VIBRATIONS OF RIGID BODIES ON ELASTIC MEDIA

A Thesis

presented for the degree of Doctor of Philosophy of the University of London and Diploma of the Imperial College

by

Ayodele Olutuminu Awojobi BSc.(Eng.)Lond.

Department of Mechanical Engineering,
Imperial College,
London S.W.7 .

ABSTRACT

Dual integral equations representing the mixed boundary-value problems of the vibrations of rigid bodies on the free surface of a semi-infinite elastic medium are developed and solved for the first time. Four cases are considered :- vertical translation and torsional oscillation of a rigid circular body and the vertical translation and rocking of an infinitely long rectangular body.

Dynamic stress distributions under the rigid bodies - which have hitherto been assumed - are obtained directly from the solutions of the above equations and are presented in graphical form as three-dimensional surfaces showing the effect of Poisson's ratio of the medium and the frequency of excitation. Resonance curves for motion of the rigid bodies are immediately derived from these stress distributions and have been compared, for the circular body, with the experiments of Arnold, Bycroft and Warburton (1955). Other published experimental results have also been used to check the above solutions. Special attention is focussed on the conditions at resonance and a single graph in each case has been prepared to show the effect of mass or inertia ratio and Poisson's ratio upon the resonant frequency factor and non-dimensional amplitude.

A method is suggested for the practical determination of the dynamic elastic constants of soil in-situ simply based on the use of this graph and the resonant frequencies of rigid circular bodies in vertical translation. This method has been

successfully applied to soil at the Imperial College Field Station, Silwood Park, Berkshire as shown in the last chapter.

Finally, the general nature of the present method of solution to mixed boundary-value problems which are reducible to dual integral equations is indicated by outlining the solution to some problems of supersonic aerofoil theory and the diffraction of an electromagnetic wave.

ACKNOWLEDGEMENTS

As interest in this field of research was roused by my supervisor's consulting work on the Mangla Dam Project, I wish to thank Dr. Grootenhuis for suggesting the problem. He has kept admirably with the pace of the work by being accessible even at odd and unofficial hours of the day.I should also thank him for stimulating interest in the field tests which were organised in his characteristic efficient manner.

Thanks are also due to Dr.R.E.Gibson and Dr.A.N.Gordon for their interests in the progress of the work and to Mr.K.Walker, Mr.N.Morgenstern and Dr.J.L.Knill for their parts in the field tests.

I should naturally not forget to thank the University of Ibadan, Nigeria for the award of a Postgraduate Scholarship during the course of the research.

CONTENTS

Page

TITLE

ABSTRACT

ACKNOWLEDGEMENTS

INTRODUCTION ..... 1 - 10

PART ONE : Development of the dual integral equations representing the mixed boundary-value problems

CHAPTER 2 Governing equations of motion ..... 11 - 14

CHAPTER 3 General solutions of the equations of motion by means of Hankel and complex Fourier transforms ..... 15 - 17

CHAPTER 4 Evaluation of the arbitrary functions in the general solutions in terms of the required boundary stresses ..... 18 - 22

CHAPTER 5 Formulation of the dual integral equations 23 - 28

PART TWO : Solution of the dual integral equations

CHAPTER 6 Solution of the static stress distribution as a limiting case of zero-frequency vibrations ..... 29 - 34

CHAPTER 7 First approximation to the solution of the vibration problems ..... 35 - 47

CHAPTER 8 Contour integration analysis of certain infinite integrals required in the complete solution ..... 48 - 61

CHAPTER 9 Successive approximations and the complete solution ..... 62 - 94

PART THREE : Experimental verification of the theory and its application to the practical determination of the dynamic elastic constants of soil in-situ

CHAPTER 10 Comparison of theory with experimental results ..... 95 - 108

CHAPTER 11 Application of the theory to the practical determination of the dynamic elastic constants of soil in-situ .....109 - 135

APPENDIX 1 : Derivation of the governing equations of motion ..... 136 - 141

APPENDIX 2 : Application of the theory to the solution of related problems in supersonic aerofoil theory and the diffraction of an electromagnetic wave..... 142 - 144

REFERENCES ..... 145 - 146

INDEX OF PRINCIPAL NOTATION 147

INTRODUCTION

1.1. Statement and scope of the problem

The object of the present investigation is to determine the response of prescribed rigid bodies on the free surface of an elastic medium when they are acted upon by harmonic forces or torques.

This problem clearly has a great number of applications in practice especially in a modern world continually subjected to the fits and starts of nuclear bomb explosions, the tremors of earthquakes, the trains of waves from moving vehicles and the shock loads from different types of impact and hammering process The vibration of buildings, transmission of noise and vibrations through foundations, stability and oscillations of dams, towers and similar large structures are other examples of the many applications of the problem to practical life.

1.2. Literature review

Several authors have attempted to solve the above problem and, broadly speaking, they fall into two main categories : those who seek a mathematical solution and those who use empirical methods.

1.2.1. Mathematical solutions

The first attempt to solve the problem seems to have been made by Reissner (1936). He considered the case of the vertical vibrations of a rigid circular body on the free surface of a semi-infinite elastic isotropic medium. He made the

assumption that the stress distribution under the rigid body was uniform and derived the displacement for the rigid body under this assumption.

An improvement over this assumption was later made by Quinlan (1953) and Sung (1953). Both assumed that the stress distribution under dynamic conditions was similar to the known static stress distribution. Before resorting to this assumed stress distribution, Quinlan remarked : "It is hopeless to attempt to solve the boundary value problem for a rigid base. However, some information may be obtained by investigating the vibrations produced by a load distribution under a static rigid base.". In their separate solutions, they assumed further that the displacement of the centre of the rigid body - derived from the assumed stress distribution - should represent the displacement of the whole rigid body.

Miller and Pursey (1954) assumed a constant stress distribution for vertical translation and a stress proportional to radial distance for rotation about an axis normal to the surfac Realising that the linear or angular displacement derived from these assumed stress distributions would not be constant under the rigid body as demanded from physical considerations, they took a simple average of the displacement under the rigid body to represent the actual displacement of the rigid body.

Yet another improvement came from Arnold, Bycroft and Warburton (1955) who considered vibrations of a rigid circular body on both a semi-infinite medium and an elastic stratum for the four modes of vertical, horizontal, torsional and rocking

vibrations. Further work on the stratum problem for vertical vibrations was later done by Warburton (1957). Their approach was to assume a stress distribution similar to the static case and to take a 'weighted' average of the resulting displacement under the rigid body. The weighting function for displacement is proportional to the assumed stress distribution.

Other authors who have worked on the assumption of a stress distribution proportional to that obtained from consideration of static loading alone include Biot (1943) and Hsieh (1962).

The only work, to the author's knowledge, which solves one aspect of the problem without assuming a stress distribution was by Reissner and Sagoci (1944) who considered the case of the torsional oscillations of a circular rigid body on an elastic half-space. Unfortunately, the use of Legendre's functions and oblate spheroidal coordinates which they employed is limited only to this one-dimensional problem.

Reissner and Sagoci (1944) in this work, had remarked that, to solve the problem otherwise would require solving an infinite number of simultaneous equations involving Bessel's functions. In a note correcting this false notion, Sneddon (1947) reformulated the problem of the dynamic stress distribution for this torsional mode only in terms of dual integral equations which he, however, did not solve.

Miller and Pursey (1955) in their second paper, although adhering to the assumption of a constant stress distribution under the rigid body, hinted that a superior approach would have been to start from the known displacement distribution.

A single integral equation of the Fredholm type and first kind involving the unknown stress distribution was derived but not solved and the hope was expressed that some future work might achieve this.

A review of some of these theories has recently appeared in a French publication by Dawance and Guillot (1963).

1.2.1.2. Mathematical solution of related problems in the diffraction of an electromagnetic wave

Dual integral equations similar to those derived by Sneddon (1947) as discussed above are known to occur in the problem of the diffraction of an electromagnetic wave incident upon a plane slit. This problem and the related problem of supersonic flow past an aerofoil are more fully discussed in Appendix 2. It is only relevant here to mention the latest reference that attempts the solution of dual integral equations. This concerns the paper of Schmeltzer and Lewin (1964) who obtained solution for the above diffraction problem by the function theoretic method. Again, like the solution of Reissner and Sagoci (1944), this method is not only cumbersome but also it is limited to this relatively simple pair of equations. None of these methods - oblate spheroidal coordinates or function theoretic methods - are applicable to the more complicated vibration problems which include the Rayleigh function (see equation 18 later) with its poles and branch-points.

1.2.2. Empirical methods

It is a matter of common experience that one main difference between a rigid body resting on a medium and the same body vibrating is that part of the medium in the latter case is also in motion. Therefore, it follows that a static stress distribution can be used, to some extent, to predict the resonant frequency of the rigid body if some mass of the medium is added on to the mass of the rigid body. The question that naturally follows is : "What proportion of the mass of the medium is to be added?"

The idea of making allowance for all parts of a vibrating system taking part in the motion is not strange in mechanical vibrations. For example, the Rayleigh energy method can be used to take account of the inertia of springs or beams partaking in vibrations. It appears, however, that energy methods will be very tedious and perhaps impossible for the present problem since displacement functions in the medium (from which velocities are to be derived) are yet unknown as these depend on the unknown stress distribution under the rigid body.

In order to answer this question of equivalent inertia of the medium, a number of empirical and semi-empirical methods have been evolved. Jacobson and Ayre (1958) suggested, for a rectangular base, that the mass of the medium to be added to the rigid body is that contained in a half of the semi-ellipsoid which has two of its semi-axes equal to half the length of the base and the third, half the width.

Another shhool of thought introduces the 'bulb of pressure' concept which considers the mass of the medium participating in the motion to be within a certain pressure zone subtended by the rigid body. A few prominent members of this idea are Crockett and Hammond (1949),Eastwood (1953) and Rao and Nagaraj (1960).

One other idea closely associated with the problem of the equivalent mass is the concept of the 'subgrade reaction' by which the elastic effect of soil on which the rigid body is resting is visualised in form of spring reactions or spring rates. The coefficients of subgrade reactions are defined in terms of load per unit deflection (horizontal or vertical) per unit area. This concept has been used, for example, by Terzaghi (1942) and more recently by Hsieh (1962).

In all these attempts, it is sufficient to summarise that, like the question of the equivalent inertia of the medium, no one has succeeded in giving a satisfactory answer to the magnitude of the coefficients of subgrade reaction in relation to the dimensions of the base of the rigid body, its mode of vibration and the elasstic properties of the soil under dynamic conditions.

Finally, there is another empirical method strongly favoured by Lorenz (e.g.1950), Tschebotarioff (e.g.1951) and Alpan (1961) which disregards completely the mass of the participating medium but studies the motion of the machine-foundation mass under the influence of the soil reaction in the form of restoring and dissipative forces. Also, isotropy or homoge-

neity of soil is considered not important. The value of this approach is lost when one considers the experimental labours involved in determining the nature of the restoring and dissipative forces.

1.2.3. The problem of the dynamic elastic constants

It is clear that whatever method of solution one adopts, the elastic constants under dynamic conditions areimportant parameters whose numerical values are ultimately required. Whilst Poisson's ratio can be assumed to be reasonably constant it is a well-known fact that the static modulus of elasticity for soil is generally lower than the dynamic modulus. This has been observed, for example, by Bernhard (1953) who used the wave propagation method of measuring dynamic modulus to compare with the static value. Also, laboratory tests on soils are very unreliable as the soil is in a disturbed state and, therefore, cannot be expected to have the same properties as the same soil under its natural conditions in-situ. The demerits of wave propagation method are discussed in Chapter1.

The method of determining elastic constants from resonance tests is now beginning to gain prominence. For example, Jones (1958) - who also used the wave propagation method - and, lately, the U.S.Army Engineer Waterways Experiment Station (1963) have performed resonant tests with rigid circular bodies in vertical translation. Jones used the theory of Sung (1953)- which has been discussed above - to calculate the shear modulus on the assumption of a Poisson's ratio of 0.5.

There is one strong objection to the method whereby resonant frequency for these rigid bodies has been determined by the above experimenters and indeed by almost all others. They have carried out the normal resonance curve procedure of measuring amplitude at various frequencies. As more fully discussed in Chapter 11, this method does not make it possible to know the real resonant frequency because of the non-linear characteristics of soil which are indeed severe at high amplitudes which are, of course, closely associated with resonance by the above methods of testing. If resonant frequency is not properly determined and therefore, not known, it is obviously useless to make use of such data to determine elastic constants especially when shear modulus is proportional to the square of frequency at a given resonant frequency factor. The order of error involved by wrong determination of resonant frequency is discussed in the comparison with the experiment of Jones (see Chapter 10).

1.3. Object of the present investigation with some comments on previous solutions

The aim has been to solve the problem stated in article 1.1 without assuming any form of stress distribution under the rigid body. It seems more direct and perhaps more logical, to use the known displacement distribution to look for the unknown stress distribution than to destroy the Known by assuming a wrong Unknown and later seek a way of straightening the Known.

Also, from article 1.2.1., it is seen that there is more than one way of assuming the Unknown and when the wrong displacement

has been derived, there is still more than one way of straightening the result. It appears feasible also to evade the mixed boundary-value problem by assuming a displacement function outside the rigid body, deriving the corresponding stress function at the boundary and adjusting this stress function until it causes the boundary stress away from the rigid body to vanish.

Surely, in all these diversities, a unique approach will be desirable - a method that will provide a satisfactory answer to the question of the equivalent mass, suggest a reliable method of determining the dynamic elastic constants of soil in-situ and above all, will provide such a general solution that will be readily applicable to related mixed boundary-value problems in other fields. The present work is an attempt in that direction.

1.4. A brief survey of the present work

Four cases of rigid bodies vibrating on the free surface of a semi-infinite elastic medium have been analysed : the vertical translation and the torsional oscillation about an axis normal to the surface of a rigid circular body and the vertical translation and rocking of an infinitely long rigid rectangular body.

The work is conveniently divided into three parts. In Part One, the three components of the vector equation of motion are derived from basic elasticity theory using cylindrical polar coordinates. The partial differential equations of motion

are then reduced to ordinary differential equations by the use of Hankel transforms (for the circular body) and Complex Fourier transforms (for the rectangular body). By retaining the exact boundary conditions, the problems are expressed in terms of dual integral equations with the transform of the dynamic stress distribution as the unknown.

In Part Two, the dual integral equations are solved first for the static case. Then a series solution for a first approximation of the vibration problems is found - from this, an answer is given to the question of equivalent inertia of the medium. Finally, a complete solution is presented based on the combined use of contour integration, extension of the dual integral equations of Titchmarsh (1937) and a systematic scheme of successive approximations. In this part, several classes of dual integral equations are solved for the first time.

The above solutions are verified in Part Three by comparison with some suitable published experimental results. Also the dynamic elastic constants of soil are determined from this theory and the results of resonance tests performed on soil at the Imperial College Field Station, Silwood Park, Berkshire and are compared with results of wave propagation and static tests on the same site and laboratory tests on samples of the same soil. In the resonance tests, the usual resonance curve technique criticised in article 1.2.3. is replaced by one defined in terms of constant small amplitude.

Finally, the application of the theory to problems of aerofoil diffraction theories is discussed in an appendix.

PART ONE

DEVELOPMENT OF THE DUAL INTEGRAL EQUATIONS REPRESENTING THE MIXED BOUNDARY-VALUE PROBLEMS

CHAPTER 2

GOVERNING EQUATIONS OF MOTION

2.1 Vector equation of motion

The motion of any particle in an isotropic elastic medium in terms of the displacement vector, $\vec{s}$, when damping is neglected is given by

$$** \quad c_1^2 \text{ grad div } \vec{s} - c_2^2 \text{ curl curl } \vec{s} = \frac{\partial^2 \vec{s}}{\partial t^2} \qquad \ldots\ldots\ldots(1)$$

where c_1 is the velocity of waves of dilatation and c_2 is the velocity of waves of distortion. The volumetric dilatation, ϵ = div $\vec{s}$ and the rotation $\vec{\omega}$ = ½curl $\vec{s}$.

2.1.1. Rigid circular body

It is convenient to resolve equation (1) into cylindrical polar coordinates in which u, v, w are the components of $\vec{s}$ in the directions r, θ, z.

Case (ai) Vertical translation In this case, axial symmetry gives v = 0 and all derivatives with respect to θ vanish, hence :-

$$c_1^2 \frac{\partial \epsilon}{\partial r} + 2c_2^2 \frac{\partial \omega_\theta}{\partial z} = \frac{\partial^2 u}{\partial t^2} \qquad \ldots\ldots\ldots(2a)$$

$$c_1^2 \frac{\partial \epsilon}{\partial z} - 2c_2^2 \frac{1}{r} \frac{\partial}{\partial r}(r\omega_\theta) = \frac{\partial^2 w}{\partial t^2} \qquad \ldots\ldots\ldots(2b)$$

** The equations of motion - the three components of equation (1) - have been derived from first principles in Appendix 1 using cylindrical polar coordinates.

where $\epsilon = \frac{u}{r} + \frac{\partial u}{\partial r} + \frac{\partial w}{\partial z}$

and the θ-component of rotation, $\omega_\theta = \frac{1}{2}(\partial u/\partial z - \partial w/\partial r)$

One method of separating ϵ and ω_θ in equations (2) is to perform the following differential operations :-

$$\left\{\frac{\partial}{\partial z}(2a) - \frac{\partial}{\partial r}(2b)\right\}$$

and

$$\left\{\left[\frac{1}{r} + \frac{\partial}{\partial r}\right](2a) + \frac{\partial}{\partial z}(2b)\right\}$$

after which equations (2) become

$$\frac{\partial^2 \epsilon}{\partial z^2} + \frac{1}{r}\frac{\partial}{\partial r}\left(r\frac{\partial \epsilon}{\partial r}\right) + \Omega_1^2 \epsilon = 0 \quad \ldots\ldots\ldots\ldots\ldots\ldots (3a)$$

$$\frac{\partial^2 \omega_\theta}{\partial z^2} + \frac{\partial}{\partial r}\left\{\frac{1}{r}\frac{\partial}{\partial r}(r\omega_\theta)\right\} + \Omega_2^2 \omega_\theta = 0 \quad \ldots\ldots\ldots (3b)$$

where it has been assumed that the oscillations are simple harmonic with an angular frequency Ω , and the notation

$$\Omega_1 = \frac{\Omega}{c_1} \qquad \Omega_2 = \frac{\Omega}{c_2}$$ is introduced.

Case (aii) Torsional oscillation about an axis normal to the surface

Here $u = w = 0$ and, again, all derivatives with respect to θ vanish. Then it can be shown that equation (1) reduces to the one-dimensional problem expressed by

$$\frac{\partial^2 v}{\partial z^2} + \frac{\partial}{\partial r}\left\{\frac{1}{r}\frac{\partial}{\partial r}(rv)\right\} + \Omega_2^2 v = 0 \quad \ldots\ldots\ldots (4)$$

It is to be noted that this mode of vibration is free from dilatation i.e. the elastic medium is in a state of pure shear.

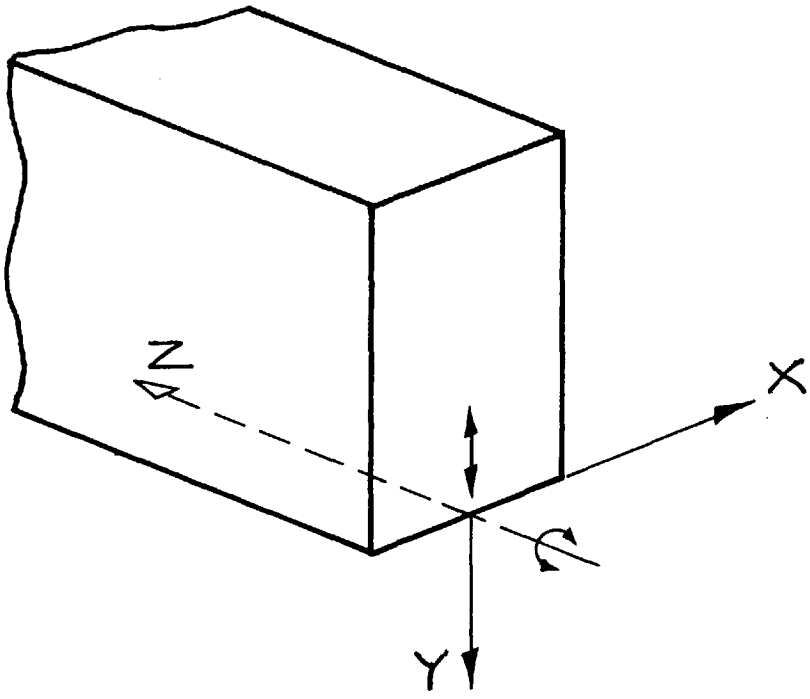


Figure 1 - Coordinate system for the rectangular bodies

2.1.2. Infinitely long rigid rectangular body

The cartesian coordinates will be adhered to, in which u, v, w are now the components of $\vec{s}$ in the directions x, y, z with the infinite length of the body along the z-axis as shown in figure 1 so that $w = 0$ and all derivatives with respect to z vanish.

Case (bi) Vertical translation

Under the above conditions, it can be shown that equation (1) reduces to

$$\nabla^2 \epsilon + \Omega_1^2 \epsilon = 0 \quad \text{.....(5a)}$$

$$\nabla^2 \omega_z + \Omega_2^2 \omega_z = 0 \quad \text{.....(5b)}$$

where $\nabla^2 = \left(\frac{\partial^2}{\partial x^2} + \frac{\partial^2}{\partial y^2}\right)$ is the two-dimensional Laplace partial differential operator, the dilatation $\epsilon = \partial u/\partial x + \partial v/\partial y$, the z-component of rotation $\omega_z = \frac{1}{2}(\partial v/\partial x - \partial u/\partial y)$ and Ω_1 and Ω_2 are as defined in equation (3).

Case (bii) Rocking about the z-axis

Equations (5a) and (5b) also apply to the rocking mode of vibration. Therefore, until the boundary displacements are introduced, it will be implied that all equations for the rigid rectangular body apply to both cases of translation and rocking.

CHAPTER 3

GENERAL SOLUTION OF THE EQUATIONS OF MOTION BY MEANS OF HANKEL AND COMPLEX FOURIER TRANSFORMS

3.1 Definition of the transform variables

The partial differential equations (3) to (5) are reduced to ordinary differential equations by introducing the following dependent variables of Hankel and Complex Fourier transforms :-

$$\left.\begin{aligned}
\text{In equation (3),}\quad \bar{\epsilon}_0(p,z) &= \int_0^\infty \epsilon(r,z) r J_0(pr)\,dr. \\
r\bar{\omega}_{\theta 1}(p,z) &= \int_0^\infty \omega_\theta(r,z) r J_1(pr)\,dr. \\
\text{In equation (4),}\quad \bar{v}(p) &= \int_0^\infty v(r) r J_1(pr)\,dr. \\
\text{In equation (5),}\quad \bar{\epsilon}(p,y) &= \int_{-\infty}^{\infty} \epsilon(x,y) e^{ipx}\,dx. \\
r\bar{\omega}_z(p,y) &= \int_{-\infty}^{\infty} \omega_z(x,y) e^{ipx}\,dx.
\end{aligned}\right\} \quad \ldots(6)$$

where the 'bar' notation over any variable indicates the corresponding transform variable.

3.2. Significance of assuming a semi-infirite medium

The elastic medium is assumed to be semi-infinite i.e. to occupy the infinite half-space below an infinitely wide horizontal plane which forms its only boundary. This assumption ensures that waves propagated from the origin are not reflected and, therefore, any interference

of waves is eliminated. Furthermore, the conditions at infinity are such that the product of functions which occurs in the process of integrating by parts vanishes: the transforms of derivatives of the functions in equations (3) to (5) can then be expressed in terms of the dependent variables of equations (6) using well-known techniques of the operational calculus.

3.3. Application of the transform variables

Eliminating r in equations (3) and (4), and x in equation (5) by introducing the parameter p of equations (6) leads to the following ordinary differential equations :-

In equation (3),

$$\frac{d^2\bar{\epsilon}_o}{dz^2} - \alpha_1^2\bar{\epsilon}_o = 0 \quad \ldots\ldots\ldots(7a)$$

$$\frac{d^2\overline{\omega}_{e1}}{dz^2} - \alpha_2^2\overline{\omega}_{e1} = 0 \quad \ldots\ldots\ldots(7b)$$

In equation (4),

$$\frac{d^2\bar{v}}{dz^2} - \alpha_2^2\bar{v} = 0 \quad \ldots\ldots\ldots(8)$$

In equation (5),

$$\frac{d^2\bar{\epsilon}}{dy^2} - \alpha_1^2\bar{\epsilon} = 0 \quad \ldots\ldots\ldots(9a)$$

$$\frac{d^2\overline{\omega}_z}{dy^2} - \alpha_2^2\overline{\omega}_z = 0 \quad \ldots\ldots\ldots(9b)$$

where the following notation has been introduced :-

$$\alpha_1^2 = p^2 - \Omega_1^2 \qquad \alpha_2^2 = p^2 - \Omega_2^2$$

3.4. General solution of the transformed equations

Since all transforms must vanish as z or y tends to infinity, we immediately have the general solution of the above ordinary differential equations as

$$\bar{\xi}_0 = A_2 e^{-\alpha_1 z} \quad \text{.....(10a)}$$

$$\bar{\omega}_{0_1} = A_1 e^{-\alpha_2 z} \quad \text{.....(10b)}$$

$$\bar{v} = B e^{-\alpha_2 z} \quad \text{.....(11)}$$

$$\bar{\xi} = C_1 e^{-\alpha_2 y} \quad \text{.....(12a)}$$

$$\bar{\omega}_z \quad C_2 e^{-\alpha_2 y} \quad \text{.....(12b)}$$

where the coefficients A, B, C are arbitrary functions of the parameter p, to be determined from the boundary conditions.

CHAPTER 4

EVALUATION OF THE ARBTRARY FUNCTIONS IN THE GENERAL SOLUTION IN TERMS OF THE REQUIRED BOUNDARY STRESSES .

4.1. Expressions for the general stress components

It is required to obtain expressions for the general state of stress in the elastic medium from which, as a particular case, the boundary stresses can be derived. Elasticity theory gives the following relations for the cases under discussion :-

4.1.1. Case (ai) Rigid circular body, vertical translation

$$\begin{aligned}\sigma_z &= \lambda\epsilon_r + (\lambda + 2G)\epsilon_z \\ &= \lambda\frac{1}{r}\frac{\partial}{\partial r}(ur) + (\lambda + 2G)\frac{\partial w}{\partial z}\end{aligned}$$

Substituting for u and w from equations (2a) and (2b) and remembering that for harmonic vibrations at an angular frequency Ω , $\frac{\partial^2}{\partial t^2}(u,w) = -\Omega^2(u,w)$

it is found after a few reductions that

$$\sigma_z = \frac{G}{\Omega_2^2}\left\{\frac{4}{r}\frac{\partial}{\partial r}\left(r\frac{\partial\omega_\theta}{\partial z}\right) - \frac{\lambda}{G}\beta^2\frac{1}{r}\frac{\partial}{\partial r}\left(r\frac{\partial\epsilon}{\partial r}\right) - \beta^4\frac{\partial^2\epsilon}{\partial z^2}\right\} \quad (13)$$

Similarly, $\tau_{rz} = G\left(\frac{\partial u}{\partial z} + \frac{\partial w}{\partial r}\right)$

$$= \frac{G}{\Omega_2^2}\left\{2\frac{\partial}{\partial r}\left[\frac{1}{r}\frac{\partial}{\partial r}(r\omega_\theta)\right] - 2\beta^2\frac{\partial^2\epsilon}{\partial r\,\partial z} - 2\frac{\partial^2\omega_\theta}{\partial z^2}\right\} \quad ..(14$$

where λ is Lame's elastic constant and G is the shear modulu
Also the ratio $= \beta = \frac{c_1}{c_2} = \frac{\Omega_2}{\Omega_1} > 1$ has been introduced.

Case (aii) Rigid circular body, torsional oscillation

In this case, the only stress component required is

$$\tau_{z\theta} = G\frac{\partial v}{\partial z} \quad \text{.....(15)}$$

4.1.2. Case (b) Rigid rectangular body

$$\sigma_y = \lambda\epsilon_x + (\lambda + 2G)\epsilon_y$$
$$= \lambda\frac{\partial u}{\partial x} + (\lambda + 2G)\frac{\partial v}{\partial y}$$

and after a few substitutions and reductions in the same manner as in case (ai), it is found that

$$\sigma_y = -\frac{G}{\Omega_2^2}\left\{\beta^4\frac{\partial^2\epsilon}{\partial y^2} + 4\frac{\partial^2\omega_z}{\partial x\partial y} + \beta^4\frac{\lambda}{G}\frac{\partial^2\epsilon}{\partial x^2}\right\} \quad \text{...(16)}$$

Similarly, $\tau_{xy} = G\left(\frac{\partial u}{\partial y} + \frac{\partial v}{\partial x}\right)$

$$= \frac{2G}{\Omega_2^2}\left\{\frac{\partial^2\omega_z}{\partial y^2} - \frac{\partial^2\omega_z}{\partial x^2} - \beta^2\frac{\partial^2\epsilon}{\partial x\partial y}\right\} \quad \text{...(17)}$$

4.2. Transforms of the general stress components

The above expressions for the stresses can be simplified by using the appropriate transforms analogous to the variables defined in equations (6). The application of the transforms leads to the following ordinary differential equations :-

$$\bar{\sigma}_{zc} = \frac{G}{\Omega_2^2}\left\{4p\frac{d\bar{\omega}_{\theta 1}}{dz} + \frac{\lambda}{G}\beta^2 p^2\bar{\epsilon}_o - \beta^4\frac{d^2\bar{\epsilon}_o}{dz^2}\right\} \quad \text{.....(13a)}$$

$$\bar{\tau}_{rz_1} = \frac{G}{\Omega_2^2}\left\{-2p^2\bar{\omega}_{\theta 1} + 2\beta^2 p\frac{d\bar{\epsilon}_o}{dz} - 2\frac{d^2\bar{\omega}_{\theta 1}}{dz^2}\right\} \quad \text{.....(14a)}$$

$$\bar{\tau}_{z\theta} = G\frac{d\bar{v}}{dz} \quad \text{.....(15a)}$$

$$\bar{\sigma}_y = -\frac{G}{\Omega_2^2}\left\{\beta^4\frac{d^2\bar{\xi}}{dy^2} - 4ip\frac{d\bar{\omega}_z}{dy} - \beta^2\frac{\lambda}{G}p^2\bar{\epsilon}\right\} \quad \text{.....(16a)}$$

$$\bar{\tau}_{xy} = \frac{2G}{\Omega_2^2}\left\{\frac{d^2\bar{\omega}_z}{dy^2} + p^2\bar{\omega}_z + ip\beta^2\frac{d\bar{\xi}}{dy}\right\} \quad \text{.....(17a)}$$

4.3. Transforms of the boundary stress components

The particular case of transforms of the boundary stress components can be deduced from equations (13a) to (17a) after the general solutions given by equations (10) to (12) have been substituted in equations (13a) to (17a), and the depth variables z(equations (10 and (11)) and y (equation (12)) are each set to zero corresponding to the surface of the medium. This procedure gives the following expressions for the boundary stress transforms in terms of the arbitrary functions :-

$$\left(\bar{\sigma}_{zz}\right)_{z=0} = \frac{G}{\Omega_2^2}\left\{-4p\alpha_2 A_1 + \beta^2\left(\frac{\lambda}{G}p^2 - \beta^2\alpha_1^2\right)A_2\right\} \quad \ldots(13b)$$

$$\left(\bar{\tau}_{rz}\right)_{z=0} = \frac{2G}{\Omega_2^2}\left\{-\left(\alpha_2^2 + p^2\right)A_1 - \beta^2\alpha_1 pA_2\right\} \quad \ldots\ldots\ldots(14b)$$

$$\left(\bar{\tau}_{z\theta}\right)_{z=0} = -EG\alpha_2 \quad \ldots\ldots\ldots(15)$$

$$\left(\bar{\sigma}_{y}\right)_{y=0} = -\frac{G}{\Omega_2^2}\left\{\beta^2\left(\beta^2\alpha_1^2 - \frac{\lambda}{G}p^2\right)C_1 + 4ip\alpha_2 C_2\right\} \quad \ldots(16b)$$

$$\left(\bar{\tau}_{xy}\right)_{y=0} = -\frac{2G}{\Omega_2^2}\left\{i\beta^2 p\alpha_1 C_1 - \left(\alpha_2^2 + p^2\right)C_2\right\} \quad \ldots\ldots\ldots(17b)$$

4.4. Representation of the unknown boundary stresses by single stress functions

It will now be assumed that the unknown stress distribution at the surface can be represented by a single function of the independent spacial variable r, for the circular body and x, for the rectangular body. Assuming also a frictionless contact between the base of the rigid body and the surface of the semi-infinite medium, except, of course, for the case of the torsional oscillation of the circular body, then :-

$$\left(\sigma_z\right)_{z=0} = \bar{\sigma}(r) \qquad \text{.....(13c)}$$

$$\left(\tau_{rz}\right)_{z=0} = 0 \qquad \text{for all } r \geqslant 0 \qquad \text{.....(14c)}$$

$$\left(\tau_{z\phi}\right)_{z=0} = \bar{\tau}(r) \qquad \text{.....(15c)}$$

$$\left(\sigma_y\right)_{y=0} = \bar{\sigma}(x) \qquad \text{.....(16c)}$$

$$\left(\tau_{xy}\right)_{y=0} = 0 \qquad \text{for all } |x| \geqslant 0 \qquad \text{.....(17c)}$$

It should be noted that the stress functions defined in equations (13c) to (17c) are kept to apply also to regions outside the rigid body. This is an important point as it distinguishes between a solution of the problems by dual integral equations and a solution by single integral equations of the Fredholm type and first kind - the latter makes use, directly, of the obvious condition of zero surface stress away from the rigid body so that its stress function applies to regions under the rigid body alone. The method of dual integral equations, however, makes use of this condition in formulating the second of the pair of equations as shown in the next chapter.

4.5. Evaluation of the arbitrary functions

The transforms of the single stress functions introduced in the last section are defined in the same manner as for the functions of equations (6). Since these single stress functions apply only to the boundarystresses, their transforms can be equated with equations (13b) to (17b) giving the following equations for the arbitrary functions

$$\frac{G}{\Omega_2^2}\left\{-4p\alpha_2 A_1 + \beta^2\left(\frac{\lambda}{G}p^2 - \beta^2\alpha_1^2\right)A_2\right\} = \bar{\sigma}(r) \qquad \text{...(13c)}$$

$$\left(\alpha_2^2 + p^2\right)A_1 + \beta^2 p\alpha_1 A_2 = 0 \qquad \text{...(14c)}$$

$$-BG\alpha_2 = \bar{\tau}(r) \quad \ldots\ldots\ldots(15d)$$

$$-\frac{G}{\Omega_2^2}\left\{\beta^2\left(\beta^2\alpha_1^2 - \frac{\lambda}{G}p^2\right)C_1 + 4ip\alpha_2 C_2\right\} = \bar{\sigma}(x) \quad \ldots\ldots(16d)$$

$$i\beta^2 p\alpha_1 C_1 - \left(\alpha_2^2 + p^2\right)C_2 = 0 \quad \ldots\ldots(17d)$$

where it should be noted that the 'bar' over $\sigma(r)$, $\tau(r)$ and $\sigma(x)$ indicates that $\bar{\sigma}(r)$, $\bar{\tau}(r)$ and $\bar{\sigma}(x)$ are functions of the parameter p and NOT functions of the spacial variables r and x.

The solutions of equations (13d) to (17d) immediately give

$$A_1 = \frac{\beta^2 p\alpha_1 \Omega_2^2 \bar{\sigma}(r)}{G\Delta(p)}$$

$$A_2 = \frac{\left(\alpha_2^2 + p^2\right)\Omega_2^2\,\bar{\sigma}(r)}{G\Delta(p)}$$

$$B = -\frac{\bar{\tau}(r)}{G\alpha_2}$$

$$C_1 = -\frac{\Omega_2^2\left(\alpha_2^2 + p^2\right)\bar{\sigma}(x)}{G\Delta(p)}$$

$$C_2 = -\frac{i\Omega_2^2\beta^2 p\alpha_1\,\bar{\sigma}(x)}{G\Delta(p)}$$

where $$\Delta(p) = \beta^2\begin{vmatrix} -4p\alpha_2 & \left(\frac{\lambda}{G}p^2 - \beta^2\alpha_1^2\right) \\ \left(\alpha_2^2 + p^2\right) & p\alpha_1 \end{vmatrix}$$

which, after some simplification gives

$$\Delta(p) = \beta^2\phi(p)$$

where $$\phi(p) = \left(2p^2 - \Omega_2^2\right)^2 - 4p^2\left(p^2 - \Omega_1^2\right)^{1/2}\left(p^2 - \Omega_2^2\right)^{1/2} \quad (18)$$

is the well-known function associated with Rayleigh surface waves.

CHAPTER 5

FORMULATION OF THE DUAL INTEGRAL EQUATIONS

5.1. Transforms of the boundary components of displacement

The next step is to obtain the transforms of the relevant components of displacement noting again that, for harmonic oscillations at an angular frequency Ω,

$$\frac{\partial^2 \vec{s}}{\partial t^2} = -\Omega^2 \vec{s}$$

5.1.1. Case (ai) Rigid circular body, vertical translation

From equation (2b), the vertical component, w is given by

$$w = -\left\{ \frac{1}{\Omega_1^2} \frac{\partial \epsilon(r,z)}{\partial z} - \frac{2}{\Omega_2^2} \frac{1}{r} \frac{\partial (r\omega_\theta)}{\partial r} \right\} \quad ..(19)$$

and its transform in relation to the definitions in equations (6) is

$$\bar{w}_o = -\frac{1}{\Omega_1^2} \frac{d\bar{\epsilon}_o}{dz} + \frac{2p}{\Omega_2^2} \bar{\omega}_{\theta 1} \quad .....(19a)$$

Using the solution in equation (10) and setting $z=0$, we obtain the transform of the boundary component of displacement:-

$$(\bar{w}_o)_{z=0} = \frac{\alpha_1}{\Omega_1^2} A_1 + \frac{2p}{\Omega_2^2} A_2 \quad .....(19b)$$

Case (aii) Rigid circular body, torsional oscillation

Since the component of displacement, v, has been given implicitly by equation (11), we obtain directly the equation corresponding to equation (19b) :-

$$(\bar{v})_{z=0} = B \quad .....(20b)$$

5.1.2. Case (b) Rigid rectangular body

It can be shown that, after some simplification of equations (5a) and (5b), the vertical component of displacement is given by

$$v = -\left(\frac{1}{\Omega_1^2}\frac{\partial \epsilon}{\partial y} + \frac{2}{\Omega_2^2}\frac{\partial \omega_z}{\partial x}\right) \qquad \ldots\ldots\ldots\ldots\ldots\ldots(21)$$

The transform of v, again using equations (6), is

$$\bar{v} = -\frac{1}{\Omega_1^2}\frac{d\bar{\epsilon}}{dy} + \frac{2ip\bar{\omega}_z}{\Omega_2^2} \qquad \ldots\ldots\ldots\ldots\ldots\ldots(21a)$$

and $$(\bar{v}_{y=0}) = \frac{\alpha_1}{\Omega_1^2}C_1 + \frac{2ip}{\Omega_2^2}C_2 \qquad \ldots\ldots\ldots\ldots\ldots\ldots(21b)$$

5.2. The inversion theorems of Hankel and Complex Fourier transforms

The functions of the spacial variables in equations (6) can be expressed in terms of the dependent variables which are functions of the parameter p by means of the following corresponding integrals obtained from the inversion theorems:-

$$\left.\begin{aligned}
\epsilon(r,z) &= \int_0^\infty \bar{\epsilon}_0(p,z)pJ_0(pr)dp. \\
\omega_\theta(r,z) &= \int_0^\infty \bar{\omega}_{\theta 1}(p,z)pJ_1(pr)dp. \\
v(r) &= \int_0^\infty \bar{v}(p)pJ_1(pr)dp. \\
\epsilon(x,y) &= \frac{1}{2\pi}\int_{-\infty}^{\infty} \bar{\epsilon}(p,y)e^{-ipx}dp. \\
\omega_z(x,y) &= \frac{1}{2\pi}\int_{-\infty}^{\infty} \bar{\omega}_z(p,y)e^{-ipx}dp.
\end{aligned}\right\} \qquad \ldots\ldots\ldots(6a)$$

5.3. Integral representation of the boundary displacements

The integrals analogous to those defined in equations (6a) will now be used to obtain expressions for the boundary displacements when use is made of equations (19b) to (21b).

5.3.1. Case (ai) Rigid circular body, vertical translation

$$w(r,0) = \int_0^\infty (\bar{w}_o)_{z=0} p J_o(pr)\,dp.$$

$$= \int_0^\infty \left(\frac{\alpha_1}{\Omega_1^2} A_1 + \frac{2p}{\Omega_2^2} A_2 \right) p J_o(pr)\,dp.$$

$$= \frac{\Omega_2^2}{G} \int_0^\infty \frac{\alpha_1 \bar{\sigma}(r)}{\phi(p)}\, p J_o(pr)\,dp. \quad \ldots\ldots\ldots (19c)$$

Case (aii) Rigid circular body, torsional oscillation

$$v(r,0) = \int_0^\infty (\bar{v})_{z=0} p J_1(pr)\,dp.$$

$$= \int_0^\infty B p J_1(pr)\,dp.$$

$$= -\frac{1}{G} \int_0^\infty \frac{\bar{\tau}(r)}{\alpha_2} p J_1(pr)\,dp \quad \ldots\ldots\ldots\ldots (20c)$$

5.3.2. Case (b) Rigid rectangular body

$$v(x,0) = \frac{1}{2\pi} \int_{-\infty}^\infty (\bar{v})_{y=0} e^{-ipx}\,dp.$$

$$= \frac{1}{2\pi} \int_{-\infty}^\infty \left(\frac{\alpha_1}{\Omega_1^2} C_1 + \frac{2ip}{\Omega_2^2} C_2 \right) e^{-ipx}\,dp.$$

$$= -\frac{\Omega_2^2}{2\pi G} \int_{-\infty}^\infty \frac{\alpha_1}{\phi(p)}\, \bar{\sigma}(x) e^{-ipx}\,dp. \quad \ldots\ldots (21c)$$

5.4. Integral representation of the boundary stresses

We shall require later the corresponding boundary stresses which have been defined in equations (13c) to (17c) as fumctions of the single spacial variables r and x. It is convenient here to express them in terms of their respective transforms by using inversion formulae analogous to those defined in equations (6a) so that

$$\sigma(r,0) = \int_0^\infty \bar{\sigma}(r)pJ_0(pr)dp. \quad \ldots\ldots\ldots(19d)$$

$$\tau(r,0) = \int_0^\infty \bar{\tau}(r)pJ_1(pr)dp. \quad \ldots\ldots\ldots(20d)$$

$$\sigma(x,0) = \frac{1}{2\pi}\int_{-\infty}^{\infty} \bar{\sigma}(x)e^{-ipx}dp. \quad \ldots\ldots\ldots(21d)$$

5.5. Derivation of the dual integral equations

With the derivation of the boundary stresses and displacements as given in the preceding articles, we are now in a position to formulate the dual integral equations representing the mixed boundary-value problems. The exact boundary conditions to be satisfied are :-

(i) Constant linear or angular displacement underneath the rigid body

and (ii) The vanishing of surface stresses away from the rigid body.

These conditions are equivalent to :-

5.5.1. Case (ai) Rigid circular body, vertical translation

Using equations (19c) and (19d), we obtain

$$\left.\begin{aligned} \frac{\Omega_2^2}{G}\int_0^\infty \frac{\alpha_1}{\phi(p)}\bar{\sigma}(r)pJ_0(pr)dp. &= w_0 \qquad 0<r<R \\ \int_0^\infty \bar{\sigma}(r)pJ_0(pr)dp. &= 0 \qquad r>R \end{aligned}\right\} \ldots\ldots(22)$$

where $w_o = w_o e^{i\Omega t}$ is the vertical displacement of the rigid body and is a constant with respect to r but varies harmonically with respect to time, t and R is the radius of the body.

Case (aii) Rigid circular body, torsional oscillation

Using equations (20c) and (20d) :-

$$\left.\begin{aligned} -\frac{1}{G}\int_0^\infty \frac{\bar{\tau}(r)}{2} pJ_1(pr)dp. &= r\theta_o \quad 0<r<R \\ \int_0^\infty \bar{\tau}(r)pJ_1(pr)dp. &= 0 \quad r>R \end{aligned}\right\} \ldots(23)$$

where $\theta_o = \theta_o e^{i\Omega t}$ is the angular displacement of the body and is, again, independent of r. Equations (23) are equivalent to those given by Sneddon (1947).

5.5.2. Case (bi) Rigid rectangular body, vertical translation

Using equations (21c) and (21d) :-

$$\left.\begin{aligned} -\frac{\Omega_2^2}{2\pi G}\int_{-\infty}^{\infty} \frac{\alpha_1}{\phi(p)}\bar{\sigma}(x)e^{-ipx}dp. &= v_o \quad |x|<b \\ \int_{-\infty}^{\infty} \bar{\sigma}(x)e^{-ipx}dp. &= 0 \quad |x|>b \end{aligned}\right\} \ldots(24a)$$

where $v_o = v_o e^{i\Omega t}$ is the vertical displacement of the body and is independent of x, and $2b$ is the width of the body. Because of the symmetry of vibrations about the z-axis, the imaginary exponential can be replaced by a cosine term and the limits of integration are then taken as zero and infinity :-

$$\left.\begin{aligned} -\frac{\Omega_2^2}{\pi G}\int_0^\infty \frac{\alpha_1}{\phi(p)}\bar{\sigma}(x)\cos(px)dp. &= v_o \quad x<b \\ \int_0^\infty \bar{\sigma}(x)\cos(px)dp. &= 0 \quad x>b \end{aligned}\right\} \ldots(24)$$

Case (bii) Rigid rectangular body, rocking mode

It is readily obvious that the anti-symmetry of the vibration in this case requires the cosine term in equations (24) to be replaced by the sine term. Remembering it is the angular displacement which is constant here with respect to the length coordinates, then corresponding to equations (24) we obtain:-

$$\left.\begin{aligned} \frac{\Omega_2^2}{\pi G}\int_0^{\infty}\frac{\alpha_1}{\phi(p)}\bar{\sigma}(x)\sin(px)dp. &= x\psi \quad x<b \\ \int_0^{\infty}\bar{\sigma}(x)\sin(px)dp. &= 0 \quad x>b \end{aligned}\right\} \ldots.(25)$$

where $\psi = \hat{\psi}e^{i\Omega t}$ is the angle of rock and is also independent of x.

It should be noted that in equations (22) to (25) α_1 and $\phi(p)$ are functions of p which have already been defined in equations (9) and (18) respectively.

5.6. The dual integral equations as an exact formulation of the mixed boundary-value problems

It is considered noteworthy to emphasise here that the pairs of equations (22) to (25) are the exact conditions which the transforms of the unknown dynamic stress distribution should satisfy in order to ensure that the mixed boundary conditions are exactly fulfilled.

The importance of this special note is two-fold: first, it makes it quite clear that the dynamic stress distribution is far from being such a simple function as can be replaced by a constant stress or static stress distribution - which are the usually assumed stresses as have been discussed in the introduction. Secondly, it expresses the need for further researches on dual integral equations by pure mathematicians who are generally fascinated by practical engineering problems reduced to such a conscise and neat form.

The general solution of these equations would lead to an answer to a hitherto unsolved problem.

PART TWO

SOLUTION OF THE DUAL INTEGRAL EQUATIONS

CHAPTER 6

SOLUTION OF THE STATIC STRESS DISTRIBUTION AS A LIMITING CASE OF ZERO-FREQUENCY VIBRATION

6.1. Purpose of the solution for the static case

It is found necessary to solve the main equations (22) to (25) for the special case of static loading for two reasons :- (a) For comparison with known stress distributions obtained by analysis of the static conditions alone and (b) For subsequent use in Chapter 7 as the first term in an expansion.

6.2. The class of dual integral equations for the static case

As the frequency of excitation tends to zero, the dual integral equations (22) to (25) reduce to the familiar equations which have been studied by Titchmarsh (1937), Busbridge (1938), Tranter (1951), Gordon (1954) and several others. The equations take the form :

$$\left.\begin{aligned} \int_0^\infty p^\alpha f(p) J_\nu(px)\,dp. &= g(x) \qquad 0<x<1 \\ \int_0^\infty f(p) J_\nu(px)\,dp. &= 0 \qquad x>1 \end{aligned}\right\} \ldots(26)$$

where $f(p)$ is the required function of p and $g(x)$ is a known function of x. The solution of $f(p)$ using Titchmarsh (1937) and Busbridge (1938), is

$$f(p) = \frac{(2p)^{1-\alpha/2}}{\Gamma(\alpha/2)} \int_0^1 u^{1+\alpha/2} J_{\nu+\alpha/2}(pu)\,du \int_0^1 g(uv) v^{\nu+1} (1-v^2)^{\alpha/2-1}\,dv. \qquad \ldots\ldots(26a)$$

provided $\alpha > 0$

or

$$f(p) = \frac{2^{-\alpha/2} p^{-\alpha}}{\Gamma(1+\alpha/2)} \left\{ p^{1+\alpha/2} J_{\frac{2\nu+\alpha}{2}}(p) \int_0^1 y^{\nu+1} (1-y^2)^{\alpha/2} g(y)\,dy. + \int_0^1 u^{\nu+1} (1-u^2)^{\alpha/2}\,du \int_0^1 g(uy)(py)^{\frac{4+\alpha}{2}} J_{\nu+1+\alpha/2}(py)\,dy \right. \qquad \ldots\ldots(26b)$$

for $\alpha > -2$ and $-(\nu+1) < \alpha - \tfrac{1}{2} < \nu+1$

6.3. Static stress distribution under the rigid circular body

Case (ai) Vertical translation

Using de'l'Hospital's rule,

$$\lim_{\Omega \to 0} \frac{\Omega_2^2 \alpha_1}{\phi(p)} = \left\{ \frac{\frac{\partial}{\partial \Omega}\left[\Omega_2^2 \alpha_1\right]}{\frac{\partial}{\partial \Omega}\left[\phi(p)\right]} \right\}_{\Omega=0}$$

from which it is found that

$$\lim_{\Omega \to 0} \frac{\Omega_2^2 \alpha_1}{\phi(p)} = \frac{1}{2\left(\beta_1^2 - 1\right)p} \qquad \text{where } \beta_1 = \frac{1}{\beta} = \frac{\Omega_1}{\Omega_2} <$$

Equations (22) then reduce to

$$\left.\begin{aligned} \int_0^\infty p^{-1} f(p) J_0(pr)\,dp. &= c \quad 0 < r < R \\ \int_0^\infty f(p) J_0(pr)\,dp. &= 0 \quad r > R \end{aligned}\right\} \ldots\ldots(27)$$

where $c = -2G\left(1 - \beta_1^2\right)w_0$ and $f(p) = \bar{\sigma}(r)p$

It is easier to solve equations (27) by using the well-known relations (Watson P405)

$$\left.\begin{aligned} \int_0^\infty p^{-1} \sin(pR) J_0(pr)\,dp. &= \pi/2 \quad 0 < r < R \\ \int_0^\infty \sin(pR) J_0(pr)\,dp. &= 0 \quad r > R \end{aligned}\right\} \ldots(27a)$$

from which, by comparison, we find the solution

$$f(p) = \frac{2}{\pi} c \sin(pR)$$

$$\text{hence } \bar{\sigma}(r) = \frac{2}{\pi} c \frac{\sin(pR)}{p} \qquad \ldots\ldots\ldots(27b)$$

and by using the inversion theorem (article 5.2.), we obtain immediately the static stress distribution :-

$$\sigma(r) = \frac{2}{\pi} c \int_0^\infty \sin(pR) J_0(pr)\,dp.$$

and using, again, Watson (P405)

$$\left.\begin{aligned} \sigma(r) &= -\frac{4G(1 - \beta_1^2)w_0}{\pi(R^2 - r^2)^{1/2}} \quad 0 < r < R \\ &= 0 \quad r > R \end{aligned}\right\} \ldots(27c)$$

This stress distribution is identical to that found by analysing the static condition alone, see for example Timoshenko (1951).

Case (aii) Torsional oscillation

Equations (23) reduce to

$$\left.\begin{aligned}\int_0^\infty \bar{\tau}(r)J_1(pr)dp. &= -G\theta r \qquad 0<r<R\\ \int_0^\infty \bar{\tau}(r)pJ_1(pr)dp. &= 0 \qquad\qquad r>R\end{aligned}\right\} \ldots.(28)$$

By introducing the non-dimensional quantities $\tilde{r} = \frac{r}{R}$, $\eta = pR$ and inserting $f(p) = p\bar{\tau}(r)$ and $f(\eta/R) = F(\eta)$, we have

$$\left.\begin{aligned}\int_0^\infty \eta^{-1}F(\eta)J_1(\eta\tilde{r})d\eta. &= c\tilde{r} \qquad 0<\tilde{r}<1\\ \int_0^\infty F(\eta)J_1(\eta\tilde{r})d\eta. &= 0 \qquad\qquad \tilde{r}>1\end{aligned}\right\} \ldots.(28a)$$

where $c = -GR\theta$.

Using the solution (26b) with $\alpha = -1$, $\nu = 1$, it is found that

$$F(\eta) = \frac{2c}{3}\sqrt{\frac{2}{\pi}}\,\eta^{1\frac{1}{2}}\left(J_{\frac{1}{2}}(\eta) + J_{2\frac{1}{2}}(\eta)\right)$$

and from the recurrence relation for Bessel's functions,

$$F(\eta) = 2c\sqrt{\frac{2}{\pi}}\eta^{\frac{1}{2}}J_{1\frac{1}{2}}(\eta)$$

or
$$p\bar{\tau}(r) = -2G\theta\sqrt{\frac{2}{\pi}}R^{1\frac{1}{2}}p^{\frac{1}{2}}J_{1\frac{1}{2}}(pR) \qquad \ldots\ldots\ldots(28b)$$

In order to obtain the stress distribution $\tau(r)$, we require the following discontinuous integral given in Bateman's Tables (Vol.2.,P.48) :-

$$\begin{aligned}\int_0^\infty p^{m-n+1}J_n(pR)J_m(pr)dp. &= \frac{2^{m-n+1}r^{m+\frac{1}{2}}(R^2-r^2)^{n-m-1}}{\Gamma(n-m)R^n} \qquad 0<r<R\\ &= 0 \qquad\qquad r>R\end{aligned}$$

Again, by the inversion theorem (article 5.2.),

$$\tau(r) = \int_0^\infty \bar{\tau}(r)pJ_1(pr)dp.$$

Substituting for $\bar{\tau}(r)$ from equation(28b) and setting $n = 1\frac{1}{2}$ and $m=1$ in the above discontinuous integral, we finally obtain

$$\left.\begin{aligned}\tau(r) &= -\frac{4}{\pi}G\theta\frac{r}{R}\left[1-\left(\frac{r}{R}\right)^2\right]^{-\frac{1}{2}} \qquad 0<r<R\\ &= 0 \qquad\qquad r>R\end{aligned}\right\} \ldots(28$$

6.4. Static stress distribution under the rigid rectangular body

Case (bi) Vertical translation

Equations (24) can be easily shown to reduce to

$$\left.\begin{aligned} c\int_0^\infty \frac{\bar{\sigma}(x)}{p}\cos(px)dp. &= 1 \quad 0<x<b \\ \int_0^\infty \bar{\sigma}(x)\cos(px)dp. &= 0 \quad x>b \end{aligned}\right\} \ldots\ldots(29)$$

where $\frac{1}{c} = -2\,G(\beta_1^2 - 1)v_o$.

It is here noted that the first integral diverges showing that the vertical deflection would become infinitely large. Since in practical problems finite displacements are obtained (infinitely long bodies do not exist) we can differentiate equation (29) under the integral sign and so obtain :-

$$\left.\begin{aligned} -c\int_0^\infty \bar{\sigma}(x)\sin(px)dp. &= 0 \quad 0<x<b \\ \int_0^\infty \bar{\sigma}(x)\cos(px)dp. &= 0 \quad x>b \end{aligned}\right\} \ldots\ldots(29a)$$

We can now spot the solution of $\bar{\sigma}(x)$ when use is made of the following results in Watson (P.405) :-

$$\int_0^\infty J_o(pb)\sin(px)dp. = 0 \quad 0<x<b$$

$$\int_0^\infty J_o(pb)\cos(px)dp. = 0 \quad x>b$$

so that $$\bar{\sigma}(x) = -\frac{1}{c}J_o(pb) \qquad \ldots\ldots(29b)$$

and by inversion, $$\sigma(x) = \frac{1}{\pi}\int_0^\infty \bar{\sigma}(x)\cos(px)dp.$$

from which we obtain

$$\left.\begin{aligned} \sigma(x) &= -\frac{2G(1-\beta_1^2)v_o}{(b^2-x^2)^{1/2}} \quad 0<x<b \\ &= 0 \quad x>b \end{aligned}\right\} \ldots(29c)$$

which is an alternative solution of the stress distribution first obtained by M. Sadowsky (1928).

Case (bii) Rocking mode

Equations (25) reduce to

$$\left.\begin{aligned}\int_0^\infty p^{-1}\bar{\sigma}(x)\sin(px)dp. &= cx \qquad 0<x<b\\ \int_0^\infty \bar{\sigma}(x)\sin(px)dp. &= 0 \qquad x>b\end{aligned}\right\}\ldots\ldots(30)$$

where $c = 2\pi G(\beta_1^2 - 1)\nu$

In order to express equations (30) in a form similar to equations (26), it is convenient to replace the sine term by its equivalent Bessel function relation and introduce non-dimensional variables analogous to those defined in case (aii) i.e.

$\sin(px) = \sqrt{\frac{\pi px}{2}}J_{\frac{1}{2}}(px)$, $f(p) = \bar{\sigma}(x)p^{\frac{1}{2}}$, $\eta = pb$, $\tilde{x} = \frac{x}{b}$

and $f\left(\frac{\eta}{b}\right) = F(\eta)$. Then equations (30) assume the form :-

$$\left.\begin{aligned}\int_0^\infty \eta^{-1}F(\eta)J_{\frac{1}{2}}(\eta\tilde{x})d\eta. &= c\sqrt{\frac{2b}{\pi}}\,\tilde{x}^{\frac{1}{2}} \qquad 0<\tilde{x}<1\\ \int_0^\infty F(\eta)J_{\frac{1}{2}}(\eta\tilde{x})d\eta. &= 0 \qquad \tilde{x}>1\end{aligned}\right\}\ldots(30a)$$

Applying the solution in equation (26b) with $\alpha = -1$, $\nu = \frac{1}{2}$, it is found that

$$\begin{aligned}F(\eta) &= cb^{\frac{1}{2}}\eta^{1\frac{1}{2}}\tfrac{1}{2}((J_0(\eta) + J_2(\eta)))\\ &= cb^{\frac{1}{2}}\eta^{\frac{1}{2}}J_1(\eta)\end{aligned}$$

where we have again made use of the recurrence relation.

Hence $\bar{\sigma}(x) = -2\pi Gb(1 - \beta_1^2)/J_1(pb)$ .....(30b)

Also, by inversion $\sigma(x) = \frac{1}{\pi}\int_0^\infty \bar{\sigma}(x)\sin(px)dp.$

The following discontinuous integral (Watson P.405) is required

$$\begin{aligned}\int_0^\infty J_m(pb)\sin(px)dp. &= \sin\left\{m \arcsin\left(\frac{x}{b}\right)\right\}(b^2 - x^2)^{-\frac{1}{2}} \qquad 0<x<b\\ &= b^m\cos(\tfrac{1}{2}m\pi)\left\{x+(x^2-b^2)^{\frac{1}{2}}\right\}^{-m}(x^2-b^2)^{-\frac{1}{2}} \qquad x>b\end{aligned}$$

For the present case of $\sigma(x)$, m=1 and, therefore,

$$\left.\begin{aligned}\sigma(x) &= -2G\nu(1 - \beta_1^2)\frac{x}{b}\left\{1 - \left(\frac{x}{b}\right)^2\right\}^{-\frac{1}{2}} \qquad 0<x<b\\ &= 0 \qquad x>b\end{aligned}\right\}\ldots(30$$

6.5. A comment on edge stresses and on the static solution

It is to be noticed that there is an infinite discontinuity of stress at the edges of the rigid body for each type of motion. These edge stresses assume finite values in practice as they are relaxed by plastic deformation of the medium.

Agreement of the stress distribution of the first three cases with known solutions obtained by different routes is a justification for the assumption made in article 4.4. that the stress distribution at the surface is a single function of the independent spacial variable. The author is not aware of any published information about the proof of the stress distribution in the case of the rocking mode of the infinitely long rectangular body. Biot (1943), however, quoted that this form of stress distribution would yield a constant angular displacement required under the rocking rectangular body.

CHAPTER 7

FIRST APPROXIMATION TO THE SOLUTION OF THE VIBRATION PROBLEMS

7.1. Fundamental assumptions of the solution

We neglect for the moment all contributions to the integrals in equations (22) to (25) from poles, branch-points and any other singularities of the functions α_2 and $\frac{\alpha_1}{\phi(p)}$ of p. We also neglect the contribution from p=0 to p=Ω_2. It is readily obvious that the error involved in this approximation increases as Ω_2 becomes large and also, as no imaginary terms are considered here, the amplitudes would be infinitely large at the resonant frequency.

However, the results are useful for low frequency factor vibrations of order less than about 0.5 which covers the range of resonant frequency factors of bodies with large mass or inertia ratios.

7.2. General analysis of the solution

The functions $\frac{\alpha_1}{\phi(p)}$ and α_2 are first replaced by their power series expansions which converge for all values of $p \gg \Omega_2$.

i.e.

$$\left.\begin{aligned} \frac{\alpha_1}{\phi(p)} &= \left\{ \sum_{s=0}^{\infty} a_{s+1} p^{1-2s} \right\}^{-1} = \frac{1}{A(p)} \\ \alpha_2 &= \sum_{k=0}^{\infty} b_{k+1} p^{1-2k} = B(p) \end{aligned}\right\} \quad \ldots(31a)$$

Equations (22) to (25) then take the form :-

$$\left.\begin{aligned} \int_0^{\infty} \frac{f(p) J_{\nu}(pr)\,dp.}{a_1 p + a_2 p^{-1} + \ldots} &= g(r) \qquad 0 < r < 1 \\ \int_0^{\infty} f(p) J_{\nu}(pr)\,dp. &= 0 \qquad r > 1 \end{aligned}\right\} \quad \ldots\ldots\ldots(31b)$$

where f(p) represents the required stress transform.

Assume that f(p) is made up of an infinite number of components i.e. $$f(p) = \sum_{s=0}^{\infty} f_{s+1}(p) \qquad \text{.....(31c)}$$

where components $f_{s+1}(p)$ satisfy the relation:-

$$\int_0^{\infty} \frac{f_{s+1}(p) J_{\nu}(pr)dp.}{a_{s+1} p^{1-2s}} = g(r) \qquad 0 < r < 1 \qquad \text{....(31d)}$$

It is clear that each component of f(p) must satisfy the second of equations (31b) since the domain $r > 1$ is stress-free. Hence the dual integral equations from which $f_{s+1}(p)$ can be formally determined are:-

$$\left.\begin{aligned} \int_0^{\infty} \frac{f_{s+1}(p) J_{\nu}(pr)dp.}{a_{s+1} p^{1-2s}} &= g(r) \qquad 0 < r < 1 \\ \int_0^{\infty} f_{s+1}(p) J_{\nu}(pr)dp. &= 0 \qquad\quad r > 1 \end{aligned}\right\} \text{....(31e)}$$

which are a special case of the equations considered in Chapter (6).

In order that f(p) in equation (31c) could be regarded as a solution of equations (31b) when $f_{s+1}(p)$ has been calculated from equations (31e), we only need to satisfy the first of equations (31b) since the second equation is obviously satisfied. Therefore, we need to show that if

$$\left.\begin{aligned} &\int_0^{\infty} \frac{f_1(p) J_{\nu}(pr)dp.}{a_1 p} = \int_0^{\infty} \frac{f_2(p) J_{\nu}(pr)dp.}{a_2 p^{-1}} = \text{....} = g(r) \\ &\text{then also} \quad \int_0^{\infty} \frac{f_1(p) + f_2(p) + \text{...}}{a_1 p + a_2 p^{-1} + \text{.....}} J_{\nu}(pr)dp. = g(r) \end{aligned}\right\} \text{..(31f)}$$

It has been found from a formal proof of equations (31f) that a necessary condition to be fulfilled by g(r) in order that equations (31f) might hold is

$$\mathcal{D}_{\nu}(r)\left\{ g(r) \right\} = 0 \qquad \text{.....(31g)}$$

where $\mathcal{D}_\nu(r)$ denotes the operator occurring in Bessel's differential equation i.e.

$$\mathcal{D}_\nu(r) = \left(\frac{\partial^2}{\partial r^2} + \frac{1}{r}\frac{\partial}{\partial r} - \frac{\nu^2}{r^2}\right) \quad \ldots\ldots\ldots(31h)$$

It is easily verified that the condition expressed by equation (31g) is satisfied by $g(r)$ and ν in all the four cases considered here so that equation (31c) gives a formal solution of the problem.

7.3. Solution for the rigid circular body

7.3.1. Case (ai) Vertical translation

The expansion in equation (31a) is found to be

$$\begin{aligned} a_1 p + a_2 p^{-1} + a_3 p^{-3} + \ldots = {} & 2(\Omega_1^2 - \Omega_2^2)p \\ & + (1\tfrac{1}{2}\Omega_1^4 - 2\Omega_1^2\Omega_2^2 + 1\tfrac{1}{2}\Omega_2^4)p^{-1} \\ & + (1\tfrac{1}{4}\Omega_1^6 - 1\tfrac{1}{2}\Omega_1^4\Omega_2^2 + \tfrac{1}{2}\Omega_1^2\Omega_2^2 + \tfrac{1}{4}\Omega_2^6)p^{-3} \\ & + \ldots\ldots\ldots\ldots\ldots\ldots(32) \end{aligned}$$

Thus corresponding to $s=0$ in equation (31e), the first component of stress, $\sigma_1(r)$, is given by

$$\left.\begin{aligned} \frac{\Omega_2^2}{G}\int_0^\infty \frac{\bar{\sigma}_1(r)pJ_0(pr)dp.}{2(\Omega_1^2 - \Omega_2^2)p} &= w_0 \qquad 0 < r < R \\ \int_0^\infty \bar{\sigma}_1(r)pJ_0(pr)dp. &= 0 \qquad r > R \end{aligned}\right\} \ldots\ldots(32a)$$

We notice that equations (32a) is the same as equations (27), so that, as expected, $\sigma_1(r)$ is the static component of stress already given by equations (27c).

The equations to be satisfied by the second component of stress, $\sigma_2(r)$, are

$$\left.\begin{aligned} \frac{\Omega_2^2}{G}\int_0^\infty \frac{\bar{\sigma}_2(r)}{a_2 p^{-1}} pJ_0(pr)dp. &= w_0 \qquad 0 < r < R \\ \int_0^\infty \bar{\sigma}_2(r)pJ_0(pr)dp. &= 0 \qquad r > R \end{aligned}\right\} \ldots(33)$$

and in terms of the non-dimensional variables defined in equations (28a), equations (33) can be expressed as

$$\left.\begin{aligned} \frac{\Omega_2^2}{Ga_2R^2}\int_0^\infty \eta F_2(\eta)J_0(\eta\tilde{r})d\eta &= w_0 \quad 0<\tilde{r}<1 \\ \int_0^\infty F_2(\eta)J_0(\eta\tilde{r})d\eta &= 0 \quad \tilde{r}>1 \end{aligned}\right\} \ldots\ldots(33a)$$

which are a particular case of equations (26) with $\alpha=1$, $\lambda'=0$ so that the solution is given by equation (26a) from which after a few reductions, we find that

$$F_2(\eta) = \frac{a_2}{\Omega_2^2}R^2Gw_0\sqrt{\frac{2}{\pi}}\eta^{-1\frac{1}{2}}J_{1\frac{1}{2}}(\eta) \quad \ldots\ldots\ldots\ldots(33b)$$

where we have made use of Sonine's first integral (Watson P.373)

$$\text{i.e.}\quad J_{m+n+1}(z) = \frac{z^{n+1}}{2^n\Gamma(n+1)}\int_0^{\pi/2}\sin^{m+1}\theta\cos^{2n+1}\theta J_m(z\sin\theta)d\theta. \quad \ldots\ldots(33c)$$

provided $m>-1$ and $n>-1$.

Reverting to the dimensional variables, equation (33b) is equivalent to

$$\sigma_2(r) = \frac{a_2}{\Omega_2^2}R^{1\frac{1}{2}}Gw_0\sqrt{\frac{2}{\pi}}p^{-1\frac{1}{2}}J_{1\frac{1}{2}}(pR)$$

and by inversion

$$\sigma_2(r) = \frac{a_2}{\Omega_2^2}R^{1\frac{1}{2}}Gw_0\sqrt{\frac{2}{\pi}}\int_0^\infty p^{-\frac{1}{2}}J_{1\frac{1}{2}}(pR)J_0(pr)dp.$$

Using the same discontinuous integral in Bateman's Tables (Vol.2., P.48) as in article 6.3. where for the present case $m=0$ and $n=1\frac{1}{2}$, we obtain

$$\left.\begin{aligned} \sigma_2(r) &= \frac{2a_2}{\pi\Omega_2^2}RGw_0\left\{1-\left(\frac{r}{R}\right)^2\right\}^{\frac{1}{2}} \quad 0<r<R \\ &= 0 \quad \ldots\ldots r>R \end{aligned}\right\} \ldots(33d)$$

In a similar manner, it is found that

$$\left.\begin{aligned} \sigma_3(r) &= \frac{2a_3Gw_0}{3^2\pi\Omega_2^2}R^3\left\{1-\left(\frac{r}{R}\right)^2\right\}^{2\frac{1}{2}} \quad 0<r<R \\ &= 0 \quad r>R \end{aligned}\right\} \ldots
$$

Hence the stress distribution in the domain $r < R$ can be written as

$$\sigma(r) = \sigma_1(r)\left\{1 + \frac{\sigma_2(r)}{\sigma_1(r)} + \frac{\sigma_3(r)}{\sigma_1(r)} + \ldots\right\}$$

$$= \sigma_1(r)\left\{1 + \frac{a_2}{1^2 a_1}R^2\overset{*}{r} + \frac{a_3}{3^2 a_1}R^4(\overset{*}{r})^2 + \ldots\right\}$$

where $\sigma_1(r)$ is the static stress distribution and the notation $\overset{*}{r} = 1 - (r/R)^2$ is used.

The numerical coefficients $\frac{1}{1^2}$ and $\frac{1}{3^2}$ have been contributed by the integral

$$I_\alpha = \frac{2^{1-\alpha/2}}{\Gamma(\alpha/2)}\int_0^1 v^{\nu+1}(1-v^2)^{\alpha/2} - 1\,dv. \text{ from equation (26}$$

and the factor $f_n = \frac{2^{1-n}}{(n)}$ of the discontinuous integral used in the inversion for $\sigma_2(r)$.

If the general term of $\sigma(r)$ has the factor $(\overset{*}{r})^s$ then for odd values of α - as in this case - it is found by inspection that α and n are given by $\alpha = 2s-1$, $n = \frac{1}{2}(2s+1)$.

Also, for odd values of α, it is easily shown that

$$\Gamma(\alpha/2) = \frac{|\alpha - 2|!!\pi^{\frac{1}{2}}}{2^{\frac{1}{2}(\alpha-1)}}$$

From these relations, it is found after some reductions that

$I_\alpha f_n = \frac{2}{\pi}\left\{(2s-1)(2s-3)!!\right\}^{-2}$ and since $\frac{2}{\pi}$ will be absorbed by the $\frac{2}{\pi}$ in $\sigma_1(r)$, we finally obtain the resultant stress as

$$\sigma(r) = \sigma_1(r)\left\{1 + \frac{1}{a_1}\sum_{s=1}^{\infty}\frac{a_{s+1}R^{2s}\left\{1-\left(\frac{r}{R}\right)^2\right\}^s}{\left\{|2s-3|!!(2s-1)\right\}^2}\right\} \quad 0<r<R$$

$$= 0 \qquad r>R$$

.....(33e)

where $\sigma_1(r)$ is the static stress distribution given by equation (27c), and the double factorial has the meaning

$s!!$ = $s(s-2)(s-4).....2$ when s is even

= $s(s-2)(s-4).....1$ when s is odd.

7.3.2. Case (aii) Torsional oscillation

Again, the first component of stress, corresponding to k=0 in equation (31a) is the same as the static stress distribution given by equation (28c).

The expansion of Ω_2^2 in equation (31a) is found to be

$$B(p) = p - \frac{\Omega_2^2}{2}p^{-1} - \frac{\Omega_2^4}{8}p^{-3} - \ldots = b_1 p + b_2 p^{-1} + b_3 p^{-3} + \ldots \quad (34)$$

so that the second component of stress is given by

$$\left.\begin{aligned} \int_0^\infty \frac{\bar{\tau}_2(r)}{b_2 p^{-1}} p J_1(pr)\,dp. &= -G\theta r \qquad 0 < r < R \\ \int_0^\infty \bar{\tau}_2(r) p J_1(pr)\,dp. &= 0 \qquad\qquad r > R \end{aligned}\right\} \ldots\ldots (34a)$$

and the solution is found to be

$$\left.\begin{aligned} \bar{\tau}_2(r) &= -\frac{4G}{3\pi}\theta b_2 r(R^2 - r^2)^{1/2} \qquad 0 < r < R \\ &= 0 \qquad\qquad r > R \end{aligned}\right\} \ldots (34b)$$

The continued process leads to an infinite series for $\tau(r)$ exactly as for the case of the vertical translation. It is found that

$$\left.\begin{aligned} \tau(r) &= \tau_1(r)\left\{1 + \sum_{k=1}^{k=\infty} \frac{b_{k+1} R^{2k}\left\{1 - \left(\frac{r}{R}\right)^2\right\}^k}{(2k+1)\left\{(2k-1)!!\right\}^2}\right\} \qquad 0 < r < R \\ &= 0 \qquad\qquad r > R \end{aligned}\right\} \ldots (3'$$

where $\tau_1(r)$ is the static stress distribution given in equation (28c).

7.4. Solution for the rigid rectangular body

Since the same function $\frac{\alpha_1}{\phi(p)}$ occurs as in the case of the vertical translation of the rigid circular body, the coefficients of the expansion are those given in equation (32).

7.4.1. Case (bi) Vertical translation

Again, the first component of stress corresponds to the static stress distribution which has been given in equation (29c) and the second component is given by

$$\left.\begin{aligned} \frac{\Omega_2^2}{\pi G}\int_0^\infty \frac{\bar{\sigma}_2(x)}{a_2 p^{-1}}\cos(px)dp. &= v_o \qquad 0<x<b \\ \int_0^\infty \bar{\sigma}_2(x)\cos(px)dp. &= 0 \qquad x>b \end{aligned}\right\} \ldots\ldots(35)$$

The solution of equations (35) is found to be

$$\left.\begin{aligned} \sigma_2(x) &= Gv_o\frac{a_2}{\Omega_2^2}b^2(b^2-x^2)^{\frac{1}{2}} \qquad 0<x<b \\ &= 0 \qquad x>b \end{aligned}\right\} \ldots\ldots(35a)$$

In a manner similar to that of case (ai), it is found that, for the series expansion for $\sigma(x)$, the corresponding product $I_\alpha f_n = 2^{-\frac{1}{2}}\left[(2s-2)!!(2s-1)!!\right]^{-1}$ is readily observed to simplify to

$$I_\alpha f_n = 2^{-\frac{1}{2}}\left[(2s-1)!\right]^{-1}$$

so that the resultant stress, $\sigma(x)$ is formally given by the series solution :-

$$\left.\begin{aligned} \sigma(x) &= \sigma_1(x)\left\{1+\frac{1}{a_1}\sum_{s=1}^{\infty}\frac{a_{s+1}b^{2s}\left[1-\left(\frac{x}{b}\right)^2\right]^s}{(2s-1)!}\right\} \qquad 0<x<b \\ &= 0 \qquad x>b \end{aligned}\right\} \ldots\ldots(35b)$$

where $\sigma_1(x)$ is given by equation (29c) and the single factorial sign has the usual meaning.

7.4.2. Case (bii) Rocking mode

$\sigma_1(x)$ is the static stress distribution and $\sigma_2(x)$ is given by

$$\left.\begin{aligned} \frac{\Omega_2^2}{\pi G}\int_0^\infty \frac{\bar{\sigma}_2(x)}{a_2 p^{-1}}\sin(px)dp. &= \gamma x \qquad 0<x<b \\ \int_0^\infty \bar{\sigma}_2(x)\sin(px)dp. &= 0 \qquad x>b \end{aligned}\right\} \ldots\ldots(36)$$

and the solution is found to be

$$\sigma_2(x) = \frac{Ga_2}{2\Omega_2^2}\rho b^2 \frac{x}{b}\left\{1 - \left(\frac{x}{b}\right)^2\right\}^{\frac{1}{2}} \quad 0 < x < b$$
$$= 0 \qquad x > b \qquad \ldots(36a)$$

The resultant stress is found to be

$$\sigma(x) = \sigma_1(x)\left\{1 + \frac{1}{a_1}\sum_{s=1}^{\infty} \frac{a_{s+1} b^{2s}\left[1 - \left(\frac{x}{b}\right)^2\right]^{\frac{1}{2}}}{(2s)!}\right\} \quad 0 < x < b$$
$$= 0 \qquad x > b \qquad \ldots(36b)$$

where $\sigma_1(x)$ is given by equation (30c).

7.5. Equivalent inertia of the medium

The above solutions provide a means of estimating the resonant frequency of a rigid body resting on an elastic medium taking into account the mass of the medium. A convenient form is to determine the proportion of mass or inertia of the elastic medium to be added to the mass of the rigid body in order to lower the natural frequency if this has been calculated on the assumption of a static stress distribution. This has been suggested by Jacobson and Ayre (1958) and others - as already discussed in the introduction - who, however, used only empirical formulae to obtain the required proportion of the elastic medium. The present article shows that the second component of the resultant stress in each of the preceding solutions is essentially the 'inertia' component and the other components above the second are higher order negligible quantities for low-frequency factor vibrations under discussion in this chapter.

7.5.1. Rigid circular body

Case (ai) Vertical translation

The equation of free vibration of a rigid body of mass m is :-

$$\left| \int_0^R \frac{\hat{\sigma}(r)}{\hat{w}_o} 2\pi r dr. \right| - m\Omega^2 = 0 \qquad \text{.....(37)}$$

where the integral represents the force contributed by the resultant stress distribution given by equation (33e).

Provided the frequency factor, defined by the non-dimensional quantity

$$\eta_2 = \frac{R\Omega}{c_2} = \frac{2\pi R}{\lambda_2}$$

is less than unity, where λ_2 is shear wavelength, the series for $\sigma(r)$ converges very rapidly and the first two terms need only be used. Equation (37), after simplifying, reduces to :-

$$R^2 \left| 2k_1 + \frac{2k_2}{3} \right| - m\Omega^2 = 0$$

where $k_1 = \dfrac{2Ga_1}{R\Omega_2^2}$ and $k_2 = \dfrac{2Ga_2 R}{\Omega_2^2}$

or

$$8GR\left(1 - \beta_1^2\right) - \left\{ m + \frac{2}{3}\pi\rho R^3 \left(\frac{3\beta_1^4 - 4\beta_1^2 + 3}{\pi} \right) \right\} \Omega^2 = 0 \qquad \text{.....(37b)}$$

where we have substituted for a_1 and a_2 from equation (32) and we recall that

$$\Omega_2^2 = \frac{\Omega^2}{c_2^2} = \frac{\Omega^2 \rho}{G}$$

It is evident from equation (37b) that a 'correction' mass of the medium to be added to the mass of the rigid body if the natural frequency were calculated on the assumption of a static stress distribution is

$$m_c = \frac{2}{3}\pi\rho R^3 \left\{ \frac{3\beta_1^4 - 4\beta_1^2 + 3}{\pi} \right\}$$

and in terms of the hemisphere of the medium subtended by the rigid body,

$m_c = f_\nu m_{HS}$ where $f_\nu = \dfrac{1}{\pi}\left(3\beta_1^4 - 4\beta_1^2 + 3\right)$ is a function of Poisson's ratio, ν, alone.

Also $m_{HS} = \frac{2}{3}\pi\rho R^3$ is the mass of the hemisphere of the medium of density ρ and radius R.

Equation (37b) finally reduces to a simple expression for the natural frequency of the body :-

$$\Omega^2 = \frac{8GR\left(1 - \beta_1^2\right)}{m + m_c} \qquad \ldots\ldots\ldots\ldots\ldots\ldots(37e)$$

and in non-dimensional variables

$$\eta_2^2 = \frac{8\left(1 - \beta_1^2\right)}{\tilde{m} + \frac{2}{3}\pi f_\nu} \qquad \ldots\ldots\ldots\ldots\ldots\ldots(37f)$$

where $\tilde{m} = \frac{m}{\rho R^3}$ is the mass ratio.

Case (aii) Torsional oscillation

Adopting a procedure similar to the above leads to the following results for the frequency equation:-

$$\Omega^2 = \frac{\frac{16}{3}GR^3}{J + J_c} \qquad \ldots\ldots\ldots\ldots\ldots\ldots(38)$$

where J is the polar inertia of the rigid body, and the correction medium inertia $J_c = f_\nu J_{HS}$ .....(38a)

where $J_{HS} = \frac{4\pi}{15}\rho R^5$ is the polar inertia of the hemisphere of the medium and $f_\nu = \frac{2}{3\pi}$ which is independent of Poisson's ratio since the medium is free from dilatation for this mode of vibration.

In terms of the non-dimensional inertia $\tilde{J} = \frac{J}{\rho R^5}$, equation (38) reduces to

$$\eta_2^2 = \frac{16}{3\left(\tilde{J} + \frac{8}{45}\right)} \qquad \ldots\ldots\ldots\ldots\ldots\ldots(38b)$$

7.5.2. Rigid rectangular body

Case (bi) Vertical translation

In this case it is found, in a manner similar to that of case (ai) that the natural frequency is given by:-

$$\Omega^2 = \frac{2\pi G\left(1 - \beta_1^2\right)}{m + m_c} \qquad \ldots\ldots\ldots\ldots\ldots\ldots(39)$$

where $m_c = f_\nu m_{SC}$ and $f_\nu = 1\tfrac{1}{2}\beta_1^4 - 2\beta_1^2 + 1\tfrac{1}{2}$ ..(39a)

and $m_{SC} = \frac{\pi}{2}\rho b^2$ is the mass per unit length of the semi-cylinder of the medium of radius equal to half the width of the rigid body; m is the mass of the rigid body per unit length.

In non-dimensional form, equation (39) reduces to

$$\eta_2^2 = \frac{2\pi\left(1 - \beta_1^2\right)}{\tilde{m} + \frac{\pi}{2} f_\nu} \qquad \ldots\ldots\ldots\ldots\ldots\ldots(39b)$$

where $\tilde{m} = \frac{m}{\rho b^2}$ is the mass ratio.

Case (bii) Rocking mode

The results corresponding to those in case (bi) are:-

$$\Omega^2 = \frac{\pi G b^2\left(1 - \beta_1^2\right)}{J + J_c + \frac{Wh}{\Omega^2}} \qquad \ldots\ldots\ldots\ldots\ldots\ldots(40)$$

where $J_c = f_\nu J_{SC}$ and $f_\nu = \tfrac{3}{8}\beta_1^4 - \tfrac{1}{2}\beta_1^2 + \tfrac{3}{8}$ ...(40a)

and $J_{SC} = \frac{\pi}{4}\rho b^4$ is the polar inertia per unit length of the semi-cylinder of the medium about the axis of rock, having a radius equal to half the width of the rigid body. Furthermore, J is the inertia, per unit length, of the rigid body about the same axis of rock; W is the weight per unit length and h is the distance of the centre of gravity from the axis of rock.

In terms of the non-dimensional inertia $\tilde{J} = \frac{J + Wh/\Omega^2}{\rho b^4}$, equation (40) becomes

$$\eta_2^2 = \frac{\pi(1 - \beta_1^2)}{\tilde{J} + \frac{\pi}{4} f_\nu} \qquad \text{.....(40b)}$$

7.6. Graphical presentation and use of the solution

The effect of Poisson's ratio, ν, of the elastic medium upon the natural frequency can be estimated from this analysis. This is shown in figure 2 for the four cases, as graphs of the correction factor f_ν against Poisson's ratio. The effect is most marked for motion in translation as was to be expected.

Although these results have been derived from a first approximation solution, the graphs of figure 2 together with equations (37f), (38b), (39b) and (40b) form a convenient and perfectly adequate means for calculating the natural frequencies of vibration for the modes considered. This solution is found, by checking with the complete solution given later, to be accurate when the resonant frequency factor is small (less than about 0.5) which is the case for rigid bodies of large mass or inertia ratios (greater than about 20).

The solution in this chapter is also verified in Chapter 10 by comparison with the experimental results of Arnold et al (1955).

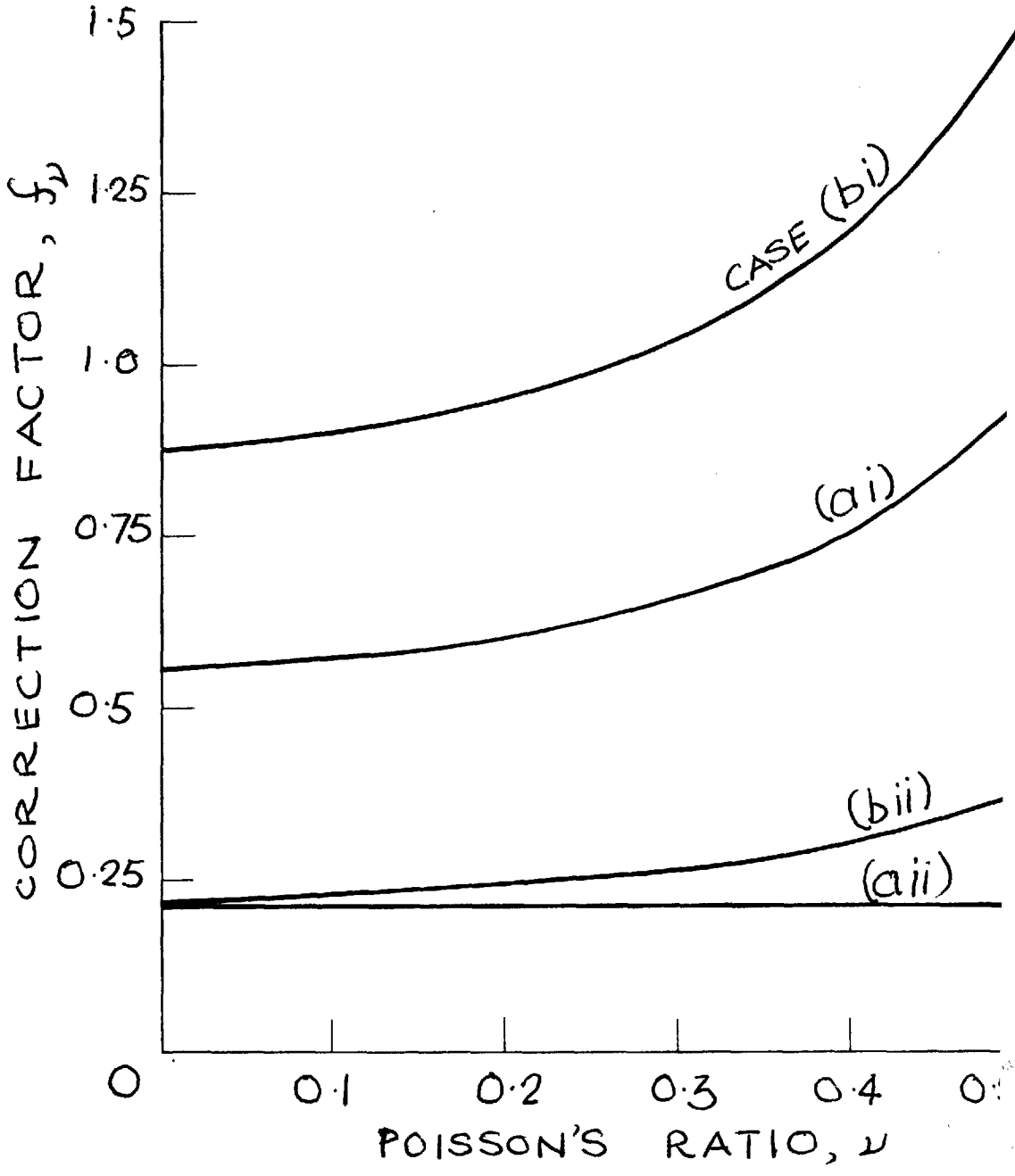


FIGURE 2: EFFECT OF POISSON'S RATIO UPON THE CORRECTION FACTOR FOR MEDIUM INERTIA

CHAPTER 8

CONTOUR INTEGRATION ANALYSIS OF CERTAIN INFINITE INTEGRALS REQUIRED IN THE COMPLETE SOLUTION .

8.1. The integrals for the rigid circular body, vertical translation

It will be seen in the next chapter that we require the solution of the general class of infinite integrals

$$I = \int_0^\infty \frac{\alpha_1 \psi(\eta)}{\phi(\eta)} d\eta .$$

which is a sum of the two integrals:

$$I_s = \int_0^\infty \frac{\alpha_1 \psi_s(\eta) \sin\eta}{\phi(\eta)} d\eta . \quad \text{where } \psi_s(\eta) \text{ is an even function (of } \eta$$

and $I_c = \int_0^\infty \frac{\alpha_1 \psi_c(\eta) \cos\eta}{\phi(\eta)} d\eta .$ where ψ_c is an odd function of η

so that $\psi(\eta) = \psi_s(\eta)\sin\eta + \psi_c(\eta)\cos\eta$ is an odd function of η.

8.1.1. Contour of integration

The integrals I_s and I_c can be derived from the single integral

$$J = \int_{\Gamma_1} \frac{\alpha_1}{\phi(\eta)} \psi(\eta) e^{i\eta} d\eta .$$

taken round a suitable contour Γ_1.

It is convenient to choose after Lamb (1904) the rectangular contour Γ_1 shown in figure 3. However, it is of no consequence if the infinitely distant parts of the contour are replaced by a semi-circular arc of infinite radius

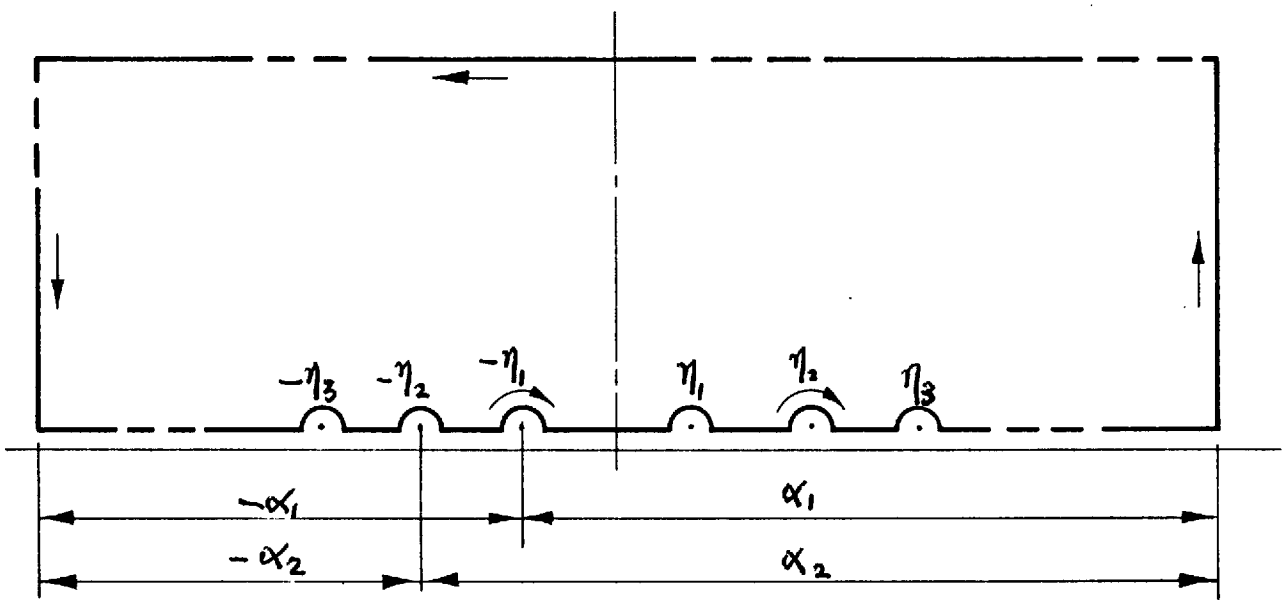


FIGURE 3 : THE CONTOUR Γ_1

since the contribution to the integral J along the infinitely distant path in each case can be shown to be zero. The singularities at the branch-points $(\pm\eta_1,0)$, $(\pm\eta_2,0)$ and at the Rayleigh poles $(\pm\eta_3,0)$- which are the principal roots of the equation $\phi(\eta) = 0$ - are by-passed by very small semi-circular indentations. Consistent signs corresponding to the principal values of the double-valued functions

$$\alpha_1(\eta) = \left(\eta^2-\eta_1^2\right)^{\frac{1}{2}}$$
$$\alpha_2(\eta) = \left(\eta^2-\eta_2^2\right)^{\frac{1}{2}}$$

which occur in the Rayleigh function $\phi(\eta)$ are shown in figure 3.

8.1.2. The contour integration

It is convenient to introduce the 'conjugate' of $\phi(\eta)$ which is denoted by $\bar{\phi}(\eta)$, i.e.

$$\phi(\eta) = \left(2\eta^2 - \eta_2^2\right)^2 - 4\eta^2\left(\eta^2 - \eta_1^2\right)^{\frac{1}{2}}\left(\eta^2 - \eta_2^2\right)^{\frac{1}{2}}$$
$$\bar{\phi}(\eta) = \left(2\eta^2 - \eta_2^2\right)^2 + 4\eta^2\left(\eta^2 - \eta_1^2\right)^{\frac{1}{2}}\left(\eta^2 - \eta_2^2\right)^{\frac{1}{2}}$$

so that

$$\phi(\eta)\bar{\phi}(\eta) = \left(2\eta^2 - \eta_2^2\right)^4 - 16\eta^4\left(\eta^2 - \eta_1^2\right)\left(\eta^2 - \eta_2^2\right) \quad \ldots\ldots(41)$$

Considering now the integral J taken round the above contour, it can be shown by Cauchy's residue theorem that, in addition to the infinitely distant parts of the contour, the contributions from each of the small semi-circles round the branch-points is zero. Since there are no poles within and on the contour, Cauchy's first theorem gives:

$$J = \int_{\Gamma_1} \frac{\alpha_1\bar{\phi}(\eta)}{\phi(\eta)} e^{i\eta} d\eta. = 0 \quad \ldots\ldots\ldots(42)$$

As the only contribution to J now comes from the path along the real axis and the semi-circles round the Rayleigh poles $(\pm\eta_3,0)$, we have

$$\int_{-\infty}^{-\eta_2} \frac{-\alpha_1 \psi_e e^{i\eta}}{\phi(\eta)} d\eta . + \int_{-\eta_2}^{-\eta_1} \frac{-\alpha_1 \psi_e e^{i\eta}}{\bar{\phi}(\eta)} d\eta . + \int_{-\eta_1}^{\infty} \frac{\alpha_1 \psi_e e^{i\eta} d\eta}{\phi(\eta)} . + \sum R = 0 \ldots (4$$

where the integrals are readily understood to be with respect to the real variable and to assume their principal values in the Cauchy sense as the radii of the small semi-circles tend to zero. $\sum R$ denotes the contributions from the poles $(\pm\eta_3, 0)$. Equation (43) reduces to

$$\int_0^{-\infty} \frac{\alpha_1}{\phi(\eta)} \psi_e e^{i\eta} d\eta . + \int_0^{\infty} \frac{\alpha_1}{\phi(\eta)} \psi_e e^{i\eta} d\eta . = 2\int_0^{-\eta_1} \frac{\alpha_1}{\phi(\eta)} \psi_e e^{i\eta} d\eta .$$

$$+ 8\int_{-\eta_1}^{-\eta_2} \frac{\eta^2 \alpha_1^2 \alpha_2 \psi_e e^{i\eta}}{\phi(\eta)\bar{\phi}(\eta)} d\eta .$$

$$- \sum R \quad \ldots\ldots\ldots\ldots (44)$$

By putting $\psi = \psi_s$ which we recall is an even function of η, we deduce

$$I_s = \int_0^{\infty} \frac{\alpha_1 \psi_s(\eta)}{\phi(\eta)} \sin\eta d\eta .$$

$$= i\left\{\int_0^{\eta_1} \frac{\alpha_1 \psi_s}{\phi(\eta)} e^{-i\eta} d\eta . + 4\int_{\eta_1}^{\eta_2} \frac{\eta^2 \alpha_1^2 \alpha_2 \psi_s}{\phi(\eta)\bar{\phi}(\eta)} e^{-i\eta} d\eta . + \tfrac{1}{2}\sum R_s\right\} \ldots (45)$$

and putting $\psi = \psi_c$ which is an odd function of η,

$$I_c = \int_0^{\infty} \frac{\alpha_1 \psi_c(\eta)}{\phi(\eta)} \cos\eta d\eta .$$

$$= \int_0^{\eta_1} \frac{\alpha_1 \psi_c}{\phi(\eta)} e^{-i\eta} d\eta . + 4\int_{\eta_1}^{\eta_2} \frac{\eta^2 \alpha_1^2 \alpha_2 \psi_c}{\phi(\eta)\bar{\phi}(\eta)} e^{-i\eta} d\eta . - \tfrac{1}{2}\sum R_c \ldots (45a)$$

From a well-known relation in the calculus of residues,

$$R(\pm\eta_3) = -\pi i\left\{\frac{\alpha_1(\eta)\psi(\eta)e^{i\eta}}{\frac{\partial}{\partial\eta}\left[\phi(\eta)\right]}\right\}_{\eta=\pm\eta_3}$$

where the negative sign indicates that the semi-circles have been traversed in the clockwise direction.

Since $\frac{\partial}{\partial\eta}\phi(\eta)$ is an odd function of η, it can be readily shown that

$$\tfrac{1}{2}\sum(iR_s - R_c) = -\pi\frac{\alpha_1(\eta_3)}{\phi'(\eta_3)}\left\{\psi_c(\eta_3)\sin\eta_3 - \psi_s(\eta_3)\cos\eta_3\right\}$$

If we now add the system of free Rayleigh waves given by the residue of the integrand at the Rayleigh pole $\eta = \eta_3$

i.e. $$I_R = -\pi i\frac{\alpha_1(\eta_3)\psi(\eta_3)}{\phi'(\eta_3)} \qquad \text{.....(45b)}$$

and introduce the following relations:

$$\left.\begin{aligned}
\psi(\eta) &= \psi_s(\eta)\sin\eta + \psi_c(\eta)\cos\eta\\
\chi(\eta) &= \psi_c(\eta)\sin\eta - \psi_s(\eta)\cos\eta\\
\bar{\alpha}_1(\eta) &= (\eta_1^2 - \eta^2)^{\frac{1}{2}} \quad \text{for} \quad 0<\eta<\eta_1\\
\bar{\alpha}_2(\eta) &= (\eta_2^2 - \eta^2)^{\frac{1}{2}} \quad \text{for} \quad \eta_1<\eta<\eta_2
\end{aligned}\right\} \qquad \text{.....(46)}$$

we finally have, by adding equations (45) to (45b) and using the relations (46) that $\int_0^\infty \frac{\alpha_1(\eta)\psi(\eta)_d\eta}{\phi(\eta)}$.

$$= -\pi\frac{\alpha_1(\eta_3)\chi(\eta_3)}{\phi'(\eta_3)} + \int_0^{\eta_1}\frac{\bar{\alpha}_1(\eta)\chi(\eta)d\eta}{\phi(\eta)} + 4\int_{\eta_1}^{\eta_2}\frac{\eta^2\alpha_1^2\bar{\alpha}_2\chi(\eta)d\eta}{\phi(\eta)\,\bar{\phi}(\eta)}$$

$$+ i\left\{-\pi\frac{\alpha_1(\eta_3)\psi(\eta_3)}{\phi'(\eta_3)} + \int_0^{\eta_1}\frac{\bar{\alpha}_1(\eta)\psi(\eta)d\eta}{\phi(\eta)} + 4\int_{\eta_1}^{\eta_2}\frac{\eta^2\alpha_1^2\bar{\alpha}_2\psi(\eta)d\eta}{\phi(\eta)\,\bar{\phi}(\eta)}\right\} \qquad \text{.....(47)}$$

from which it will be observed that the real part can be computed from $\chi(\eta)$ while the imaginary part comes from the original function $\psi(\eta)$.

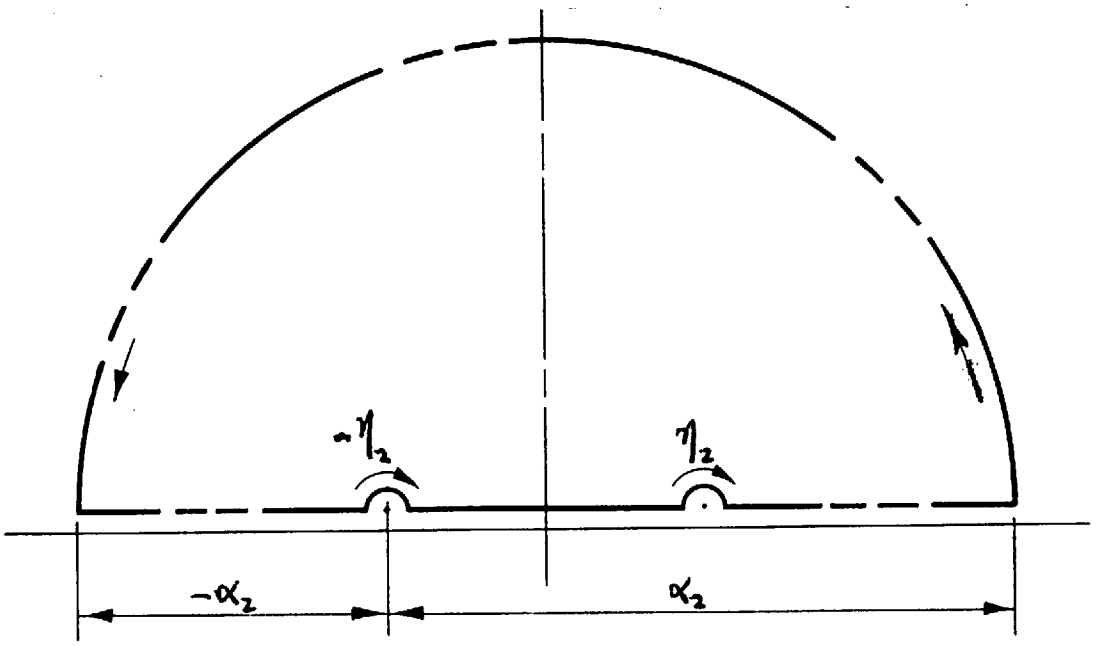


FIGURE 4 : THE CONTOUR Γ_2

8.2. The integrals for the rigid circular body, torsional oscillation.

The integral corresponding to the above case is

$$I' = \int_0^\infty \frac{\psi(\eta)\,d\eta}{(\eta^2-\eta_2^2)^{1/2}}$$ which is a sum of the integrals

$$I'_s = \int_0^\infty \frac{\psi_s(\eta)\sin\eta\,d\eta}{\alpha_2(\eta)}$$ where ψ_s is an even function of η

$$I'_c = \int_0^\infty \frac{\psi_c(\eta)\cos\eta\,d\eta}{\alpha_2(\eta)}$$ where ψ_c is an odd function of η.

8.2.1. Contour of integration

The contour chosen is similar to the above contour except for the fact that there is only a pair of semi-circular indentations corresponding to the branch-points $(\pm\eta_2,0)$ of the double-valued function $\alpha_2 = (\eta^2-\eta_2^2)^{1/2}$ as shown in figure 4.

That the medium is here free from dilatation is marked in figure 4 by the absence of the Rayleigh poles $(\pm\eta_3,0)$ of figure 3 and the branch-points $(\pm\eta_1,0)$ associated with the dilatational waves.

8.2.2. The contour integration

By taking the integral $J' = \int_{\Gamma_2} \frac{\psi(\eta)e^{i\eta}\,d\eta}{(\eta^2-\eta_2^2)^{1/2}}$ round the contour of figure 4 and noting that the contribution from either the large or small semi-circle is zero since, for the latter,

$$\lim_{\eta \to \eta_2} \left\{ \frac{\psi(\eta)e^{i\eta}}{\frac{\partial}{\partial\eta}\left[\eta^2-\eta_2^2\right]^{1/2}} \right\} = 0$$

we have, in the notation of the vertical translation analysis, the following final result corresponding to equation (47).-

$$\int_0^{\infty} \frac{\chi(\eta)d\eta.}{(\eta^2-\eta_2^2)^{\frac{1}{2}}} = -\int_0^{\eta_2} \frac{\chi(\eta)d\eta.}{\bar{\alpha}_2(\eta)} - i\int_0^{\eta_2} \frac{\chi(\eta)d\eta.}{\bar{\alpha}_2(\eta)} \quad \ldots.(48)$$

from which it is observed that the real part corresponds to the contribution to the integral for values of η from η_2 to ∞ while the imaginary part represents the contribution in the range $0<\eta<\eta_2$ as expected.

8.3. The integrals for the rigid rectangular body

Case (bi) Vertical translation

The required integrals take the form

$$I_c = \int_0^{\infty} \frac{\alpha_1(\eta)\chi(\eta)J_\nu(\eta)\cos(\eta x)d\eta.}{\phi(\eta)}$$

where $\chi(\eta)J_\nu(\eta)$ is an even function of η.

Case (bii) Rocking mode

In this case

$$I_s = \int_0^{\infty} \frac{\alpha_1(\eta)\chi(\eta)J_\nu(\eta)\sin(\eta x)d\eta.}{\phi(\eta)}$$

where $\chi(\eta)J_\nu(\eta)$ is here an odd function of η.

It should be noted that the integrands in both cases of the rigid rectangular body are even functions of η while the integral in the case of the vertical translation of the rigid circular body is an odd function of η. This difference calls for a modification of the contour of figure 3 as shown below.

8.3.1. Contours of integration

Figure 5 shows the contours required for the evaluatio of the above integrals. The upper contour - Γ_3 - is, in effect, a modification of the contour Γ_1 of figure 3 with

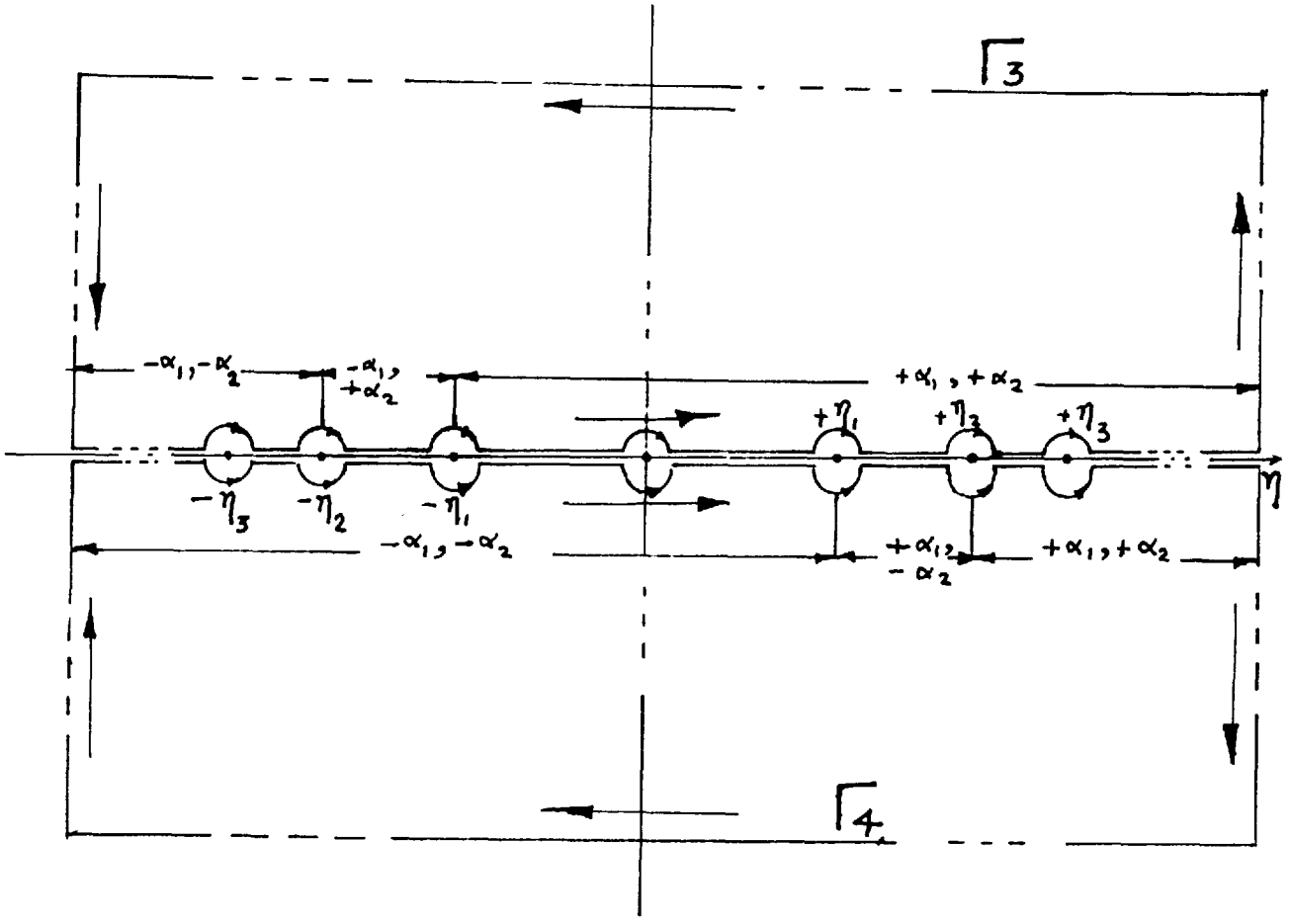


FIGURE 5 — THE PAIR OF CONTOURS Γ_3 AND Γ_4

an additional semi-circular indentation at the origin. The contour Γ_4 in the lower half-plane is the image of Γ_3. Consistent signs of the double-valued functions α_1 and α_2 are also shown.

The semi-circles at the origin ensure that the integrand - which contains Bessel function of the second kind as will be seen in article 8.3.2. - is analytic throughout the domain of integration.

8.3.2. Contour integration

Both integrals I_c and I_s can be deduced from the single integral

$$I = \int_{-\infty}^{\infty} \frac{\alpha_1(\eta)\psi(\eta)J_\nu(\eta)e^{i\eta x}d\eta}{\phi(\eta)}.$$

It is convenient to replace $J_\nu(\eta)$ by its equivalent relation :-

$$J_\nu(\eta) = \tfrac{1}{2}\left[H^1_\nu(\eta) + H^2_\nu(\eta)\right]$$

where H_ν denotes Bessel function of the third kind or Hankel function. It is to be noted that the introduction of this functiom calls for the addition of the semi-circular indentations at the origin of figure 5 since the function tends to infinity at the origin

i.e.
$$H^1_\nu(\eta) = J_\nu(\eta) + iY_\nu(\eta)$$
$$H^2_\nu(\eta) = J_\nu(\eta) - iY_\nu(\eta)$$

and $\lim_{\eta \to 0} Y_\nu(\eta) = \infty$

where $Y_\nu(\eta)$ is Bessel function of the second kind. With the introduction of the Hankel functions, we can now write $I = I_1 + I_2$

where $I_1 = \tfrac{1}{2}\int_{-\infty}^{\infty} \frac{\alpha_1(\eta)\psi(\eta)H^1_\nu(\eta)e^{i\eta x}d\eta}{\phi(\eta)}$ and $I_2 = \tfrac{1}{2}\int_{-\infty}^{\infty} \frac{\alpha_1(\eta)\psi(\eta)H^2_\nu(\eta)e^{i\eta x}d$

It can be shown that I_1 and I_2 can be evaluated when the integrals

$$J_1 = \int_{\Gamma_3} \frac{\alpha_1 \psi(\eta) H_\nu^1(\eta) e^{i\eta x} d\eta}{\phi(\eta)}.$$

and

$$J_2 = \int_{\Gamma_4} \frac{\alpha_1 \psi(\eta) H_\nu^2(\eta) e^{i\eta x} d\eta}{\phi(\eta)}.$$

are taken round the contours in the upper and lower half-planes respectively. It will be noted that in the upper half-plane $0 \leqslant \arg \eta \leqslant \pi$ and in the lower half-plane $-\pi \leqslant \arg \eta \leqslant 0$. Also, it can beshown that the contributions to the above integrals come only from the paths along the real axis and the semi-circles round the Rayleigh poles.

Therefore, we have, after a few reductions and in a manner similar to the case of the rigid circular body, vertical translation, that the above contour integration gives

$$2\int_0^\infty \frac{\alpha_1 \psi(\eta) J_\nu(\eta) e^{i\eta x} d\eta}{\phi(\eta)} - \int_0^\infty \frac{\alpha_1 \psi(-\eta)}{\phi(\eta)} \left[H_\nu^1(-\eta) + H_\nu^2(-\eta) \right] e^{-i\eta x} d\eta.$$

$$= 2\int_0^{\eta_1} \frac{\alpha_1}{\phi(\eta)} \left[-\psi(-\eta) H_\nu^1(-\eta) e^{-i\eta x} + \psi(\eta) H_\nu^2(\eta) e^{i\eta x} \right] d\eta.$$

$$+ 8 \int_{\eta_1}^{\eta_2} \frac{\eta^2 \alpha_1^2 \alpha_2}{\phi(\eta) \bar{\phi}(\eta)} \left[-\psi(-\eta) \frac{H_\nu^1(-\eta)}{e^{i\eta x}} + \psi(\eta) H_\nu^2 e^{i\eta x} \right] d\eta.$$

$$- \sum (R_1 + R_2) \qquad \ldots\ldots\ldots\ldots\ldots\ldots\ldots\ldots\ldots\ldots (49)$$

where $\sum (R_1 + R_2)$ denotes the contributions from the Rayleigh poles.

In order to simplify equation (49), we make use of the following relations from Watson (article 3.62):-

$$H_\nu^1(ze^{m\pi i}) = \frac{\sin(1-m)\nu\pi}{\sin(\nu\pi)} H_\nu^1(z) - \frac{e^{-\nu\pi i} \sin(m\nu\pi)}{\sin(\nu\pi)} H_\nu^2(z)$$

and $$H_\nu^2(ze^{m\pi i}) = \frac{\sin(1+m)\nu\pi}{\sin(\nu\pi)} H_\nu^2(z) + \frac{e^{\nu\pi i} \sin(m\nu\pi)}{\sin(\nu\pi)} H_\nu^1(z)$$

which are seen to be indeterminate for integral values of ν.

However, using de l'Hospital's rule, it is easily shown from these relations that

$$H_\nu^1(-\eta) = -H_\nu^2(\eta) \quad \text{for even values of } \nu$$
$$= H_\nu^2(\eta) \quad \text{for odd values of } \nu$$
$$\text{and } H_\nu^2(-\eta) = -H_\nu^1(\eta) \quad \text{for even values of } \nu$$
$$= H_\nu^1(\eta) \quad \text{for odd values of } \nu$$

8.3.2.1. Vertical translation

When the above relations are now introduced in equation (49) and it is remembered that for this case $\psi(\eta)J_\nu(\eta)$ is even, it is found that equation (49) reduces to

$$\int_0^\infty \frac{\alpha_1\psi(\eta)}{\phi(\eta)}J_\nu(\eta)\cos(\eta x)d\eta = \int_0^{\eta_1}\frac{\alpha_1\psi(\eta)}{\phi(\eta)}H_\nu^2\cos(\eta x)d\eta + 4\int_{\eta_1}^{\eta_2}\frac{\eta^2\alpha_1^2\alpha_2\psi(\eta)}{\phi(\eta)\bar{\phi}(\eta)}H_\nu^2(\eta)\cos(\eta x)d\eta - \tfrac{1}{4}\sum(R_1+R_2) \qquad \text{.....(49a)}$$

Noting that the contour Γ_4 is traversed in the positive (counter-clockwise) direction and Γ_3 in the negative direction and using the relation

$$H_\nu^1(\eta) - H_\nu^2(\eta) = 2iY_\nu(\eta)$$

we find from Cauchy's residue theorem that

$$\sum(R_1+R_2) = \frac{4\pi\alpha_1(\eta_3)\psi(\eta_3)Y_\nu(\eta_3)\cos(\eta_3 x)}{\phi'(\eta_3)}$$

and equation (49a) then reduces to

$$\int_0^\infty \frac{\alpha_1\psi(\eta)}{\phi(\eta)}J_\nu(\eta)\cos(\eta x)d\eta = -i\pi\frac{\alpha_1(\eta_3)\psi(\eta_3)}{\phi(\eta_3)}H_\nu^2(\eta_3)\cos(\eta_3 x) + \int_0^{\eta_1}\frac{\alpha_1\psi(\eta)}{\phi(\eta)}H_\nu^2(\eta)\cos(\eta x)d\eta + 4\int_{\eta_1}^{\eta_2}\frac{\eta^2\alpha_1^2\alpha_2}{\eta_1\phi(\eta)\bar{\phi}(\eta)}\psi(\eta)H_\nu^2(\eta)\cos(\eta x)d\eta \qquad \text{.....(49b)}$$

where the free Rayleigh waves have already been superimposed on equation (49a) in the same manner as in the case of the rigid circular body, vertical translation.

By resolving equation (49b) into its real and imaginary parts, we finally obtain:-

$$\int_0^{\infty} \frac{\alpha_1 \psi(\eta) J_\nu(\eta)}{\phi(\eta)} \cos(\eta x)\, d\eta = -\frac{\pi \alpha_1(\eta_3) \psi(\eta_3) Y_\nu(\eta_3)}{\phi'(\eta_3)} \cos(\eta_3 x)$$

$$+ \int_0^{\eta_1} \frac{\bar{\alpha}_1 \psi(\eta) Y_\nu(\eta)}{\phi(\eta)} \cos(\eta x)\, d\eta + 4 \int_{\eta_1}^{\infty} \frac{2\eta^2 \alpha_1^2 \bar{\alpha}_2 \psi(\eta) Y_\nu(\eta)}{\phi(\eta)\bar{\phi}(\eta)} \cos(\eta x)\, d\eta$$

$$-i \left[\frac{\alpha_1(\eta_3) \psi(\eta_3) J_\nu(\eta_3)}{\phi(\eta_3)} \cos(\eta_3 x) - \int_0^{\eta_1} \frac{\bar{\alpha}_1 \psi(\eta) J_\nu(\eta)}{\phi(\eta)} \cos(\eta x)\, d\eta \right.$$

$$\left. - 4 \int_{\eta_1}^{\infty} \frac{2\eta^2 \alpha_1^2 \bar{\alpha}_2 \psi(\eta) J_\nu(\eta)}{\phi(\eta)\bar{\phi}(\eta)} \cos(\eta x)\, d\eta \right] \qquad \text{.....(50)}$$

where, in a manner analogous to the case of the circular body, the real part comes from $Y_\nu(\eta)\psi(\eta)$ and the imaginary part is obtained from the original function $J_\nu(\eta)\psi(\eta)$.

8.3.2.2. Case (bii) Rocking mode

If the above procedure is repeated with the opposite condition that $\psi(\eta)J_\nu(\eta)$ is an odd function of η, it is found that the solution for

$$I_s = \int_0^{\infty} \frac{\alpha_1 \psi(\eta) J_\nu(\eta)}{\phi(\eta)} \sin(\eta x)\, d\eta.$$

is exactly the same as in equation (50) with the only exception that every cosine term is replaced by the corresponding sine term.

8.4. Evaluation of the finite integrals

The preceding articles show that the purpose of the contour integrations is to reduce the infinite integrals to a sum of finite integrals and residue terms.

The rest of the evaluation is accomplished by splittin the finite integrals into a sufficient number of intervals that would make the application of Simpson's rule to be accurate to three significant figures. Also, the Bessel functions are to be replaced by their equivalent power series so that the final results are in terms of a power series of the frequency factor η_2 and the spacial variables r(for the circular body) and x (for the rectangular body). This procedure is given in fuller details in the next chapter.

CHAPTER 9

SUCCESSIVE APPROXIMATIONS AND THE COMPLETE SOLUTION

9.1. The damping effect of wave dispersion in a semi-infinite elastic medium

It was stated in article 7.1. that the first approximation solution would yield infinitely large amplitudes at the resonant frequency factors. This is, of course, physically incorrect as with a semi-infinite medium, dispersion of elastic waves away from the source of the motion will occur. The energy associated with this dispersion will never return since there are no boundaries to reflect the waves.

This dispersion of waves has the same effect as damping in limiting the motion at resonance. It will here be referred to as dispersion damping in which no energy is actually dissipated into heat to distinguish it from thermal damping in which an energy conversion does occur. This latter type of damping is not taken into account in this analysis but is discussed in general comments later.

Dispersion damping can be allowed for by considering the terms in quadrature (the imaginary) arising from the poles and branch-points of the Rayleigh function. The rest of this chapter is, therefore, devoted to the complete analysis which includes the quadrature components of stress and displacement.

9.2. An outline of the general procedure in the successive approximations

In this article, a procedure will be derived for solving the main equations (22) to (25) including the quadrature terms taking as a starting point the solution of the first approximation - chapter 7.

The non-dimensional form of equations (22) to (25) can be written as

$$\left.\begin{aligned} \int_0^\infty \frac{\alpha_1 F(\eta)}{\phi(\eta)} J_\nu(\eta\tilde{r})d\eta. &= g(\tilde{r}) \qquad 0<\tilde{r}<1 \\ \int_0^\infty F(\eta) J_\nu(\eta\tilde{r})d\eta. &= 0 \qquad \tilde{r}>1 \end{aligned}\right\} \ldots\ldots(51)$$

except for the case of the torsional oscillation of the rigid circular body in which the function $\frac{\alpha_1}{\phi(\eta)}$ is replaced by $\frac{1}{\alpha_2}$.

Suppose that in equations (51)

$$F(\eta) = F_{11}(\eta) + F_{12}(\eta) \qquad \ldots\ldots\ldots\ldots(51a)$$

where $F_{11}(\eta)$ is the solution corresponding to the first approximation i.e. $F_{11}(\eta)$ satisfies the pair of equations:

$$\left.\begin{aligned} \int_0^\infty \frac{F_{11}(\eta)}{A(\eta)} J_\nu(\eta\tilde{r})d\eta. &= g(\tilde{r}) \qquad 0<\tilde{r}<1 \\ \int_0^\infty F_{11}(\eta) J_\nu(\eta\tilde{r})d\eta. &= 0 \qquad \tilde{r}>1 \end{aligned}\right\} \ldots\ldots(51b)$$

where $A(\eta)$ is the series expansion given in equation (31a), in its non-dimensional form.

Substituting equation (51a) in equation (51) leads to the following pair of equations for the determination of $F_{12}(\eta)$.

$$\left.\begin{aligned} \int_0^\infty \frac{\alpha_1 F_{12}(\eta)}{\phi(\eta)} J_\nu(\eta\tilde{r})d\eta. &= g(\tilde{r}) - \epsilon_{11}(\tilde{r}) \qquad 0<\tilde{r}<1 \\ \int_0^\infty F_{12}(\eta) J_\nu(\eta r)d\eta. &= 0 \qquad \tilde{r}>1 \end{aligned}\right\} \ldots(52)$$

where $\epsilon_{11}(\tilde{r}) = \int_0^\infty \frac{\alpha_1 F_{11}(\eta)}{\phi(\eta)} J_\nu(\eta\tilde{r})d\eta.$ is now a known function of $\tilde{r}$.

If we put $F_{12}(\eta) = F_{22}(\eta) + F_{23}(\eta)$ .....(52a)

where $F_{22}(\eta)$ is the solution of the pair of equations :-

$$\left.\begin{aligned} \int_0^\infty \frac{F_{22}(\eta)}{A(\eta)} J_\nu(\eta\tilde{r})d\eta. &= g(\tilde{r}) - \epsilon_{11}(\tilde{r}) \quad 0<\tilde{r}<1 \\ \int_0^\infty F_{22}(\eta)J_\nu(\eta\tilde{r})d\eta. &= 0 \qquad\qquad \tilde{r}>1 \end{aligned}\right\} ..(52b)$$

then $F_{23}(\eta)$ can be obtained, after the substitution of equation (52a) in equations (52), from the pair of equations:-

$$\left.\begin{aligned} \int_0^\infty \frac{\alpha_1 F_{23}(\eta)}{\phi(\eta)} J_\nu(\eta\tilde{r})d\eta. &= g(\tilde{r}) - \epsilon_{11}(\tilde{r}) - \epsilon_{22}(\tilde{r}) \quad 0<\tilde{r}<1 \\ \int_0^\infty F_{23}(\eta)J_\nu(\eta\tilde{r})d\eta. &= 0 \qquad\qquad \tilde{r}>1 \end{aligned}\right\} ..(53)$$

The pattern of the procedure is now obvious and we generalise the solution of $F(\eta)$ by

$$F(\eta) = \sum_{k=1}^{\infty} F_{kk}(\eta) \qquad .....(54)$$

where $F_{kk}(\eta)$ is to be determined from the pair of equations:-

$$\left.\begin{aligned} \int_0^\infty \frac{F_{kk}(\eta)}{A(\eta)} J_\nu(\eta\tilde{r})d\eta. &= g(\tilde{r}) - \sum_{m=1}^{m=k-1} \epsilon_{mm}(\tilde{r}) \quad 0<\tilde{r}<1 \\ \int_0^\infty F_{kk}(\eta)J_\nu(\eta\tilde{r})d\eta. &= 0 \qquad\qquad \tilde{r}>1 \end{aligned}\right\} ..(54a)$$

where $\epsilon_{mm}(\tilde{r}) = \int_0^\infty \frac{\alpha_1 F_{mm}}{\phi(\eta)}(\eta)J_\nu(\eta\tilde{r})d\eta.$ $1 \leqslant m \leqslant k$ .....(54b)

and is a known function of $\tilde{r}$.

By evaluating equation (54b), we can solve equations (54a) in terms of the first approximation solution $F_{11}(\eta)$.

Remembering also that $F_{11}(\eta)$ is in itself an infinite series i.e.

$$F_{11}(\eta) = \sum_{j=1}^{\infty} F_j(\eta) \quad \ldots\ldots\ldots\ldots\ldots(55)$$

then thesolution of $F_{kk}(\eta)$ can be expressed as a function of $F_j(\eta)$.

The method of the above general analysis is now to be indicated by solving completely the present problems and it will be shown how $F_{kk}(\eta)$, for values of $k>2$, can be computed from a systematic scheme based on $F_{22}(\eta)$.

9.3. Complete sclution of the rigid circular body, vertical translation

9.3.1. Solution of $F_{22}(\eta)$

With k=2 in equations (54a), $F_{22}(\eta)$ is the solution of the pair of equations :-

$$\left.\begin{aligned} \eta_2^2 \int_0^{\infty} \frac{F_{22}(\eta)}{A(\eta)} J_0(\eta\tilde{r})d\eta. &= c - \epsilon_{11}(\tilde{r}) \quad 0<\tilde{r}<1 \\ \int_0^{\infty} F_{22}(\eta) J_0(\eta\tilde{r})d\eta. &= 0 \qquad\qquad \tilde{r}>1 \end{aligned}\right\} \ldots\ldots(56)$$

where $c = Gw_0$, $\epsilon_{11}(\tilde{r}) = \eta_2^2 \int_0^{\infty} \frac{\alpha_1 F_{11}(\eta)}{\phi(\eta)} J_0(\eta\tilde{r})d\eta$.

and from the solution of chapter 7,

$$F_{11}(\eta) = c\left\{\frac{2a_1}{\pi\Omega_2^2}\sin\eta + \frac{a_2R^2}{\Omega_2^2}\sqrt{\frac{2}{\pi}}\eta^{-\frac{1}{2}}J_{1\frac{1}{2}}(\eta) + \frac{a_3R^4}{3\Omega_2^2}\sqrt{\frac{2}{\pi}}\eta^{-1\frac{1}{2}}J_{2\frac{1}{2}}(\eta) + \ldots\right\} \quad \ldots\ldots\ldots(56a)$$

9.3.1.1. Use of contour integration of Chapter 8 in evaluating $\epsilon_{11}(\tilde{r})$

It is readily obvious that the integral expression for $\epsilon_{11}(\tilde{r})$ above belongs to the class of integrals discussed in article 8.1. in which

$$I = \int_0^\infty \frac{\alpha_1 \psi(\eta)}{\phi(\eta)} d\eta .$$

By comparing I with $\epsilon_{11}(\tilde{r})$, the latter can be evaluated by setting

$$\psi(\eta) = \eta^2 F_{11}(\eta) J_0(\eta \tilde{r})$$

In order to obtain the corresponding expression for $\chi(\eta)$ of equation (46), we determine ψ_s and $\psi_c(\eta)$ of article 8.1. from $F_{11}(\eta)$ by replacing the Bessel functions by their equivalent trigonometric functions i.e.

$$J_{1\frac{1}{2}}(\eta) = \sqrt{\frac{2}{\pi}} \eta^{-\frac{1}{2}} \left(\frac{\sin\eta}{\eta} - \cos\eta \right)$$

$$J_{2\frac{1}{2}}(\eta) = \sqrt{\frac{2}{\pi}} \eta^{-\frac{1}{2}} \left(\frac{3-\eta^2}{\eta^2} \sin\eta - \frac{3}{\eta} \cos\eta \right)$$

As stated in article 8.4., the finite integrals in equation (47) have been evaluated by splitting the intervals into sufficient number of strips to make Simpson's rule accurate to three significant figures. A preliminary procedure is to resolve the functions into their power series equivalents and to take the first few terms . The following new variable is also introduced:-

$$\zeta = \frac{\eta}{\eta_2}$$

by which the non-dimensional lengths are referred to η_2. It is then found that the finite integrals of equation (47) take the form:

$$I_1 = \int_0^{\beta_1} \frac{\sqrt{\beta_1^2 - \zeta^2}\, \zeta^m d\zeta}{\left(\frac{1}{2} - \zeta^2\right)^2 + \zeta^2 \sqrt{\left(\beta_1^2 - \zeta^2\right)\left(1 - \zeta^2\right)}} \qquad m=0,1,2,\ldots$$

$$I_2 = \int_{\beta_1}^1 \frac{\zeta^2 \sqrt{1 - \zeta^2}\left(\zeta^2 - \beta_1^2\right) \zeta^m d\zeta}{\left(\zeta^2 - \frac{1}{2}\right)^4 - \zeta^4 \left(\zeta^2 - \beta_1^2\right)\left(\zeta^2 - 1\right)} \qquad m=0,1,2,\ldots$$

These integrals have been evaluated for four values of Poisson's ratio : 0, ¼, 1/3 and ½ for which the corresponding values of β_1^2 are ½, 1/3, ¼ and 0 respectively. Further procedures for the case of zero Poisson's ratio are presented here as specimen since the experiments of Arnold et al(1955) with which this theory is compared in the next chapter were performed on foam rubber of negligible Poisson's ratio, as the elastic medium. Hence the integrals reduce to :

$$I_1 = \int_0^{\frac{1}{\sqrt{2}}} \frac{\sqrt{\tfrac{1}{2} - \zeta^2}\,\zeta^m d\zeta}{\left(\tfrac{1}{2} - \zeta^2\right)^2 + \zeta^2\sqrt{\left(\tfrac{1}{2} - \zeta^2\right)\left(1 - \zeta^2\right)}}$$

$$I_2 = \int_{\frac{1}{\sqrt{2}}}^{1} \frac{\zeta^2\sqrt{1 - \zeta^2}\left(\zeta^2 - \tfrac{1}{2}\right)\zeta^m d\zeta}{\left(\zeta^2 - \tfrac{1}{2}\right)^4 - \zeta^4\left(\zeta^2 - \tfrac{1}{2}\right)\left(\zeta^2 - 1\right)}$$

In I_1 put $\zeta = \frac{1}{\sqrt{2}}\sin\theta$ and in I_2 put $\zeta = \sin\theta$, then the integrals reduce to :-

$$I_1 = 2^{1-m/2}\int_0^{\pi/2} \frac{\sin^m\theta d\theta}{\cos^2\theta + \sin^2\theta(1 + \sec 2\theta)^{\frac{1}{2}}}$$

$$I_2 = \int_{\pi/4}^{\pi/2} \frac{\sin^m\theta d\theta}{\sin^2\theta - \tfrac{1}{8}\sec^2\theta\,\mathrm{cosec}^2\theta\cos^3(2\theta)}$$

and, with this simplification, the rest of the evaluation is accomplished by the application of Simpson's rule.

In order to evaluate the residue terms of equation (47), we need to determine the Rayleigh pole $(\eta_3, 0)$ of the integrand i.e. the principal root of the equation $\phi(\eta)=0$ which, again, for the case of zero Poisson's ratio is:

$$(\zeta^2 - \tfrac{1}{2})^2 - \zeta^2(\zeta^2 - \tfrac{1}{2})^{\frac{1}{2}}(\zeta^2 - 1)^{\frac{1}{2}} = 0 \quad \ldots\ldots\ldots (57)$$

It is easily seen that a pair of roots is $\zeta^2 = \tfrac{1}{2}$, factorising and solving the resulting quadratic in ζ^2 the other roots are found to be $\zeta^2 = \tfrac{1}{4}(3 \pm \sqrt{5})$. However, after Rayleigh (1885) it can be shown that the only root corresponding to the principal values of the radicals is that for which $\zeta \geq 1$ i.e. on the contour of figure 3, $\eta_3 > \eta_2 > \eta_1$

Accordingly, the principal roots of equation (57) are

$$\zeta^2 = \pm \tfrac{1}{4}(3 + \sqrt{5}) \quad \text{or} \quad \zeta = \pm 1.144$$

Finally, taking only the first two terms of $J_o(\eta \tilde{r})$, it is found that the above analysis leads to the following expression, for the case of zero Poisson's ratio :-

$$\epsilon_{11}(\tilde{r}) = Gw_o \left\{ \left[\left(1 - 0.875\eta_2^2 + 0.120\eta_2^4 - 0.015\eta_2^6\right) + \tfrac{1}{4}\left(0.959\eta_2^4 - 0.105\eta_2^6\right)\tilde{r} \right. \right.$$
$$\left. \left. -i\eta_2 \left[\left(0.864 - 0.410\eta_2^2 + 0.0224\eta_2^4\right) - \tfrac{1}{4}\left(0.954\eta_2^2 - 0.465\eta_2^4\right)\tilde{r}^2 \right] \right.$$

in which higher order quantities are negligible and therefore not included.

9.3.1.2. Solution of a class of dual integral equations related to $F_{22}(\eta)$.

When the above expression for $\epsilon_{11}(\tilde{r})$ is inserted in equation (56), we notice that the solution for $F_{22}(\eta)$ is of order η_2^2 in the real part and of order η_2 in the imaginary part as should be expected. Also, we are involved in the solution of the pair of equations, considering only the dominant term of the series $A(\eta)$:

$$\left.\begin{aligned}\int_0^\infty \frac{F_{22}^b(\eta)}{a_1\eta} J_0(\eta\tilde{r})d\eta. &= \tilde{r}^2 \qquad 0 \leq \tilde{r} < 1\\ \int_0^\infty F_{22}^b(\eta) J_0(\eta\tilde{r})d\eta. &= 0 \qquad \tilde{r} > 1\end{aligned}\right\} \ldots\ldots\ldots(58)$$

where, for convenience, the coefficients of $\tilde{r}^2$, which are only functions of η_2, have been omitted.

It is here noted that the conditions of the Busbridge solution (equation (26b)) are violated by equations (58). However, these equations can be solved if we employ the same technique of using the operator $\mathcal{D}_\mu(r)$ - equation (31b) - to reduce equations (58) to a form amenable to solution by means of equation (26b). As the differential operation on equation (58) absorbs part of the solution of $F_{22}^b(\eta)$ since $\mathcal{D}_0(r)$ operating on a constant is zero, it can be shown that the complete solution of equations (58) is :-

$$F_{22}^b(\eta) = F_1(\eta) + \frac{32F_2(\eta)}{7\eta_2^2} \qquad \ldots\ldots\ldots\ldots(58a)$$

where $F_1(\eta)$ and $F_2(\eta)$ are the first two terms in the expansion of $F_{11}(\eta)$ - then, with negligible errors of order η_2^6, we can approximate $F_1(\eta) = F_{11}(\eta) - F_2(\eta)$.

It is found from the foregoing analyses that the solution of $F_{22}(\eta)$ is given by

$$F_{22}(\eta) = \gamma_{11}F_{11}(\eta) + \delta_{11}F_2(\eta) \qquad \ldots\ldots\ldots\ldots(59)$$

where, again for the case of zero Poisson's ratio,

$$\gamma_{11} = 0.875\eta_2^2\left(1-0.412\eta_2^2+0.0469\eta_2^4\right)+i0.864\eta_2\left(1-0.751\eta_2^2+0.16\eta\right)$$

$$\delta_{11} = -0.875\eta_2^2\left(1.25-0.412\eta_2^2+0.0297\eta_2^4\right)+ i0.864\eta_2\left(-1.26+0.892\eta_2^2 -0.135\eta_2^4\right)$$

9.3.2. Solution of $F_{33}(\eta)$

By putting k = 3 in equation (54a), we obtain the equations for $F_{33}(\eta)$. It is clear from the solution of $F_{22}(\eta)$ in equation (59) that we need to evaluate

$$\epsilon_2(r) = \eta_2^2 \int_0^{\infty} \frac{\alpha_1 F_2(\eta)}{\phi(\eta)} J_0(\eta \tilde{r}) d\eta .$$

which is part of the solution of $\epsilon_{11}(\tilde{r})$ and can, therefore, be written down by inspection. It is found that

$$\epsilon_2(\tilde{r}) = -Gw_0 \left\{ \begin{array}{l} \left[0.440\eta_2^2 - 0.0964\eta_2^4 + 0.0066\eta_2^6 \right) \\ \left. -\tfrac{1}{4}\left(0.878\eta_2^2 + 0.443\eta_2^4 - 0.115\eta_2^6\right)\tilde{r}^2 \right] \\ +i\eta_2 \left[\left(-0.253\eta_2^2 + 0.0279\eta_2^4\right) + \tfrac{1}{4}\left(0.279\eta_2^4\right)\tilde{r}^2 \right] \end{array} \right\}$$

and after some reductions, the solution of $F_{33}(\eta)$ is found to be

$$\begin{aligned} F_{33}(\eta) &= \left(\kappa_{11}^2 + \delta_{11}\kappa\right) F_{11}(\eta) + \left(\gamma_{11}\delta_{11} + \xi\delta_{11}\right) F_2(\eta) \\ &= \gamma_{22} F_{11}(\eta) + \delta_{22} F_2(\eta) \qquad \ldots\ldots\ldots\ldots\ldots (59a) \end{aligned}$$

where $\kappa = 0.875\eta_2^2\left(0.252 - 0.236\eta_2^2 + 0.0405\eta_2^4\right)$
$+ i0.864\eta_2\left(-0.239\eta_2^2 + 0.113\eta_2^4\right)$

$\xi = -0.875\eta_2^2\left(0.330 - 0.276\eta_2^2 + 0.033\eta_2^4\right)$
$+ i0.864\eta_2\left(0.382\eta_2^2 - 0.081\eta_2^4\right)$

It should be noted that equation (59a) gives explicitly how γ_{22} and δ_{22} can be calculated from γ_{11} and δ_{11}.

9.3.3. Expression for the general term $F_{kk}(\eta)$

With the determination of κ, ξ, γ_{11} and δ_{11} of equations (59) and (59a), we can obtain directly $F_{44}(\eta)$, $F_{55}(\eta)$ .....from the general relation:-

$$F_{kk}(\eta) = \left(\gamma_{11}\gamma_{k-2,k-2} + \kappa\delta_{k-2,k-2}\right)F_{11}(\eta) + \left(\gamma_{11}\delta_{k-2,k-2} + \xi\delta_{k-2,k-2}\right)F_2(\eta) \qquad k>2$$

$$= F_{11}(\eta)\,\gamma_{k-1,k-1} + F_2(\eta)\,\delta_{k-1,k-1} \quad \ldots\ldots(59b)$$

which shows that $\gamma_{k-1,k-1}$ and $\delta_{k-1,k-1}$ can be readily computed from a systematic scheme based on κ, ξ, δ_{11} and γ_{11} of equations (59) and (59a).

9.3.4. Expression for the required stress transform $F(\eta)$

Finally, from equation (54), the transform of the required stress function expressed in terms of the non-dimensional variable η, is given by

$$F(\eta) = \sum_{k=1}^{\infty} F_{kk}(\eta)$$

$$= F_{11}(\eta) + \sum_{k=2}^{\infty} F_{kk}(\eta)$$

and substituting for $F_{kk}(\eta)$ from equation (59b),

$$F(\eta) = \left[1 + \sum_{m=1}^{\infty}\gamma_{mm}\right]F_{11}(\eta) \left[\sum_{m=1}^{\infty}\delta_{mm}\right]F_2(\eta)$$

remembering also that $F_{11}(\eta) = F_1(\eta) + F_2(\eta) + F_3(\eta) + O(\eta_2^6)$ we finally have, with very negligible errors of order η_2^6

$$F(\eta) = \left[1 + \sum_{m=1}^{\infty} mm\right]F_1(\eta) + \left[1 + \sum_{m=1}^{\infty}\left(\gamma_{mm} + \delta_{mm}\right)\right]F_2(\eta) + \left[1 + \sum_{m=1}^{\infty}\gamma_{mm}\right]F_3(\eta) \quad \ldots\ldots(60)$$

9.3.5. Use of equation (60) in deriving complete solution from first approximation solution

The interpretation of equation (60) is obvious when it is remembered that $F_1(\eta)$, $F_2(\eta)$, $F_3(\eta)$ are the first three terms of the first approximation solution of

chapter 7 corresponding to static or first component of stress, the inertia or second component of stress and the relatively small third component of stress.

In order to derive the complete solution of any expression from the first approximation solution, it is only required to write out the first three terms of the corresponding expression in the first approximation solution and multiply them by the factors which are the coefficients of $F_{1,2,3}(\eta)$ respectively in equation (60). This important procedure is indicated in the next article.

9.35.1 The complete equation of forced vibrations

The equation of forced vibrations, using the approximate solution of chapter 7 is, correct to the third term and for the case of zero Poisson's ratio :

$$\left[4 - (m + 1.167)\eta_2^2 - 0.025\eta_2^4\right] GR\hat{w}_o = \hat{F} \quad \ldots\ldots(61)$$

where $\hat{F}$ is the amplitude of the harmonic exciting force. We notice that the terms 4, $-1.167\eta_2^2$ and $-0.025\eta_2^4$ are due to the first three terms of $F_{11}(\eta)$. Using the coefficients equation (60), we readily deduce the* vector equation of forced vibrations from equation (61) :

$$\left[1+\sum_{m=1}^{\infty}\gamma_{mm}\right]4 - \left\{\tilde{m} + \left[1 + \sum_{m=1}^{\infty}\left(\gamma_{mm} + \delta_{mm}\right)\right]1.167\right\}\eta_2^2 - \left[1+\sum_{m=1}^{\infty}\gamma_{mm}\right]0.025\eta_2^4$$

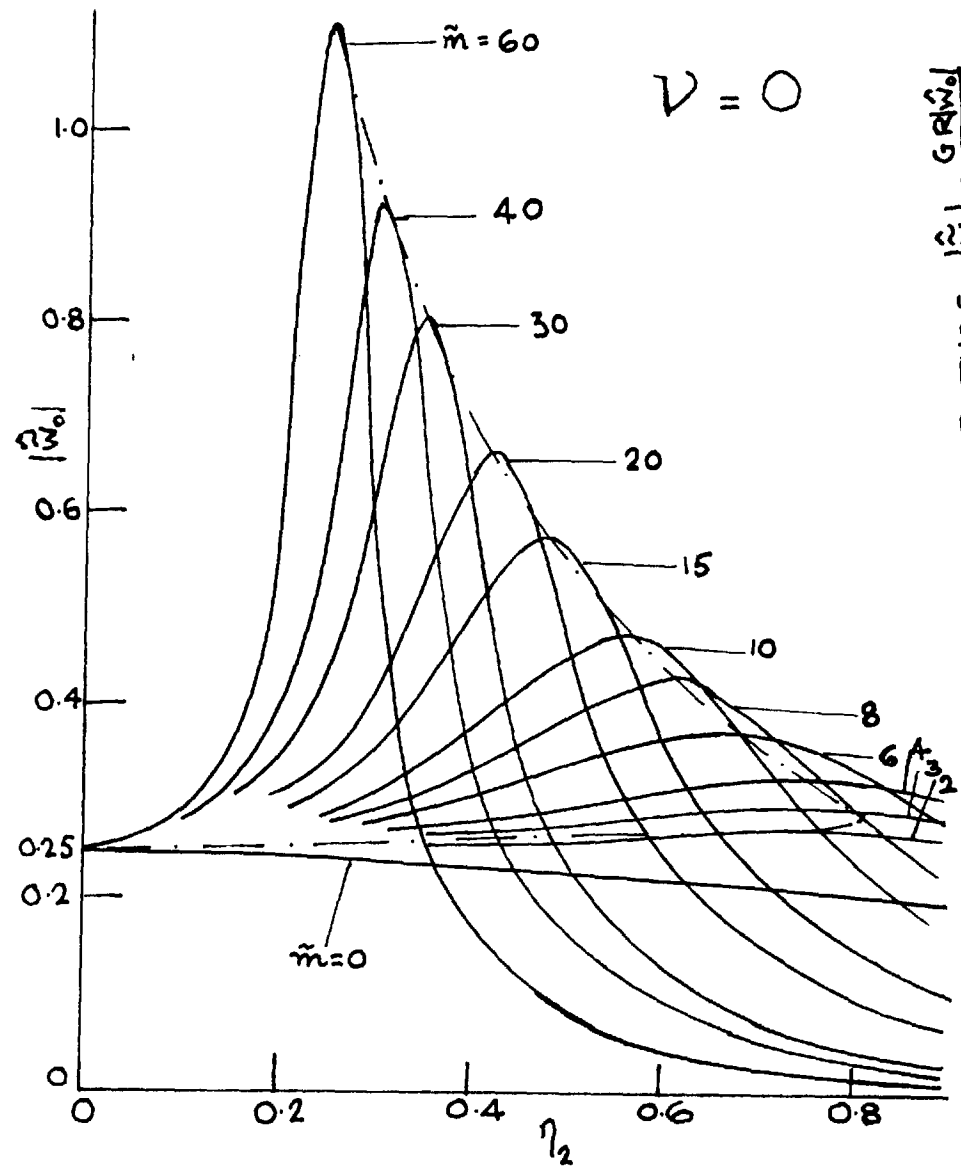
$$= \frac{\hat{F}}{GR\hat{w}_o} \quad \ldots\ldots(61a)$$

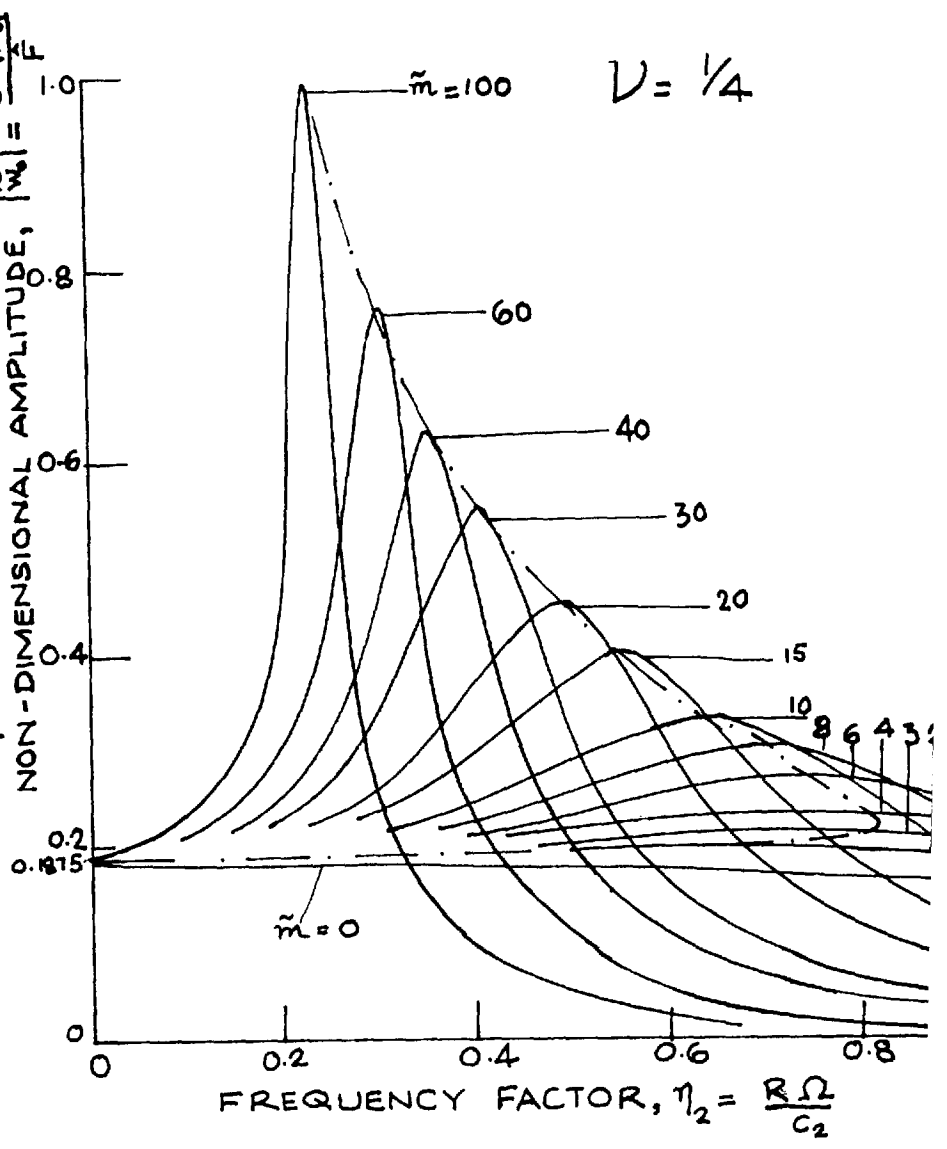
Hence, the non-dimensional amplitude $\frac{GR\hat{w}_o}{\hat{F}}$ is given by:

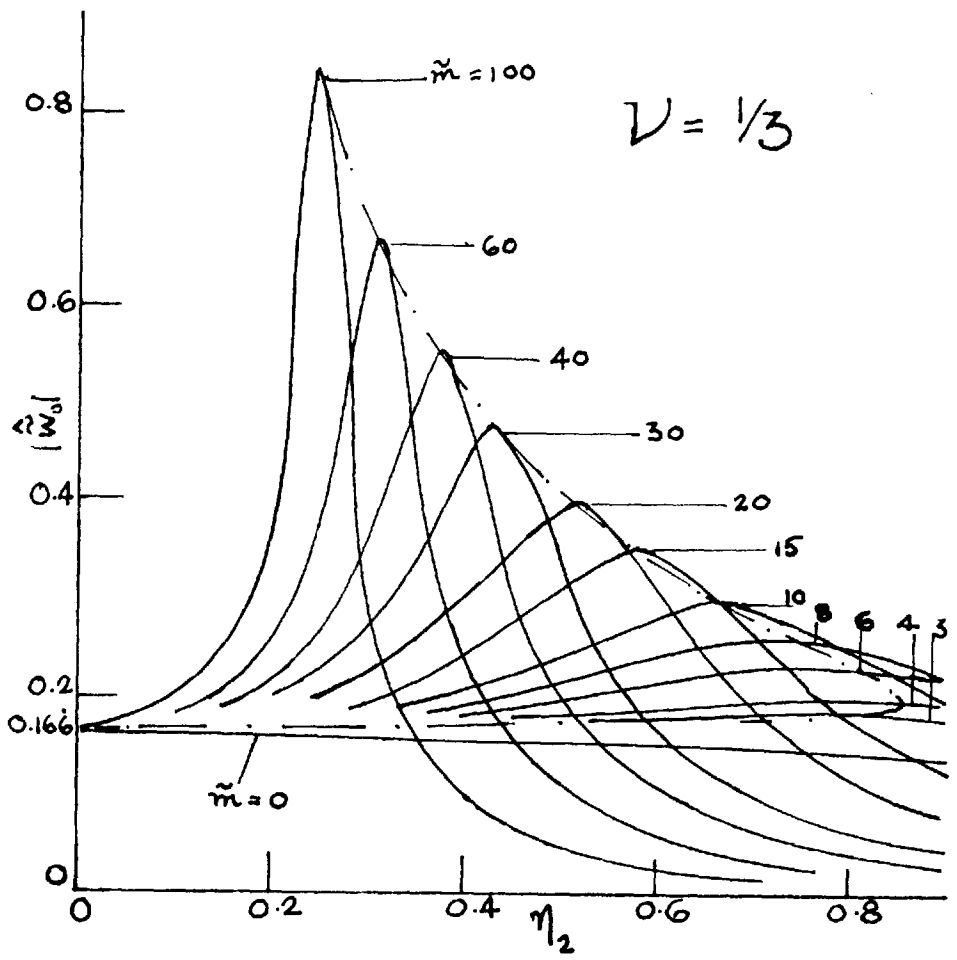
$$\tilde{\hat{w}}_o = \frac{1}{P + iQ} \quad \text{or} \quad |\tilde{\hat{w}}_o| = \frac{1}{\sqrt{(P^2 + Q^2)}} \quad \ldots\ldots(62)$$

---

* The use of 'vector' is appropriate since the coefficients γ_{mm} and δ_{mm} are complex quantities.







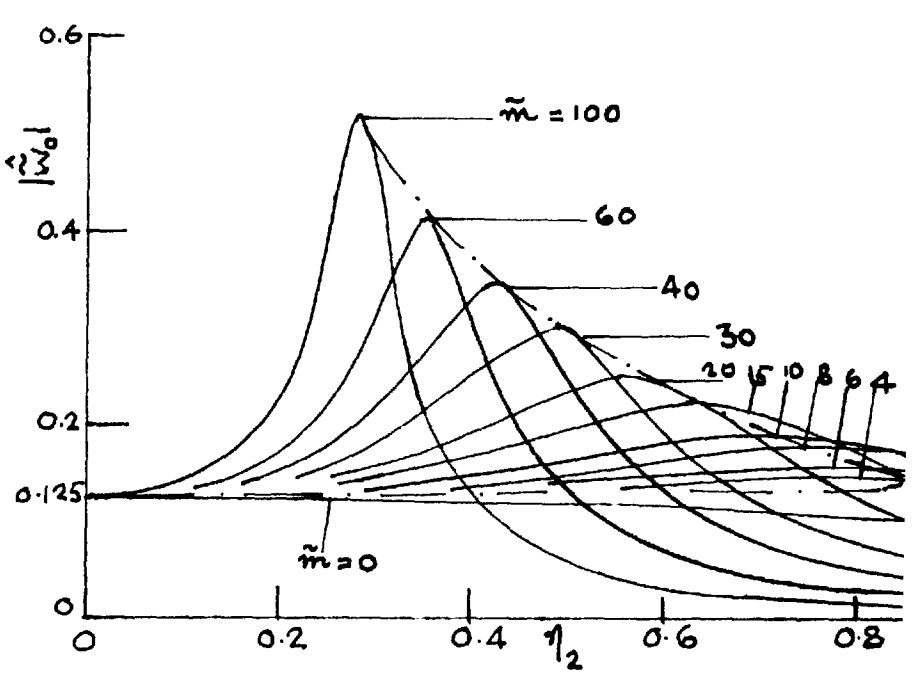


FIGURE 6 - RESONANCE CURVES AT CONSTANT MASS RATIO, $\tilde{m}$ & POISSON'S RATIO, ν FOR CASE (ai)
(RIGID CIRCULAR BODY, VERTICAL TRANSLATION)

and from a computation of γ_{mm} and δ_{mm} up to m=7, it is found, correct to three significant figures and with higher order quantities neglected, that P and Q are given by

$$\left.\begin{aligned} P &= 4 - (\tilde{m} + 1.167)\eta_2^2 + 3.50\eta_2^2\left(0.148 + 0.0347\eta_2^2\right) \\ Q &= 3.456\,\eta_2\left(1 + 0.0506\eta_2^2\right) . \end{aligned}\right\} \quad \ldots(62a)$$

The results expressed by equations (62) and (62a) are presented in Figure 6a for different values of the mass ratio, $\tilde{m}$ ranging from 0 to 100. Also, in the next chapter, these equations are used to derive the resonance curves of specified values of $\tilde{m}$ corresponding to the mass ratios of the rigid bodies used in the experiments by Arnold et al.

9.3.5.2 Complete solution of the dynamic stress distribution

The procedure described in article 9.3.5. has been adopted in the same manner as in article 9.3.5.1. to derive the complete solution of the dynamic stress distribution from the resultant stress distribution of the first approximation - equation (33e). Thus, using the first three terms of this equation

$$\sigma_{11}(r) = \sigma_1(r) + \sigma_2(r) + \sigma_3(r)$$

The complete solution is again a modification of this relation obtained by multiplying the first three components of stress by the corresponding factors given in equation (60).

The result of this procedure is given in graphical form in figures 8a and 8b in which the complete solution of the dynamic stress distribution has been resolved into in-phase and quadrature components.

9.3.6. Complete solutions for cases of Poisson's ratio = 1/4, 1/3 and 1/2

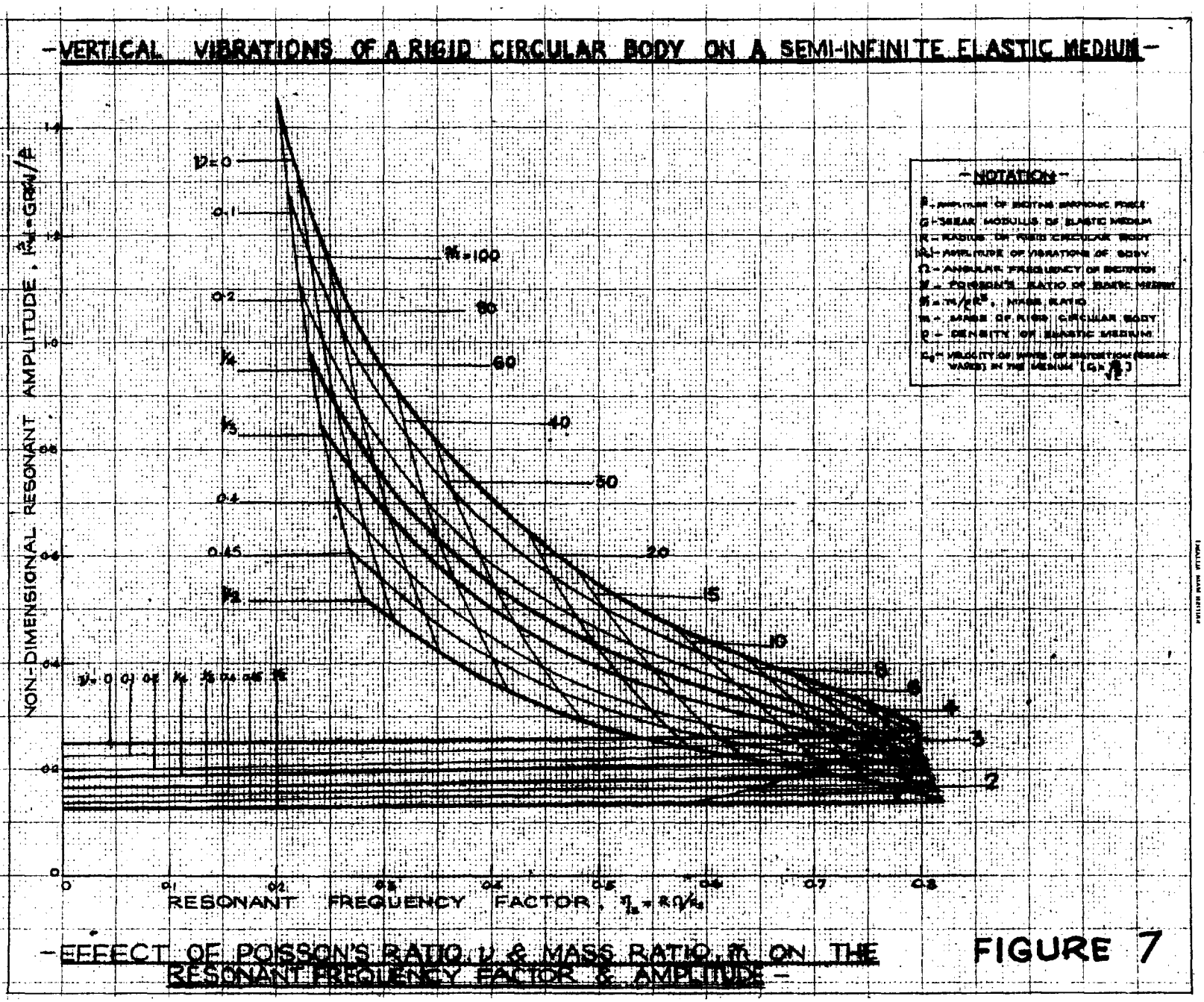
It is recalled here that the whole of the preceding complete solutions applies to the case of zero Poisson's ratio which has been chosen as a specimen of the computations

involved in this analysis. However, in order to cover the whole range of Poisson's ratio - which is 0 to 0.5 for engineering materials - the preceding procedures have been repeated for the three values of Poisson's ratio given above. For this purpose, it is only necessary to present the different values of the coefficients a_1, a_2 and a_3 of the first three terms in the expansion of equation (31a) ; the roots $(\pm\eta_3, 0)$ of the equation $\phi(\eta) = 0$ for the Rayleigh poles of figure 3 and, finally, the corresponding values of β_1 for the limits of integration in equation (47). These values are presented below in Table 1.

The complete solution for all FOUR values of Poisson's ratio are presented in graphical forms in figures 6,7 and 8. These curves are discussed in the next chapter.

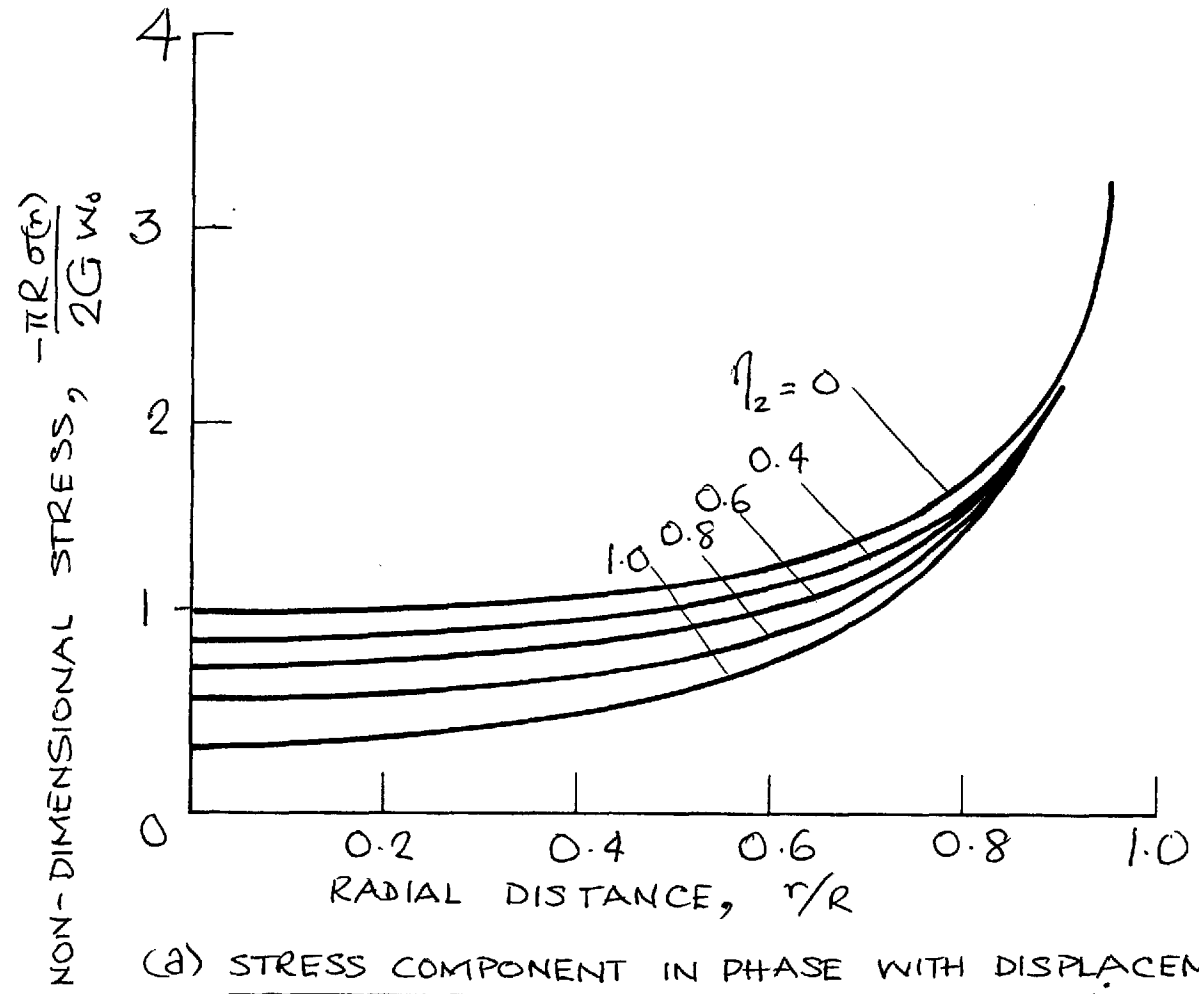
TABLE 1

ν	$\frac{a_1}{\Omega_2^2}$	$\frac{a_2}{\Omega_2^4}$	$\frac{a_3}{\Omega_2^6}$	$\frac{\eta_3}{\eta_2}$	β_1 :
0	-1	7/8	9/32	1.144	$1/2^{1/2}$
1/4	-4/3	1	8/27	1.088	$1/3^{1/2}$
1/3	-3/2	$\frac{35}{32}$	$\frac{77}{256}$	1.072	1/2
1/2	-2	3/2	1/4	1.047	0

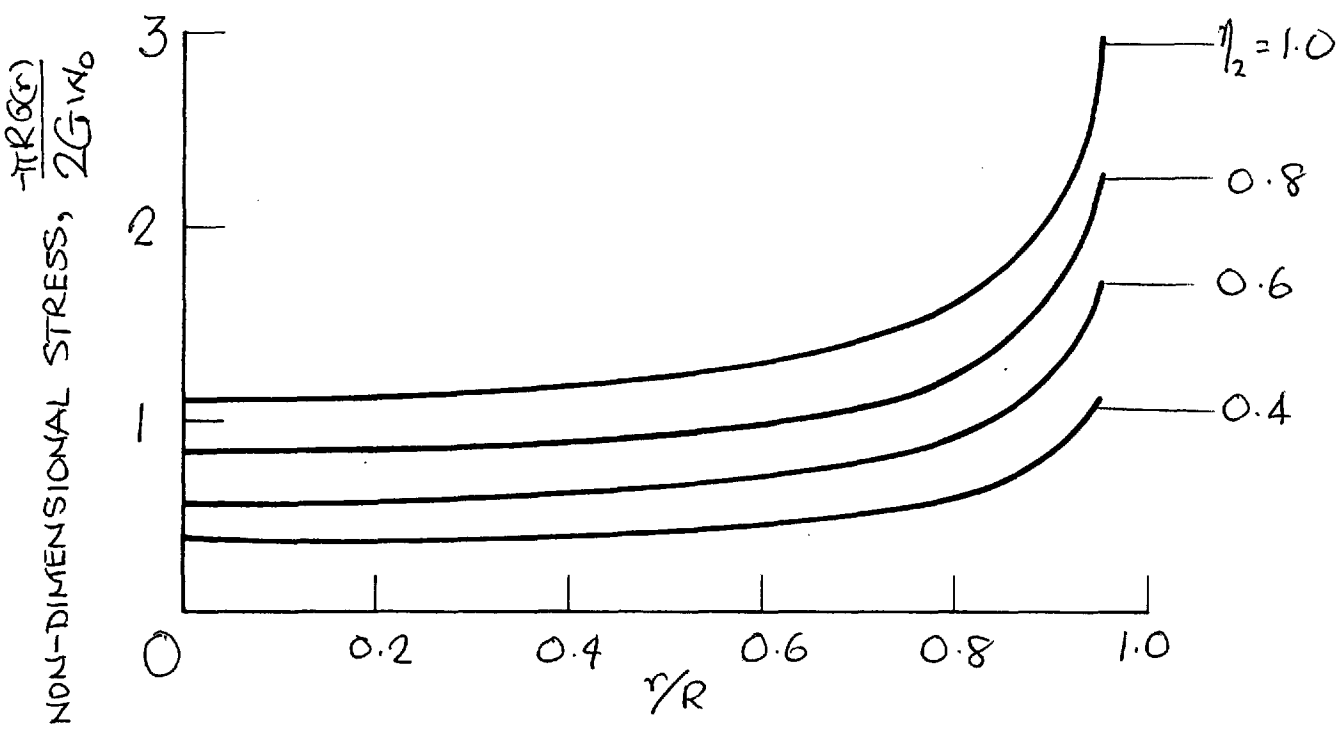


EFFECT OF POISSON'S RATIO ν & MASS RATIO β ON THE RESONANT FREQUENCY FACTOR & AMPLITUDE

FIGURE 7



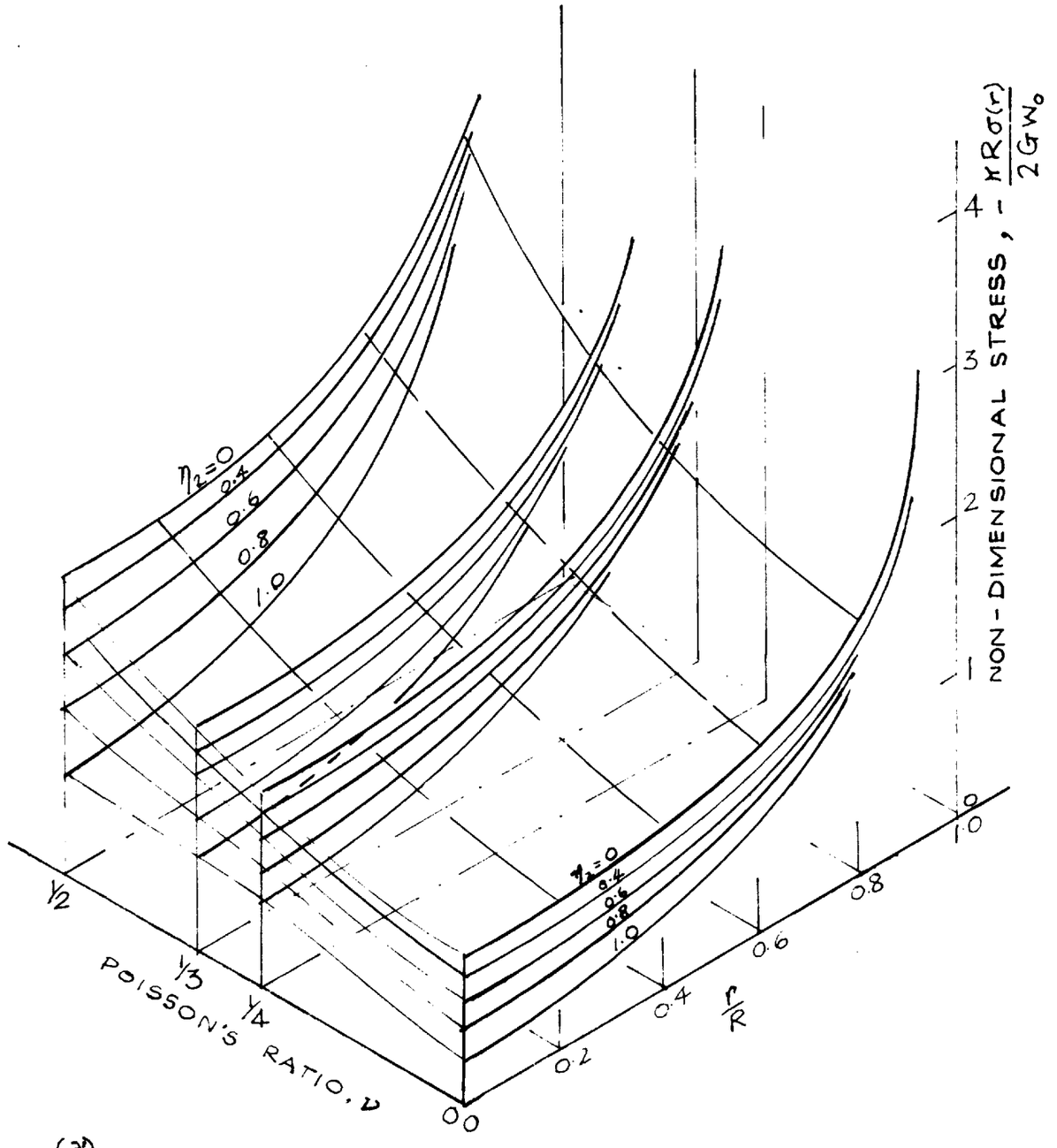
(a) STRESS COMPONENT IN PHASE WITH DISPLACEMENT



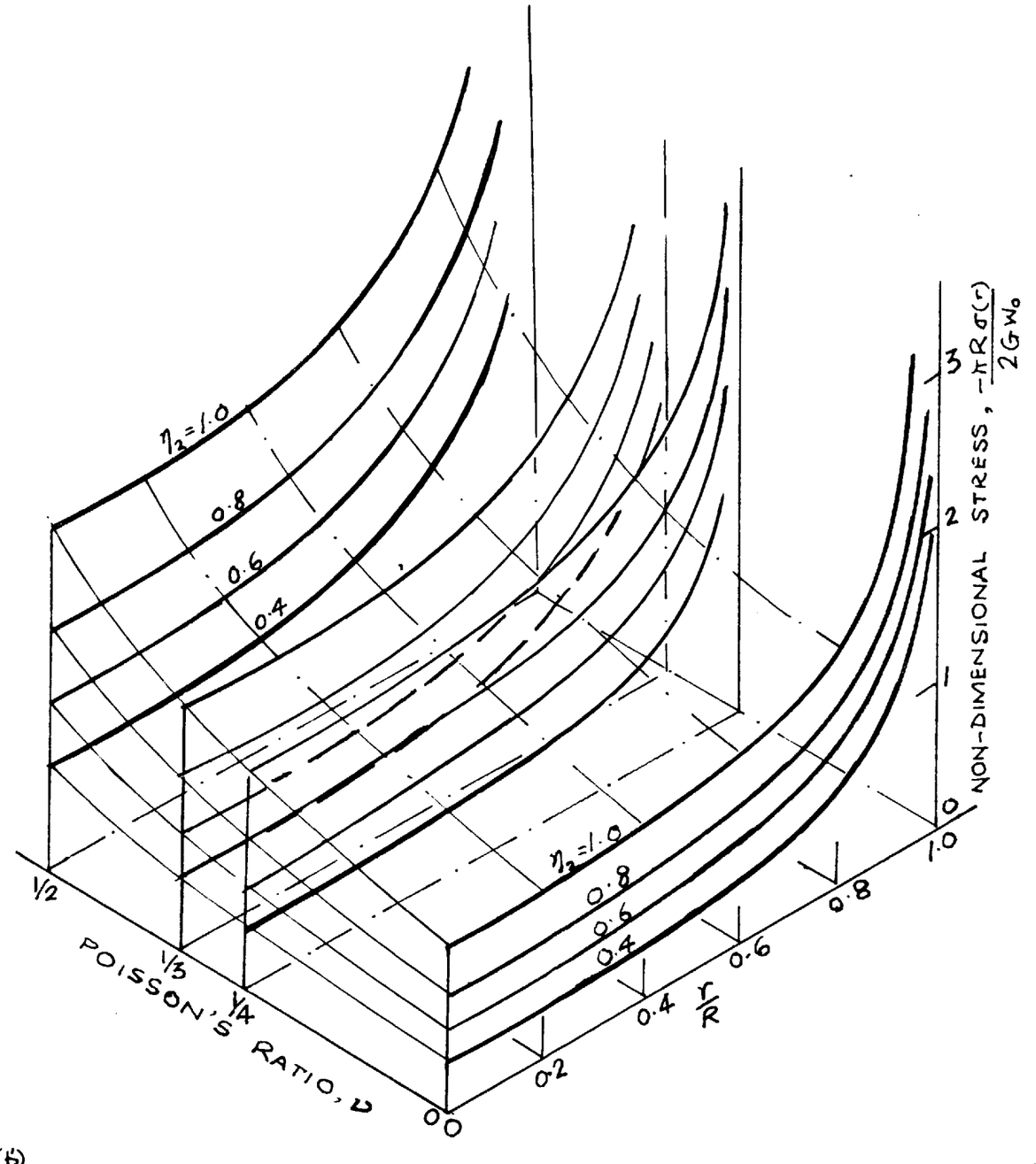
(b) STRESS COMPONENT IN QUADRATURE WITH DISPLACEMENT

FIGURE 8: STRESS DISTRIBUTION UNDER A RIGID CIRCULAR BODY IN VERTICAL TRANSLATION

(POISSON'S RATIO = 0)



(a) STRESS COMPONENT IN PHASE WITH DISPLACEMENT —



(b) STRESS COMPONENT IN QUADRATURE WITH DISPLACEMENT

FIGURE 8' – EFFECT OF POISSON'S RATIO & FREQUENCY FACTOR, η_2, UPON THE STRESS DISTRIBUTION UNDER A CIRCULAR RIGID BODY IN VERTICAL TRANSLATION - (CASE ai)

9.4. Complete solution of the rigid circular body, torsional oscillation

9.4.1. Solution of $F_{22}(\eta)$

Similar to the case of vertical translation, $F_{22}(\eta)$ is to be determined from the pair of equations :-

$$\left.\begin{aligned} \int_0^\infty \frac{F_{22}(\eta)}{B(\eta)} J_1(\eta\tilde{r})d\eta &= k\tilde{r} - \epsilon_{11}(\tilde{r}) \qquad 0<\tilde{r}<1 \\ \int_0^\infty F_{22}(\eta) J_1(\eta\tilde{r})d\eta &= 0 \qquad\qquad \tilde{r}>1 \end{aligned}\right\} \quad \ldots.(63)$$

where $B(\eta)$ is the non-dimensional form of the expansion in equation (31a) and $k = -GR\theta$.

Also, $$\epsilon_{11}(\tilde{r}) = \int_0^\infty \frac{F_{11}(\eta) J_1(\eta\tilde{r})d\eta}{\sqrt{\eta^2 - \eta_2^2}}.$$

where $$F_{11}(\eta) = -2\sqrt{\frac{2}{\pi}}\, GR\theta\left[\eta^{1/2} J_{1\frac{1}{2}}(\eta) - \frac{\eta_2^2}{6}\eta^{-1/2} J_{2\frac{1}{2}}(\eta) + \ldots\right]$$

which is obtained from the solution of chapter 7.

9.4.1.1. Expression for $\epsilon_{11}(\tilde{r})$

By taking the first two terms of $J_1(\eta\tilde{r})$ and using equation (48) of the contour integration analysis, it is found that

$$\epsilon_{11}(\tilde{r}) = k\tilde{r}\left\{\left[\left(1+0.167\eta_2^2-0.0573\eta_2^4+0.000870\eta_2^6\right) - \left(0.0182\eta_2^4-0.00585\eta_2^6\right)\tilde{r}^2\right] - i\frac{4\eta_2^3}{9\pi}\left[\left(1-0.113\eta_2^2+0.00440\eta_2^4\right) - \left(0.100\eta_2^2-0.0119\eta_2^4+0.000276\eta_2^6\right)\tilde{r}^2\right]\right\}$$

9.4.1.2. Solution of a class of dual integral equations related to $F_{22}(\eta)$

When $\epsilon_{11}(\tilde{r})$ is substituted in equation (63), it is obvious that we are involved in the solution of the pair of equations :-

$$\left.\begin{aligned} \int_0^{\infty} \frac{F_{22}^{b}(\eta)}{a_1\eta} J_1(\eta\tilde{r})d\eta. &= \tilde{r}^3 \qquad 0<\tilde{r}<1 \\ \int_0^{\infty} F_{22}^{b}(\eta) J_1(\eta\tilde{r})d\eta. &= 0 \qquad \tilde{r}>1 \end{aligned}\right\} \ldots\ldots\ldots(64)$$

Since a direct application of equation (26b) leads to the intractable integral

$$\int_0^1 y^{4\frac{1}{2}} J_{1\frac{1}{2}}(\eta y)dy.$$

we obtain a formal solution of equation (64) by applying the operator $\mathcal{D}_1(r)$ of equation (31b) from which it is found that

$$F_{22}^{b}(\eta) = F_1(\eta) + \frac{16}{\eta_2^2} F_2(\eta)$$

Finally, after some reductions, we obtain

$$F_{22}(\eta) = \gamma_{11} F_{11}(\eta) + \delta_{11} F_2(\eta) \ldots\ldots(65)$$

where $\gamma_{11} = \left[-0.167\eta_2^2\left(1-0.452\eta_2^2+0.0403\eta_2^4\right) + i\,\frac{4\eta_2^3}{9\pi}\left(1-0.213\eta_2^2+0.0163\eta_2^4\right) \right]$

$$\delta_{11} = \left[0.292\eta_2^2\left(1-0.383\eta_2^2+0.20\eta_2^4\right) - i\frac{64\eta_2^3}{90}\left(1-0.182\eta_2^2+0.0102\eta_2^4\right) \right]$$

9.4.2. Solution of $F_{33}(\eta)$, $F_{kk}(\eta)$ and the required $F(\eta)$

In a manner similar to that of the vertical translation, it is found that

$$F_{33}(\eta) = \left(\gamma_{11}^2 + \kappa\delta_{11}\right)F_{11}(\eta) + \left(\gamma_{11}\delta_{11} + \xi\delta_{11}\right)F_2(\eta)$$

$$= \gamma_{22}F_{11}(\eta) + \delta_{22}F_2(\eta) \quad \ldots\ldots\ldots\ldots\ldots\ldots(65a)$$

where it is found that

$$\kappa = 0.167\eta_2^2\left(0.125+0.0313\eta_2^2-0.00580\eta_2^4\right) - i\frac{4\eta_2^3}{9\gamma}\left(0.030\eta_2^2 - 0.00170\eta_2^4\right)$$

$$\xi = -0.167\eta_2^2\left(0.125+0.0625\eta_2^2-0.0469\eta_2^4\right) + i\frac{4\eta_2^3}{9\gamma}\left(0.0527-0.00650\eta_2^2+0.00020\eta_2^4\right)$$

Now that the basic quantities γ_{11}, δ_{11}, κ and ξ have been derived, the solutions of the general term $F_{kk}(\eta)$ and the required non-dimensional stress transform $F(\eta)$ follow exactly as in the case of the vertical translation.

9.4.3. Complete equation of forced vibrations

The equation of forced vibrations, deduced from equation (38b) of the first approximation solution is, correct to the first two terms of $F_{11}(\ )$:-

$$\left[\frac{16}{3} - \left(\tilde{J} + \frac{8}{45}\right)\eta_2^2\right] GR^3\hat{\theta} = \hat{T} \quad \ldots\ldots\ldots\ldots\ldots\ldots(66)$$

where $\hat{T}$ is the amplitude of the exciting harmonic torque.

As discussed in article 9.3.5., the complete equation of forced vibrations can be deduced from equation (66) using the computation of γ_{mm} and δ_{mm} for the present case. The final result for the non-dimensional amplitude $\tilde{\hat{\theta}} = \frac{GR^3\hat{\theta}}{\hat{T}}$

is found to be given by:

$$\hat{\tilde{\theta}} = \frac{1}{P + iQ} \quad \text{or} \quad |\hat{\tilde{\theta}}| = \frac{1}{\sqrt{(P^2+Q^2)}} \qquad .....(66a)$$

where $P = \frac{16}{3} - \left(\tilde{J} + \frac{8}{45}\right)\eta_2^2 - \frac{8}{9}\eta_2^2\left(1-0.630\eta_2^2+0.347\eta_2^4-0.193\eta_2^6 + 0.119\eta_2^8-0.0683\eta_2^{10}+0.0372\eta_2^{12}\right)$

$$Q = \frac{64\eta_2^3}{27\pi}\left(1-0.560\eta_2^2+0.325\eta_2^4-0.180\eta_2^6+0.103\eta_2^8 - 0.0524\eta_2^{10}+ 0.0370\eta_2^{12}\right)$$

It is recalled that the result is independent of Poisson's ratio so that there is only one family of resonance curves for different values of the inertia ratio $\tilde{J}$ as shown in figure 9.

The results of equation (66a) are also compared with the experimental results of Arnold et al(1955) for specified values of $\tilde{J}$ in chapter 10.

9.4.4. Complete solution of the dynamic stress distribution

The method of solution is, again, the same as described in article 9.3.5.2. for the case of vertical translation. The results are presented in a graphical form in figure 11.

9.5. Complete solution for the rigid rectangular body

9.5.1. Similarity between solution for the rectangular body and case (ai)

It is important to state that the procedure for the case of the rigid rectangular body (both vertical translation and rocking mode) is, in most details, the same as for the rigid circular body, vertical translation.

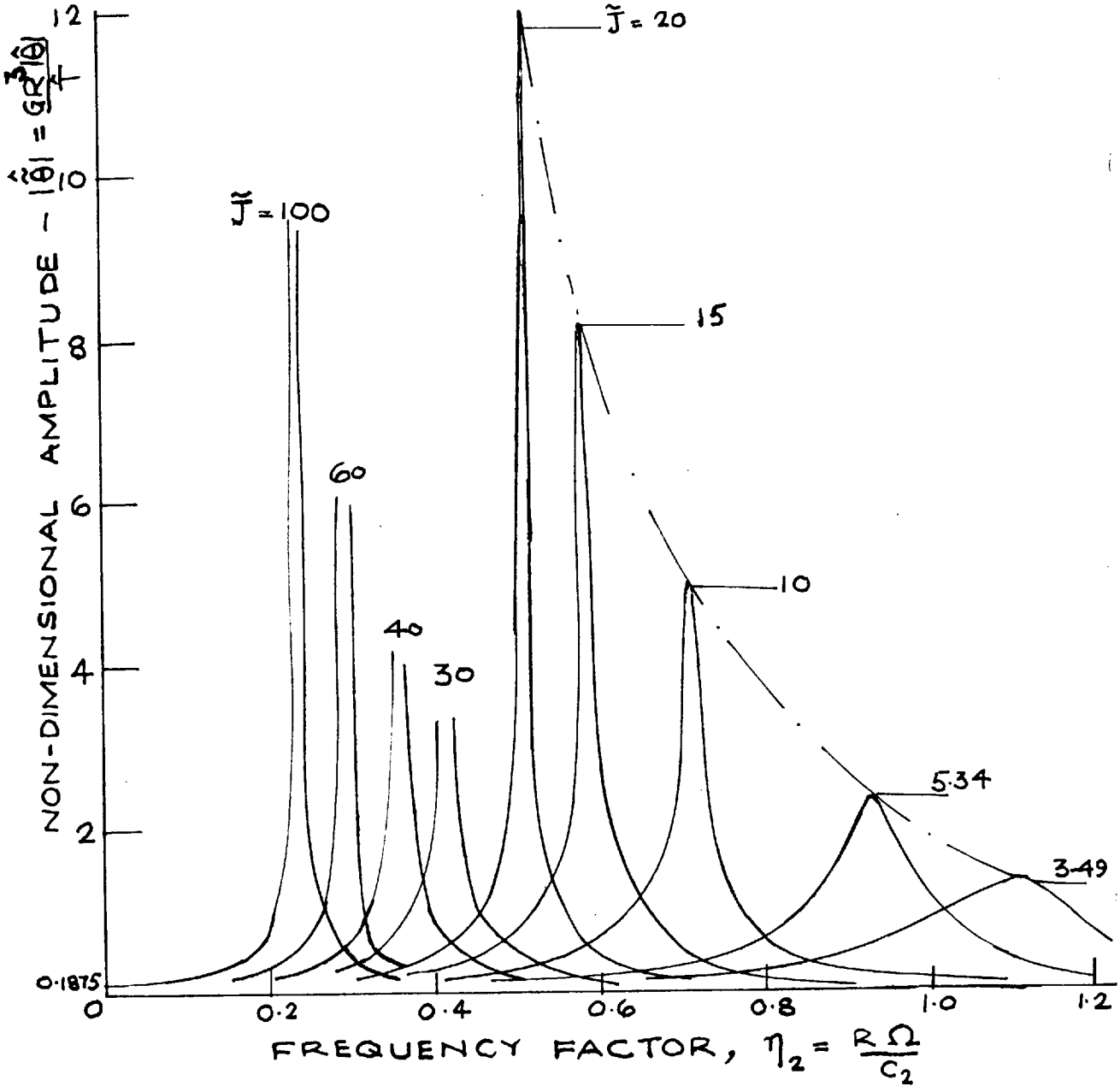


FIGURE 9 – RESONANCE CURVES AT CONSTANT INERTIA RATIO, $\tilde{J}$ FOR CASE (aii) – RIGID CIRCULAR BODY, TORSIONAL OSCILLATION.

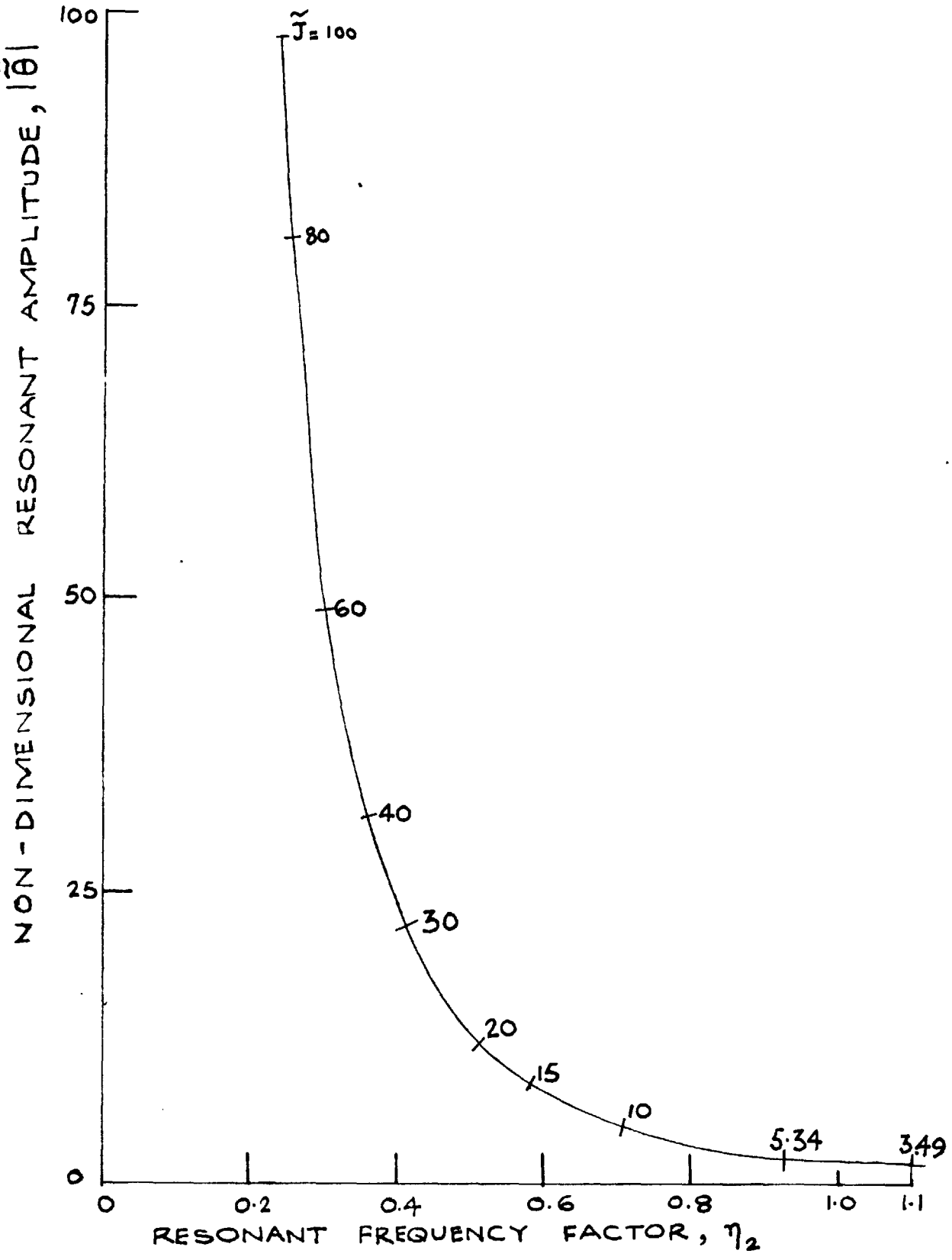
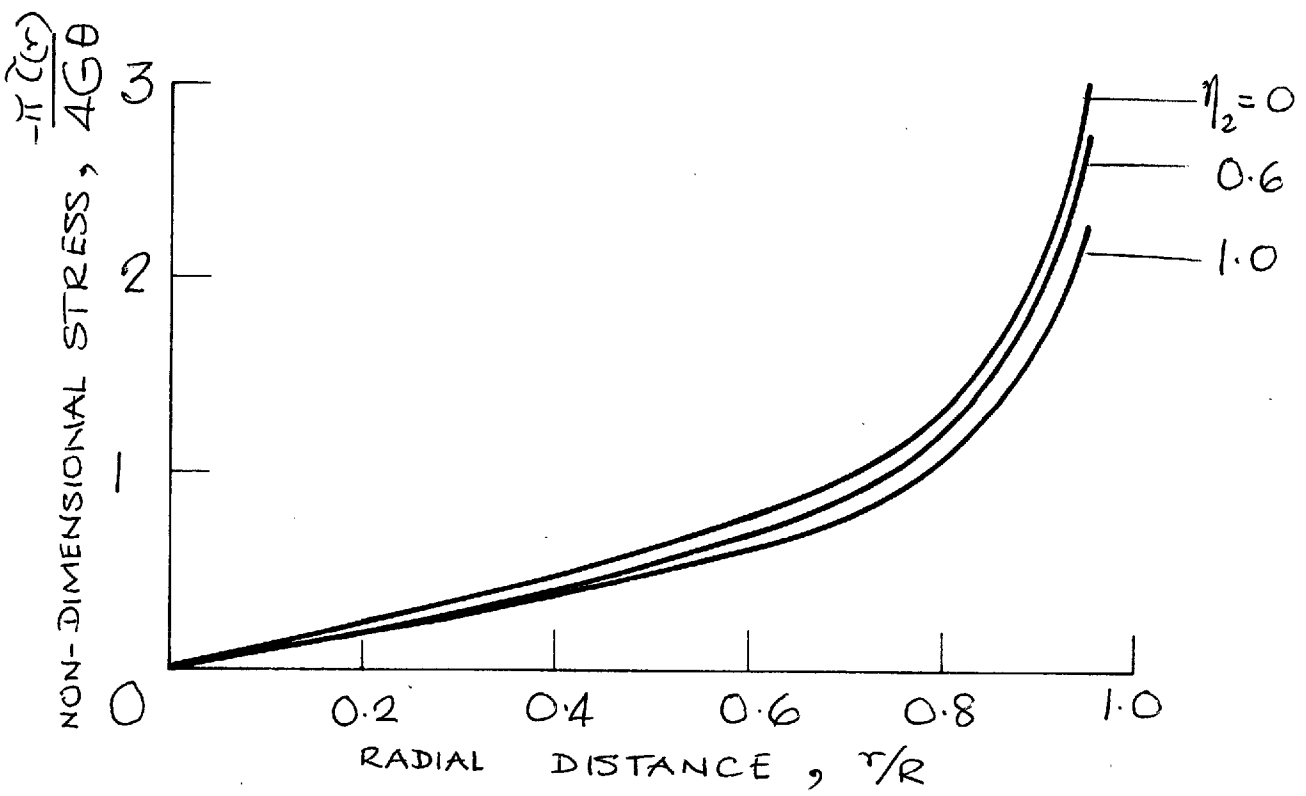
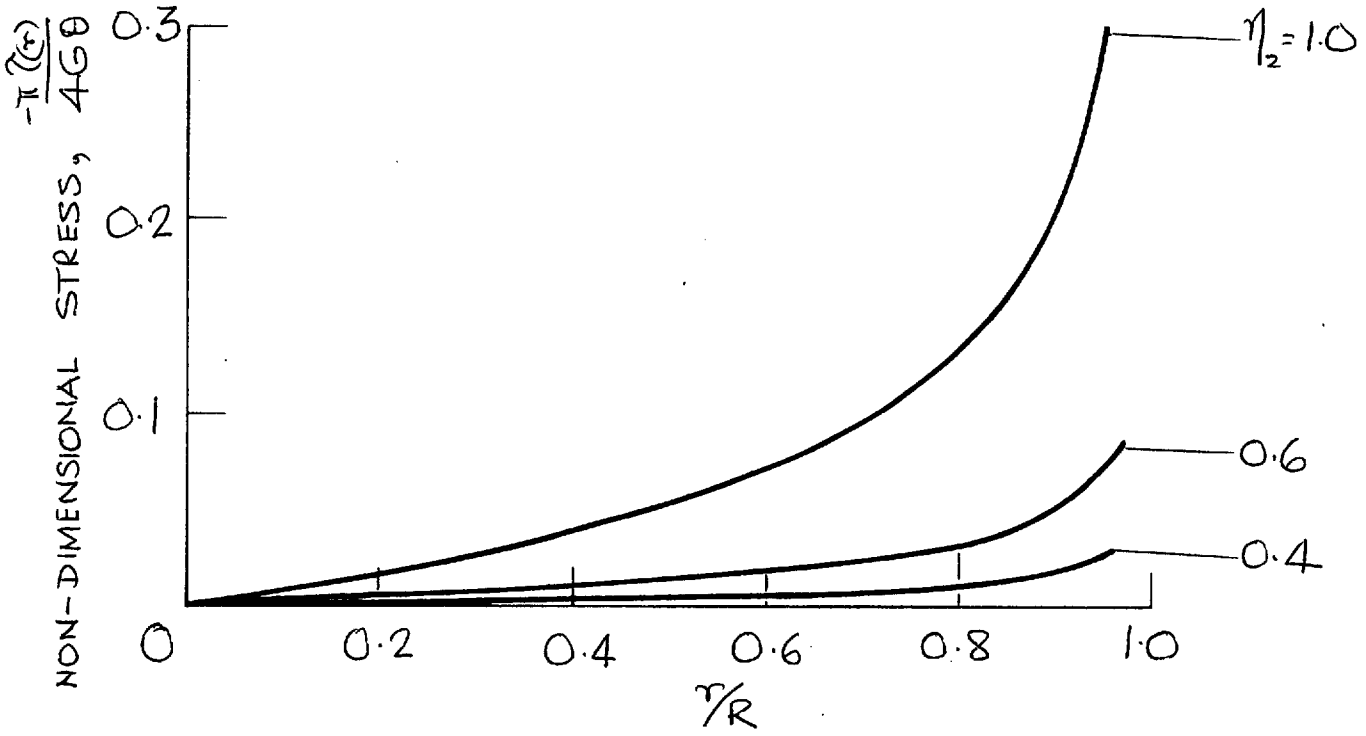


FIGURE 10 - EFFECT OF INERTIA RATIO, $\tilde{J}$, UPON RESONANT AMPLITUDE AND FREQUENCY FACTOR (CASE a (Torsional oscillation, circular body))



(d) STRESS COMPONENT IN PHASE WITH DISPLACEMENT



(b) STRESS COMPONENT IN QUADRATURE WITH DISPLACEMENT

FIGURE 11: STRESS DISTRIBUTION UNDER A RIGID CIRCULAR BODY IN TORSIONAL OSCILLATION

This is because the main equations (22),(24) and (25) contain the same function $\frac{\alpha_1}{\phi(\eta)}$ so that the values in Table 1 for the four cases of Poisson's ratio considered are the same in all the cases.

Also the important generalisation of $F(\eta)$ in equation (60) whereby complete solutions can be deduced from the corresponding first approximation solutions applies here.

9.5.2. Evaluation of integrals involving $Y_\nu(\eta)$

The only point worthy of note is the computation of $\epsilon_{11}(\tilde{x})$ - the analogue of $\epsilon_{11}(\tilde{f})$ of case (ai) - which contains integrals involving Bessel's function of the second kind, whenever the integrands tend to infinity at the lower limit of integration. This is the case only for vertical translation of the rectangular body in which, we recall, the theoretical vertical static displacement is infinitely large.

As a preliminary, $Y_\nu(\eta)$ is replaced by its power series :

$$Y_\nu(\eta) = \frac{2}{\pi} J_\nu(\eta)\left[\ln\left(\frac{\eta}{2}\right)+\gamma\right] - \frac{1}{\pi}\sum_{r=0}^{\nu-1}\left(\frac{\eta}{2}\right)^{-\nu+2r}\frac{(\nu-r-1)!}{r!}$$

$$- \frac{1}{\pi}\sum_{r=0}^{\infty}(-1)^r\frac{\left(\frac{\eta}{2}\right)^{\nu+2r}}{r!(\nu+r)!}\left[\sum_{s=1}^{\nu+r}\left(\frac{1}{s}\right) + \sum_{s=1}^{r}\left(\frac{1}{s}\right)\right]$$

where $\gamma = \lim_{r\to\infty}\left[\sum_{s=1}^{r}\left(\frac{1}{s}\right) - \ln r\right] = 0.577216$ is Euler's constant. By replacing η by $\zeta\,\eta_2$ so that

$$\ln\frac{\eta}{2} = \ln\eta_2 - \ln 2 + \ln\zeta$$

('ln' denotes the Naperian logarithm), it is found that one part of the solution of the integral involving $Y_\nu(\eta)$ can be deduced from the corresponding integrals containing $J_\nu(\eta)$ which have been analysed for the case of the circular body.

The remaining component of the $Y_\nu(\eta)$ integrals is that which contains the logarithmic terms and is treated in the following manner :-

In cases where the integrand is finite at the origin, the usual procedure of applying Simpson's rule is adopted without any modification. However, when the integrand tends to infinity at the origin, the integral is first split into two thus:

$$I = I_1 + I_2$$

where $I = \int_0^{\zeta_2} F(\zeta)\ln\zeta\, d\zeta$. $I_1 = \int_0^{\epsilon} F(\zeta)\ln\zeta\, d\zeta$. $I_2 = \int_{\epsilon}^{\zeta_2} F(\zeta)\ln\zeta\, d\zeta$.

in which ϵ is chosen to be very small compared with ζ_2. It should be noted that $F(0)$ is finite although $F(\zeta)\ln\zeta$ is taken to be unbounded at the origin.

I_2 can be evaluated directly by Simpsons rule and, for I_1 we can replace $F(\zeta)$ by $\bar{F}(\zeta)$ - its mean value in the very small interval 0 to ϵ.

Then $I_1 = \bar{F}(\zeta)\int_0^{\epsilon}\ln\zeta\, d\zeta$.

$= \epsilon\,\bar{F}(\zeta)(\ln\epsilon - 1)$ where use has been made of the well-known result $\lim_{\zeta\to 0}\zeta\ln\zeta = 0$.

9.5.3. The functions $F_{11}(\eta)$

It is sufficient to give the first approximation solution which is the basis of the computations of the complete solution.

Case (bi) Vertical translation

$$F_{11}(\eta) = \frac{Gw_o}{\Omega_2^2}\left[a_1\eta^{\frac{1}{2}}J_0(\eta) + a_2b^2\eta^{-\frac{1}{2}}J_1(\eta) + \tfrac{1}{2}a_3b^4\eta^{-1\frac{1}{2}}J_2(\eta)+\ldots\right]$$

Case (bii) Rocking mode

$$F_{11}(\eta) = \frac{G/b^{\frac{1}{2}}}{\Omega_2^2}\left[a_1\eta^{\frac{1}{2}}J_1(\eta) + \tfrac{1}{2}a_2b^2\eta^{-\frac{1}{2}}J_2(\eta) + \tfrac{1}{8}a_3b^4\eta^{-1\frac{1}{2}}J_3(\eta)+\ldots\right]$$

9.5.4. Resonance curves and stress surfaces

The method of deriving the complete solution $F(\eta)$ of the non-dimensional stress transform from the first approximation solution $F_{11}(\eta)$ given in the last article is the same as in the case of the vertical translation of the rigid circular body. Also, the complete equation of forced vibrations and the dynamic stress distribution are derived from the corresponding first approximation solution and the complete solution $F(\eta)$ in the same manner as described in article 9.3.5.

The results of these complete solutions are presented as resonance curves and stress surfaces for the four values of Poisson's ratio considered in figures 12 to 14 (for vertical translation) and figures 15 to 17 (for the rocking mode). In figures 12 and 13, $\hat{F}$ represents the amplitude of the harmonic exciting force per unit length of the rigid body and $\tilde{m}$ is the same mass ratio defined in equation (39b). In figures 15 and 16, $\hat{T}$ is the amplitude of the exciting torque per unit length and $\tilde{J}$ is the same inertia ratio defined in equation (40b).

The results of this chapter are discussed in the next chapter.

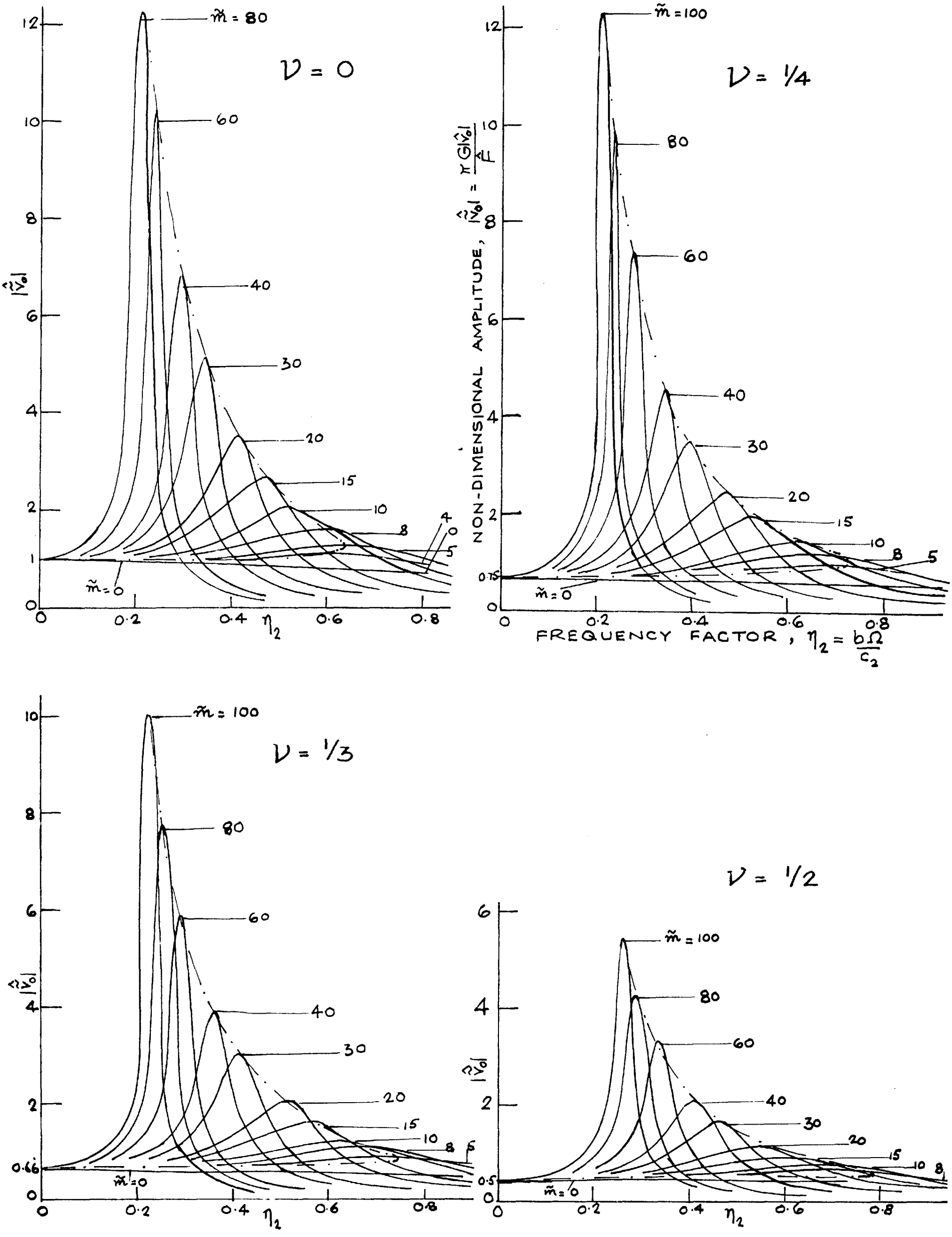


FIGURE 12 - RESONANCE CURVES AT CONSTANT MASS RATIOS, $\tilde{m}$ & POISSON'S RATIO, ν FOR CASE(bi)
(RECTANGULAR BODY, VERTICAL TRANSLATION)

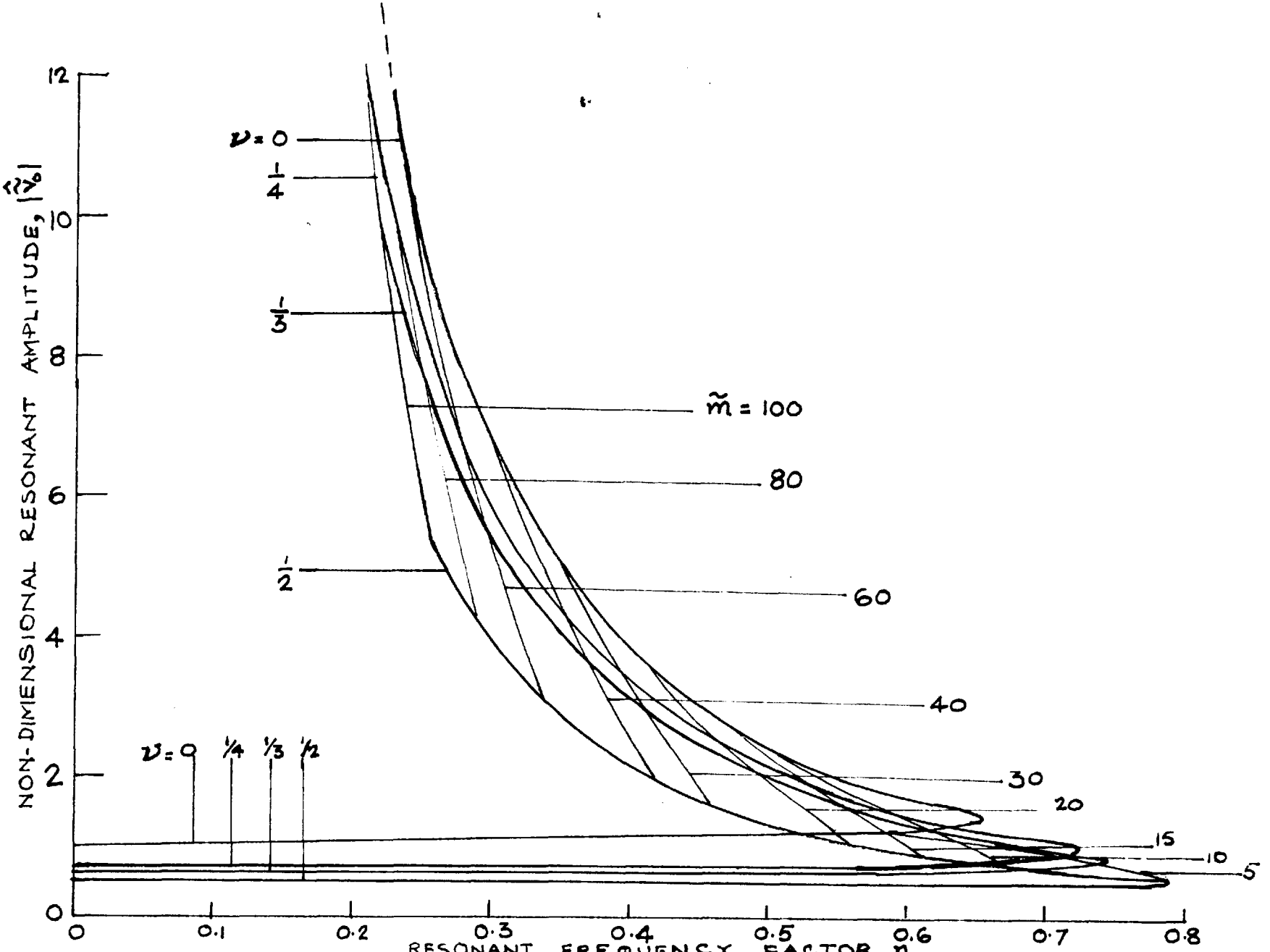
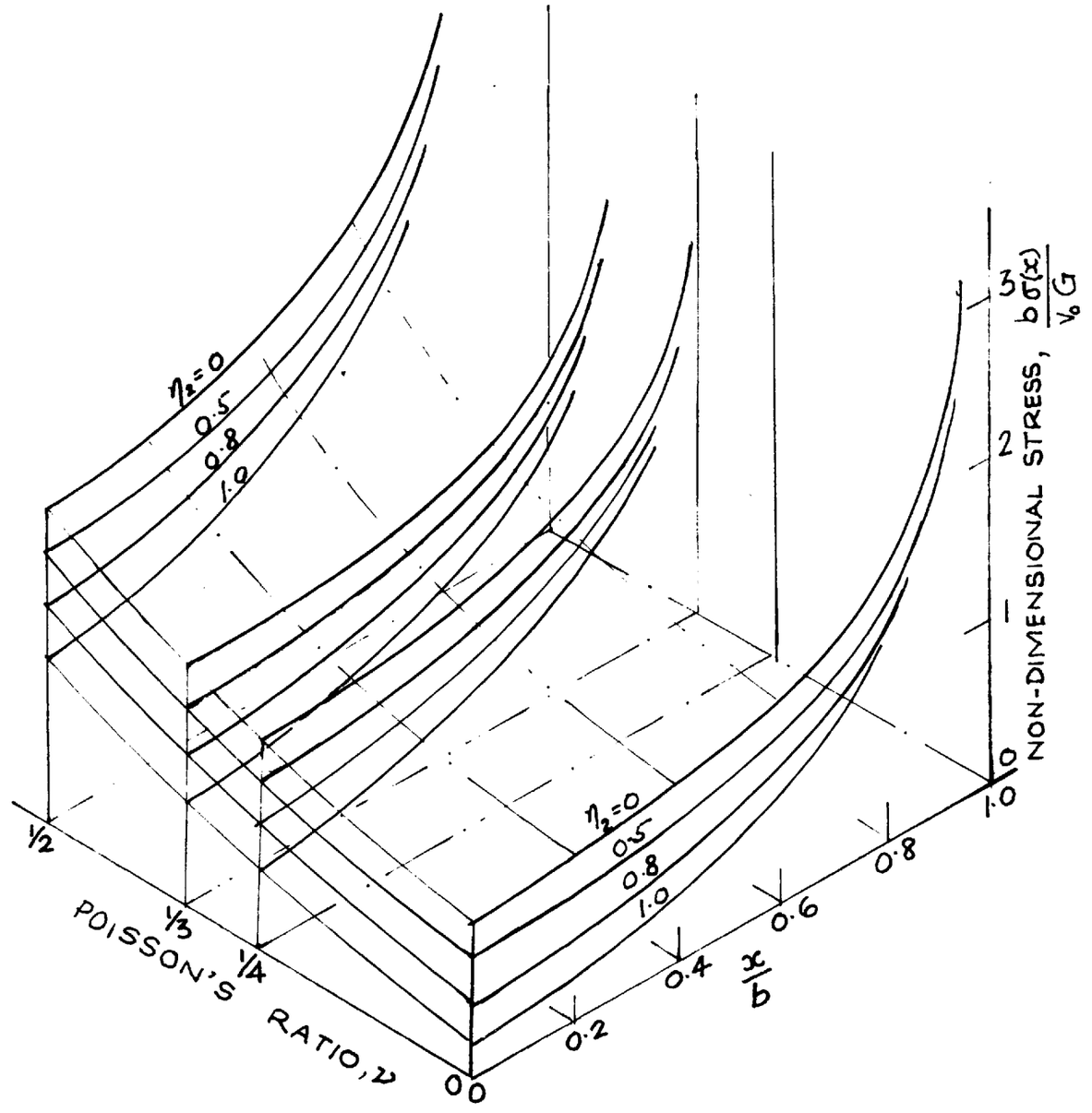
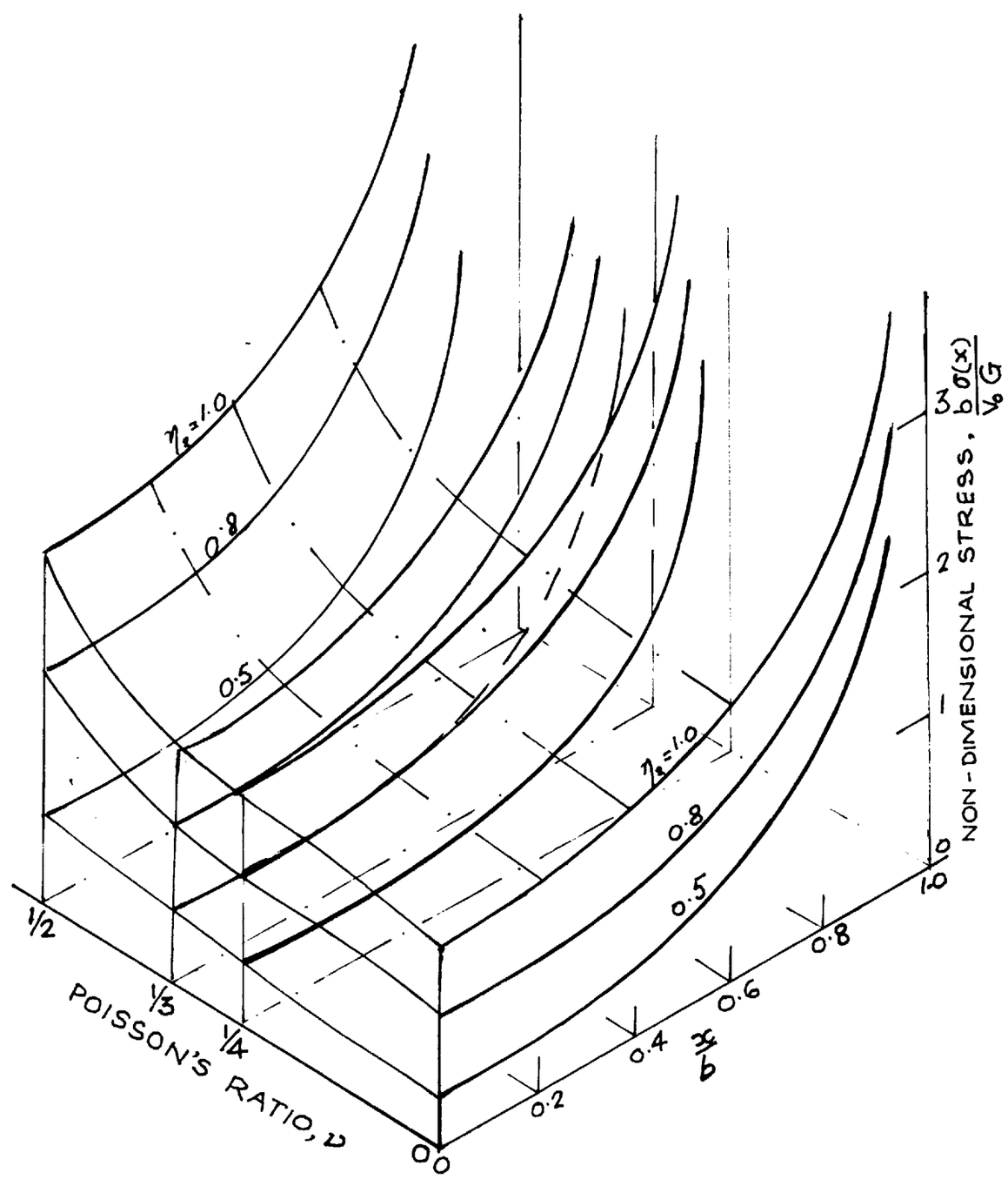


FIGURE 13 – EFFECT OF MASS RATIO, $\tilde{m}$, & POISSON'S RATIO, ν, UPON RESONANT AMPLITUDE & FREQUENCY FACTOR [CASE (bi) – Rectangular body in translation]



(a) STRESS COMPONENT IN PHASE WITH DISPLACEMENT



(b) STRESS COMPONENT IN QUADRATURE WITH DISPLACEMENT

FIGURE 14 – EFFECT OF POISSON'S RATIO & FREQUENCY FACTOR, η_2, UPON THE STRESS DISTRIBUTION UNDER AN INFINITELY LONG, RECTANGULAR RIGID BODY IN VERTICAL TRANSLATION – (CASE bi)

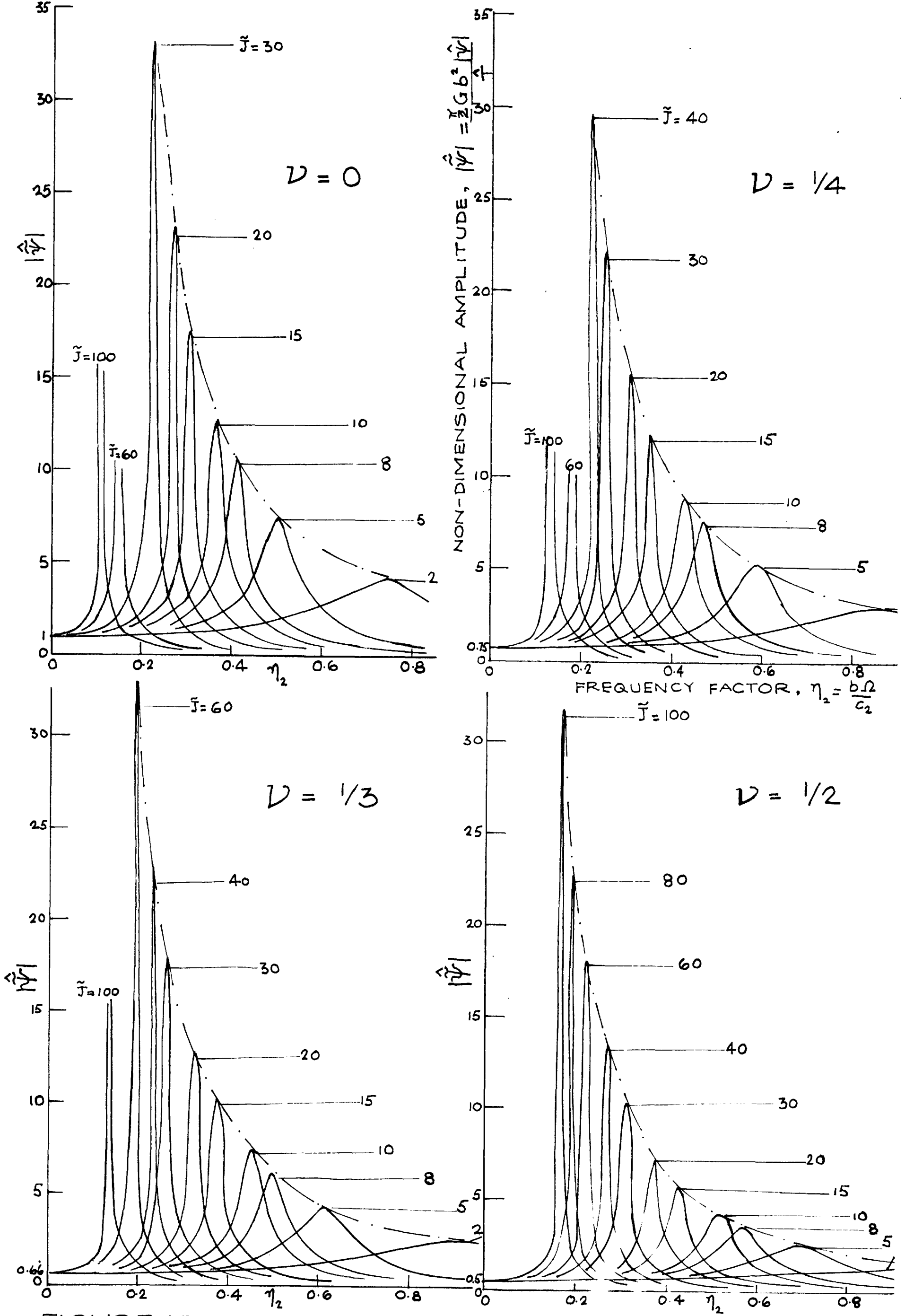


FIGURE 15 – RESONANCE CURVES AT CONSTANT INERTIA RATIOS, $\tilde{J}$ & POISSON'S RATIO, ν FOR CASE (bii 'RECTANGULAR BODY, ROCKING MODE)

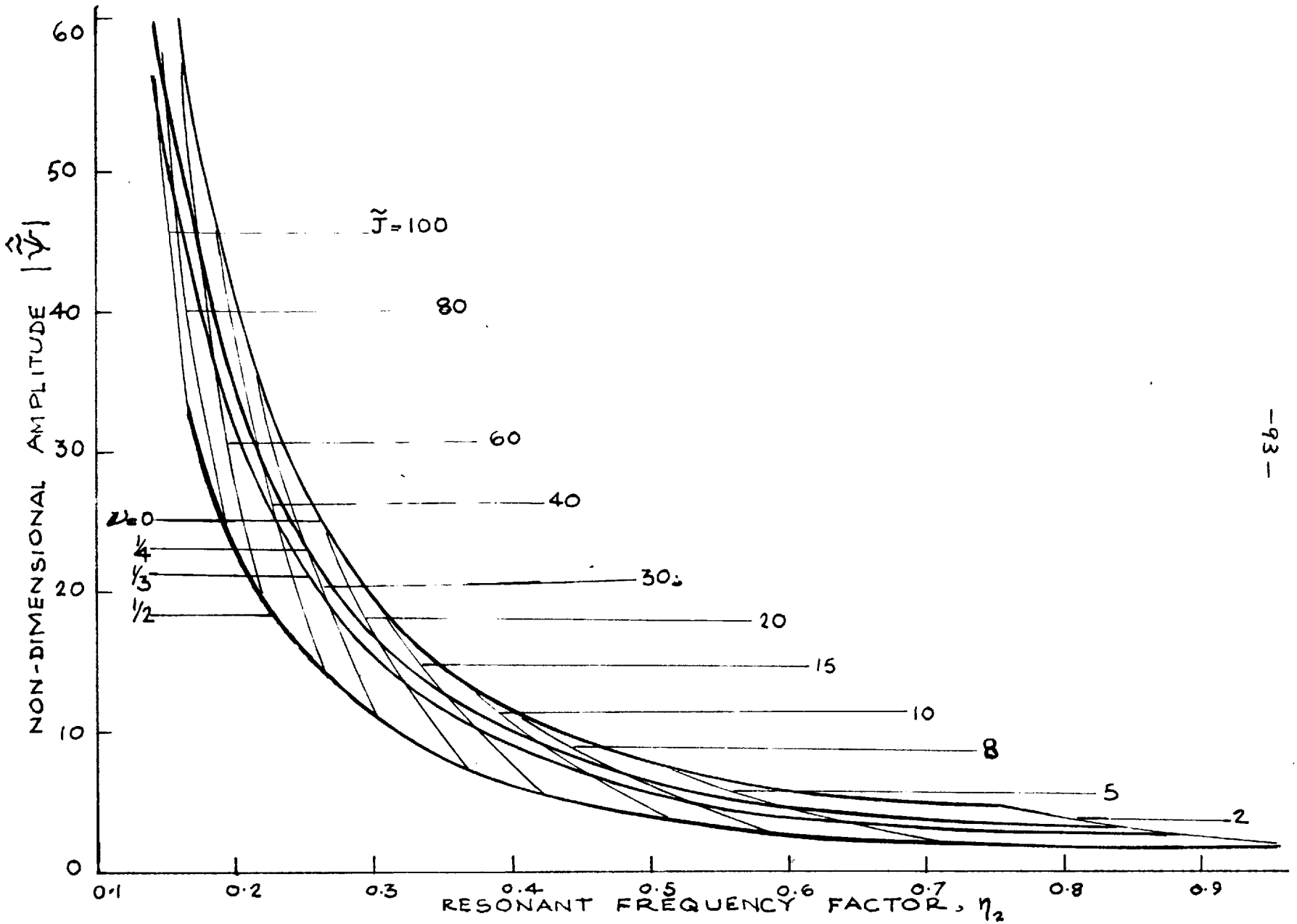
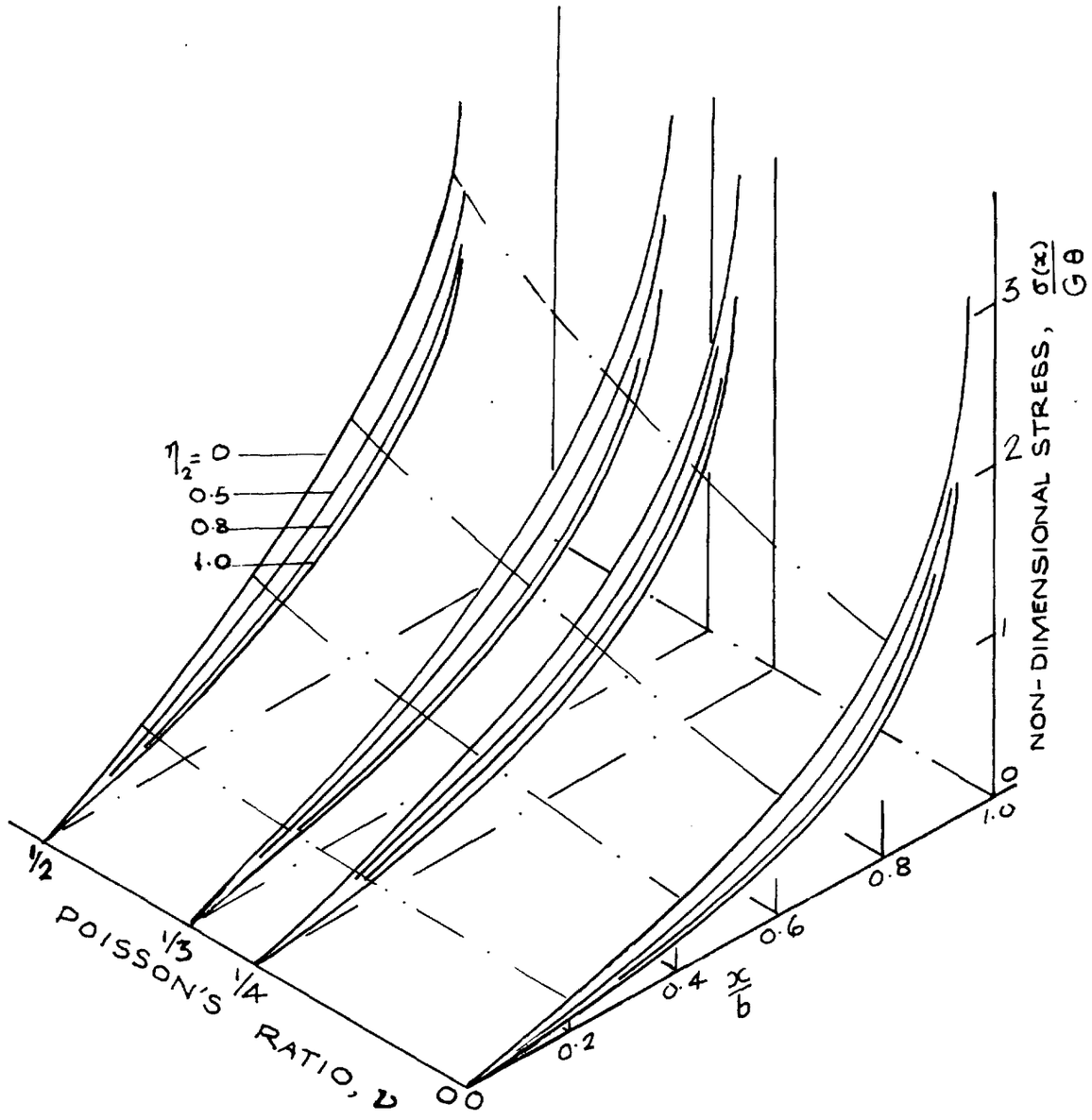
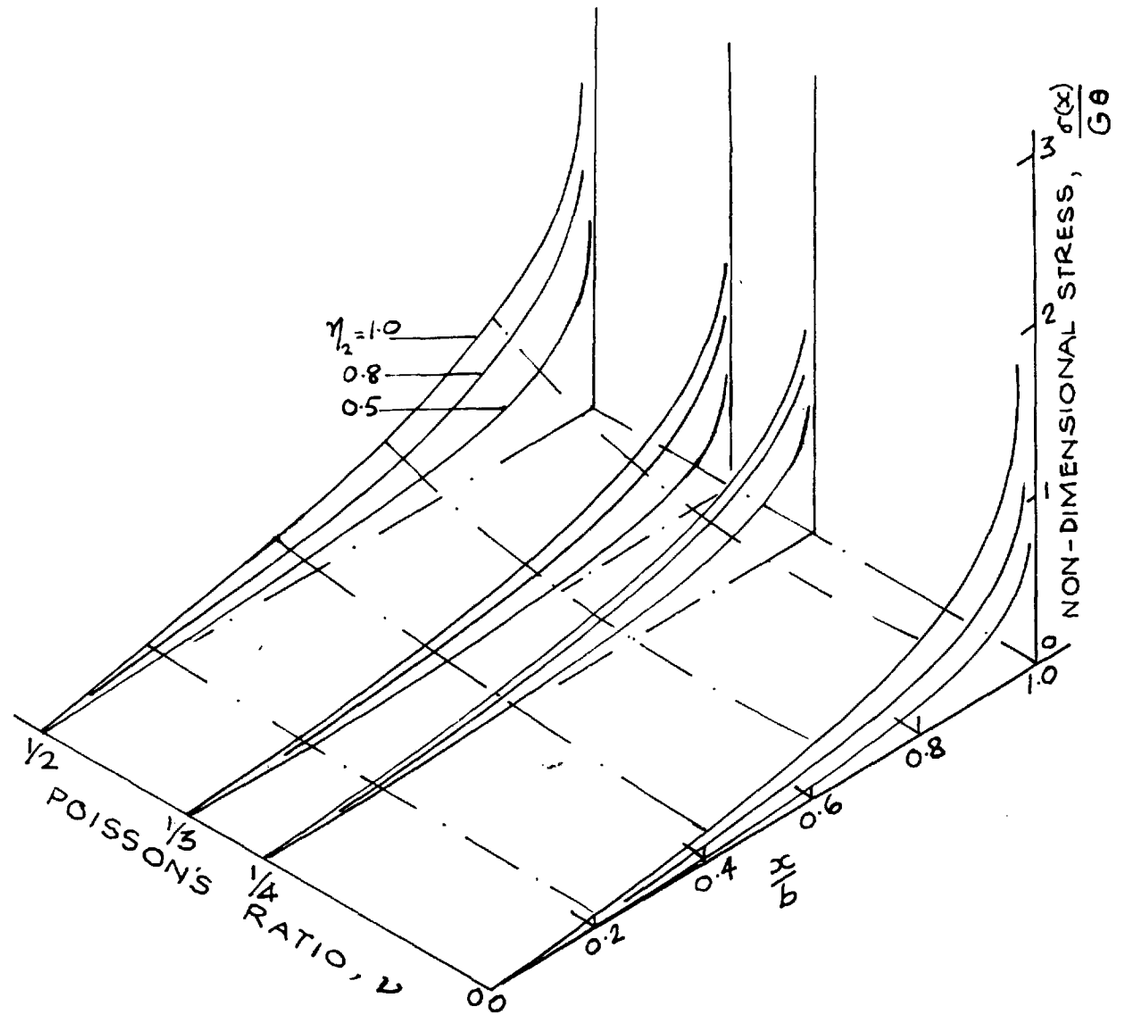


FIGURE 16 - EFFECT OF INERTIA RATIO, $\tilde{J}$, & POISSON'S RATIO, ν, UPO RESONANT FREQUENCY FACTOR & AMPLITUDE (CASE bii) - (Rectangular body, rocking mode)



(a) STRESS COMPONENT IN PHASE WITH DISPLACEMENT



(b) STRESS COMPONENT IN QUADRATURE WITH DISPLACEMEN

FIGURE 17 – EFFECT OF POISSON'S RATIO & FREQUENCY FACTOR, η_2, UPON THE STRESS DISTRIBUTION UNDER AN INFINITELY LONG, RECTANGULAR RIGID BODY IN ROCKING MODE – (CASE. bii)

PART THREE

EXPERIMENTAL VERIFICATION OF THE THEORY AND ITS APPLICATION TO THE PRACTICAL DETERMINATION OF THE DYNAMIC ELASTIC CONSTANTS OF SOIL IN-SITU.

CHAPTER 10

COMPARISON OF THE THEORY WITH EXPERIMENTAL RESULTS

10.1. Introduction

In this chapter, the predictions of the present theory are justified by comparison with published results of laboratory and field tests.

Most published results lack information on the dynamic elastic constants on which numerical comparison can be based. Personal correspondences in a few cases have shown that these constants were, in fact, not determined for the medium on which the rigid bodies were vibrating. However, any information which includes the resonant frequencies and mass ratios for more than one test can be used to determine these constants when use is made of the method recommended in the next chapter These constants can then be used to predict further results on the same medium. This procedure has been adopted in the comparison with the experiments of Eastwood (1953) as will be seen later in this chapter. In some cases - Kanai (1961) and Jones (1958) - shear modulus has been compared with their own values obtained from the wave propagation tests.

Finally, the chapter contains discussions on differences between theory and experimental results, comments on the test procedures of the authors cited and general discussions on some of the theoretical curves.

10.2. The experiments of Arnold, Bycroft and Warburton (1955)

The most reliable experiments seem to have been performed by the above authors. This was because great care was taken to satisfy the assumptions of the theory as much as possible. Foam rubber - the elastic medium used - can be accepted as a uniform isotropic material. The size of the rubber, twelve 3'x3'x1", is very large compared with 0.375 to 2.25" which were the radii of the rigid circular discs used. Thus, with the negligible reflection of waves from the edges as quoted by the authors, the foam rubber is a very fair approximation to a semi-infinite medium. Also, the exciting force was produced electromagnetically and can, therefore, be easily controlled.

The elastic constants for the medium are quoted in table 1 of their paper but it is unfortunate that the method whereby these constants were obtained was not stated.

10.2.1. Justification of the first approximation solution

It was stated in chapter 7 that the first approximation solution is perfectly adequate for estimating the resonant frequencies for bodies with large mass or inertia ratios since these have low resonant frequency factors.

This statement is justified by comparison with two of the experiments of Arnold et al (1955) for the vertical translation and torsional oscillation of the rigid circular body when use is made of equations (37f) and (38b). It can be seen from Table 2 that there is perfect agreement when the resonant frequency factor is small.

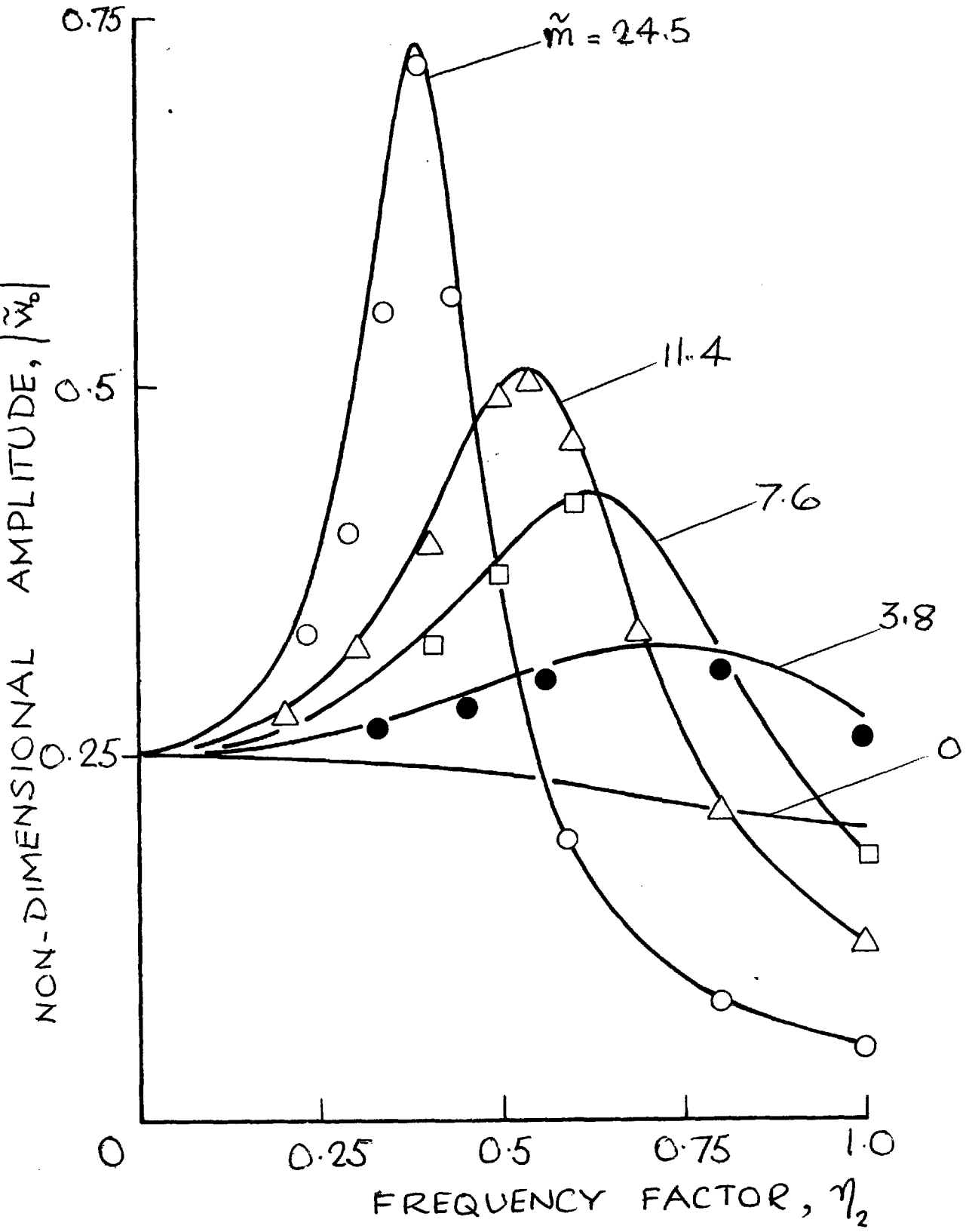
TABLE 2

Case	Mass or Inertia Ratio	Resonant frequency factor	
		Theory	Experiment
(ai)	24.5	0.395	0.395
$\nu = 0$	11.4	0.564	0.55
	7.6	0.675	0.63
(aii)	5.34	0.982	0.92

10.2.2. The complete solution

The results of the complete solution in the last chapter have been compared with the experimental points due to Arnold et al (1955). These are shown in figures 18 and 19 for the two cases of vertical translation and torsional oscillation respectively. Figure 19 also includes theoretical curves due to Arnold et al (1955).

One point of interest is brought out clearly in the above figures - there appears to be more thermal damping for motion in rotation than in translation. In other words, dispersion damping for the case of translation is very much greater than thermal damping for the same mode and this condition is reverse for the case of rotation. This is not unexpected when one considers the magnitude of the quadrature components of stress in comparison with the in-phase components for all cases in translation and those in rotation as shown in the stress distribution figures.



——— PRESENT THEORY, $\nu = 0$

○△□● EXPERIMENTAL RESULTS BY ARNOLD et al (1955)

FIGURE 18: RESONANCE CURVES FO

VERTICAL TRANSLATION OF RIGID CIRCULA

BODY

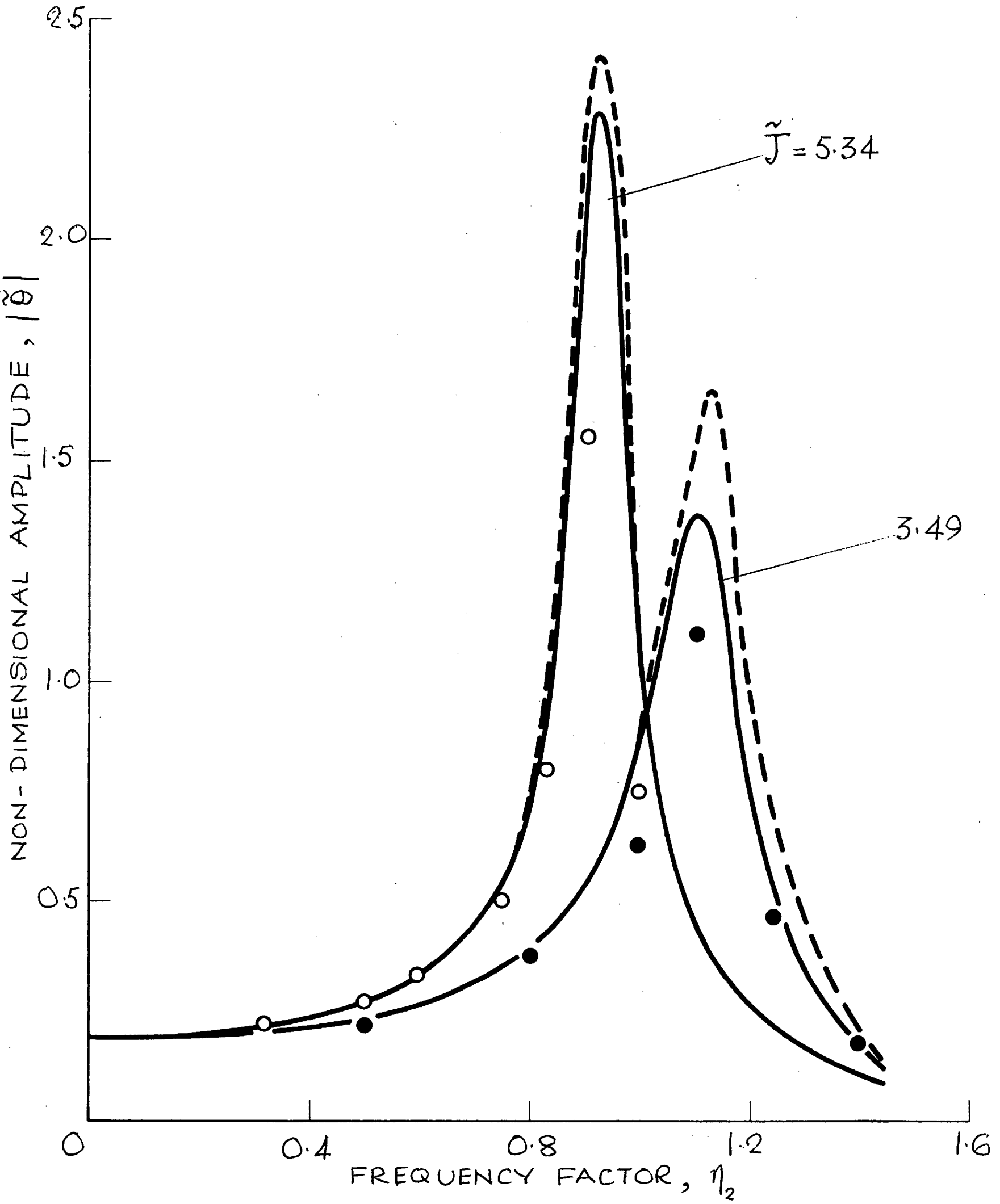


FIGURE 19: RESONANCE CURVES FOR TORSIONAL OSCILLATION OF RIGID CIRCULAR BODY

10.3. Laboratory and field experiments on soils

Although foam rubber serves as an ideal elastic medium, it is obviously not the type of medium that rigid bodies generally rest on in practical life. Therefore, it becomes very essential to be able to interpret results of vibration tests on soils as this is one of the main problems that confron us. This has been realised, for example, by Warburton (1957) who concluded his paper by stating that the theoretical results would be used in a later publication to predict resonant frequencies for a soil-mass system.

Notwithstanding the fact that soil is known to have non-linear characteristics (as discussed in the next chapter), the results of the present theory can be adapted to soil vibration problems under some specified assumptions which are stated in each case.

10.3.1. The experiments of Eastwood (1953)

Laboratory experiments on dry and inundated sand have been performed by Eastwood (1953). The sand was contained in a tank 4' cubed and according to him there were no appreciable reflections of waves from its boundaries. The relevant experimental results give the variation of mass ratio (expressed as dead load per unit area) with natural frequency for vertical translation of rigid circular and long rectangula bodies.

The method of determining the natural frequency was to subject the body to a vertical blow and to measure the frequen of the free oscillations that followed. This is not considered

to be sufficiently satisfactory since it required re-compacting the sand after each test thereby disturbing the state of the medium.

Poisson's ratio and shear modulus were not determined by Eastwood as personal correspondence revealed. Also, it can be easily checked from his experimental points (by considering the product of radius or semi-width and frequency at constant mass ratio) that the shear modulus was not constant throughout the test since the above product is found not constant. The density was maintained (by regular compaction) at 108.1 lb/cu.f so that the dead load given is easily converted to mass ratio.

It will now be assumed, for the purpose of this comparison, that shear modulus varies with frequency but remains constant at the same frequency. Thus, by choosing two experimental points of nearly the same resonant frequencies as 'reference points' - these pairs are encircled in figure 20 - knowing their mass ratios and corresponding radii, then the appropriate Poisson's ratio curve in figure 7 is that for which the frequency factors of the intersections of the mass ratios are in the same ratio as the radii. For example, the upper encircled pair of points in figure 20(a) have mass ratios of 22.2 and 12.6 which intersect the 1/3 Poisson's ratio curve of figure 7 at resonant frequency factors of 0.490 and 0.614 respectively which are in the same ratio as the radii 4" and 5" corresponding to the points. The Poisson's ratio having been determined, experimental points for one rigid body are used to determine the variation of frequency factor with

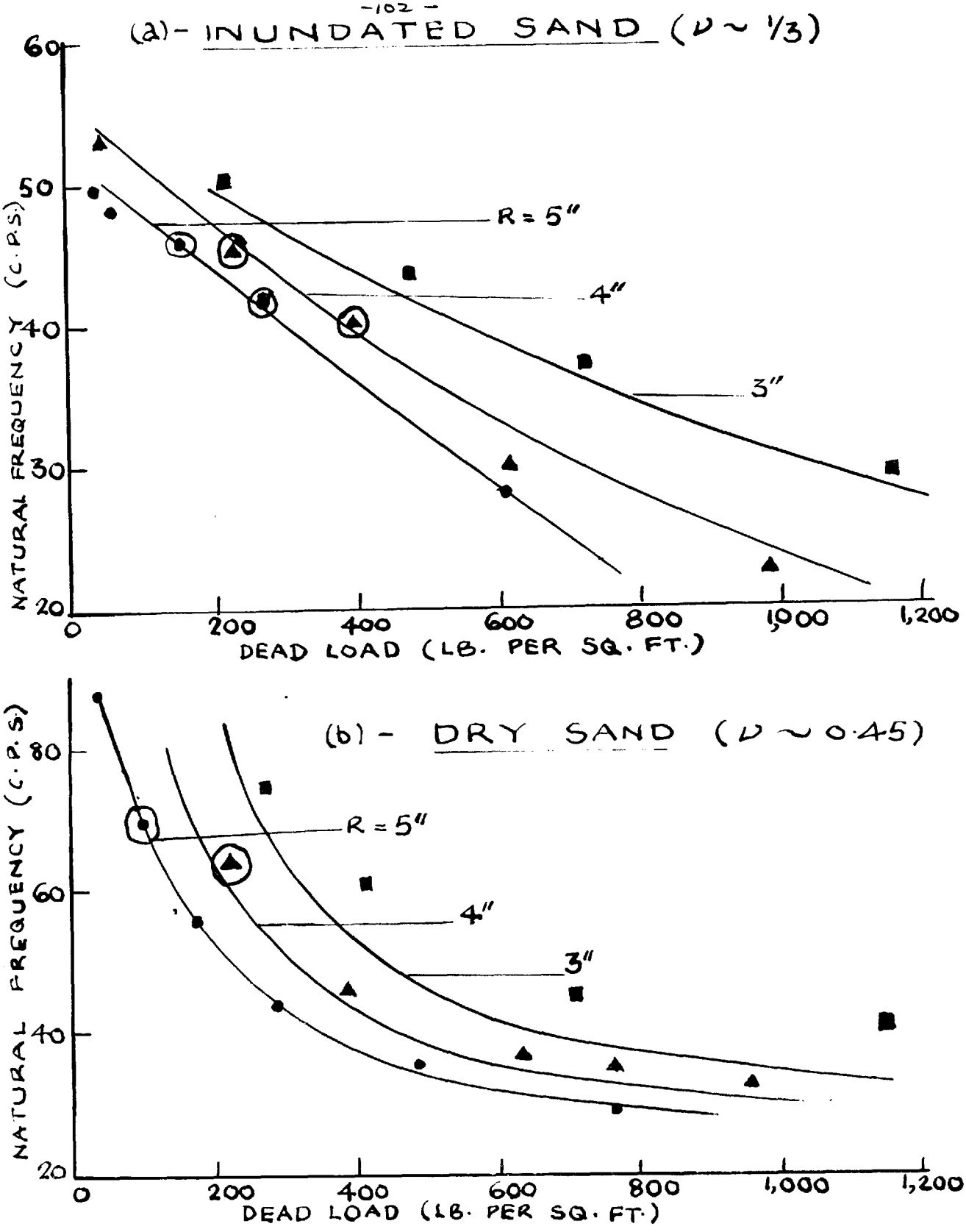


FIGURE 20: VARIATION OF NATURAL FREQUENCY WITH DEAD LOAD PER UNIT AREA FOR CIRCULAR RIGID BODIES IN VERTICAL TRANSLATION ON SAND

◉ ◉ REFERENCE POINTS (SEE ARTICLE 10.3.1)
● ▲ ■ EXPERIMENTAL POINTS (EASTWOOD, 1953)
——— PRESENT THEORY

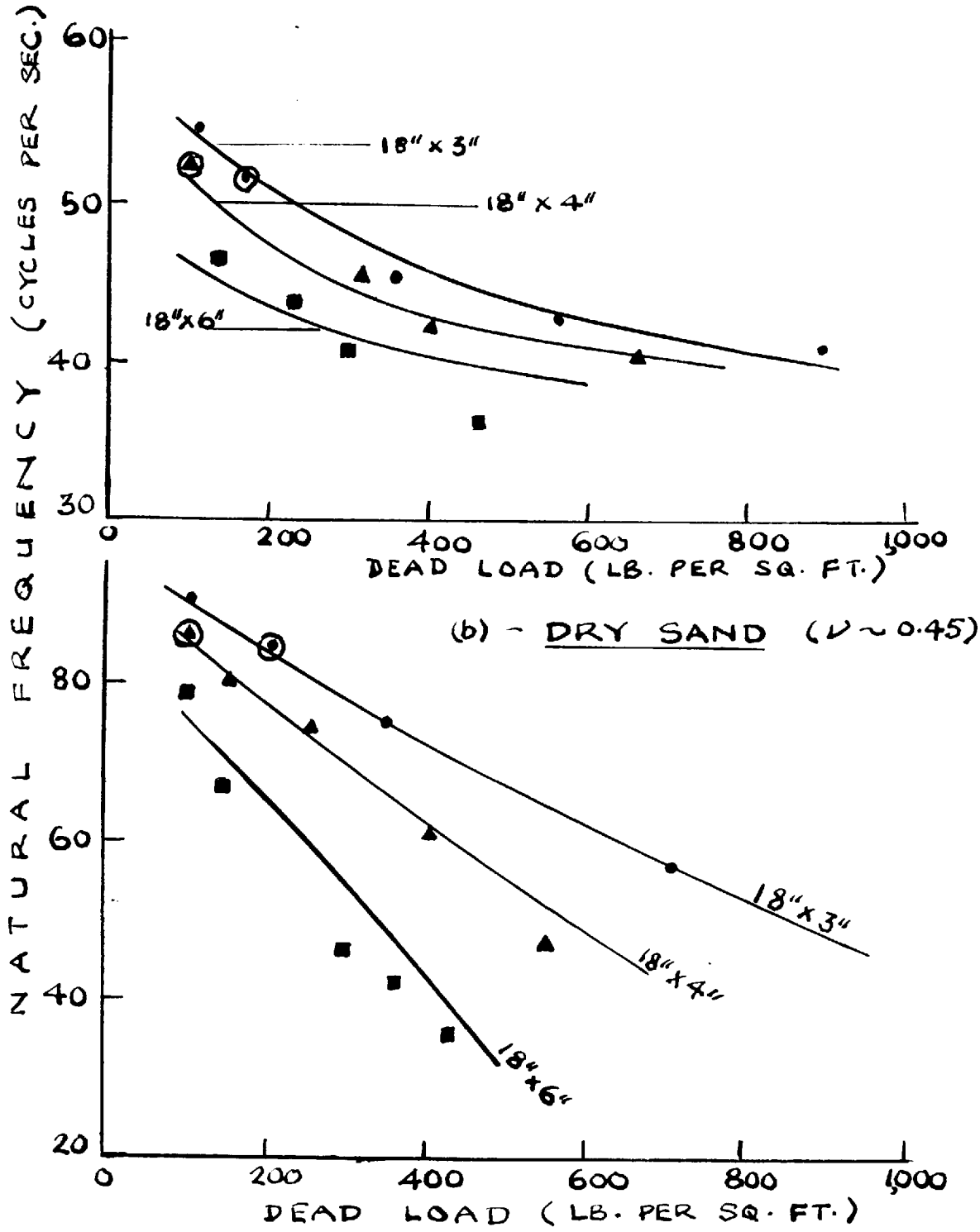


FIGURE 21: VARIATION OF NATURAL FREQUENCY WITH DEAD LOAD PER UNIT AREA FOR RECTANGULAR RIGID BODIES IN VERTICAL TRANSLATION ON SAND

● ▲ ■ EXPERIMENTAL POINTS (EASTWOOD, 1953)
——— PRESENT THEORY

frequency and from this the theoretical curves for the others are derived. The whole of the comparison is shown by figures 20 and 21.

10.3.2. The experiments of Jones (1958)

Jones attempted in 1958 to determine the dynamic elastic constants of soil in-situ by two methods : the wave propagation method and the resonance method. In the former, the velocities of Rayleigh waves propagated from an electrodynamic vibrator were measured and in the latter, the resonant frequencies of several rigid circular bodies were determined for vertical vibrations. Jones assumed a Poisson's ratio of 0.5 for the purposes of calculating the shear modulus from the Rayleigh wave velocity. He obtained 5,750 and 1,870 lb/sq.in. for sites A and B respectively (see P.16 of his paper). The resonance data for these sites are given in Table 3 of his paper and when use is made of figure 7 of the present theory, it is found that shear modulus, assuming Poisson's ratio of 0.5, varies as shown in the following table :

TABLE 3

Site	Mass ratio	Shear modulus lb./sq.in.
A	51	4,410
	109	4,530
B	51	1,270
	80	1,430
	109	1,500

It can be seen that these values are not only much lower than his own values but also are not the same for each site. The explanation to these differences immediately comes from the method which Jones used to determine his resonant frequencies - the usual resonance method of keeping force constant and varyin amplitude until the maximum is attained. As shown in the next chapter, this method is unreliable as far as soil is concerned because of its non-linear characteristics which become severe at high amplitudes.

This fact is more vividly brought out by reference to the tests of Jones on sites C and D as shown by the results in Table 4 of his paper where we see that two natural frequencies are obtained with two different constant currents i.e. forces (since electromagnetic force is proportional to current). Thus, with the uncertainty of the correct resonant frequency, it is not worthwhile using the present theory to determine Poisson's ratio. Since the error involved in the calculation of the shear modulus is proportional to the square of the frequency, then in a case like site C, line 13, with resonant frequencies ranging from 77.5 to 67.5 for 0.5 and 1.5A. current respectively, the values of the shear modulus(for any Poisson' ratio) would differ by 31.5%. Therefore, this method of determining resonant frequency is not suitable for soils. An alternative method, described in the next chapter has proved very successful.

10.3.3. The experiments of Bycroft (1959)

Bycroft has carried out a field test for vertical and horizontal translation of a circular concrete block of diameter 5' and depth 1' on soil of which he assumed a Poisson's ratio of 0.45 and a shear modulus derived from Boussinesq's equation and the results of his in-situ static tests. The exciting force was produced by out-of-balance weights placed on the concrete and operated by a belt drive from an electric motor a few feet from the vibrator.

Although this method of dynamic soil test using static modulus is not considered satisfactory (see next chapter), yet the experiment is cited here as the only available experiment which confirms that rigid bodies of small mass ratios (less than about 3) do not have an observable resonant frequency when performing vertical vibrations since the theoretical peak is too close to the static deflection. The fact that the above rigid body had a mass ratio of 2.53 and no peak appears in its resonance curve is a justification of the doubling back of the curves in figure 7.

This phenomenon, peculiar to vertical translation cases and absent in rotation cases, is a direct consequence of the high dispersion damping in translational modes. This can be checked mathematically by investigating the decreasing or increasing nature of the resonance curves near zero frequency factor.

10.3.4. The experiments of Kanai and Yoshizawa(1961)

Experiments on actual buildings have been carried out by the above authors of the Earthquake Research Instute, Tokyo, for the case of the rocking of buildings whose lengths are much greater than their widths. Also, the experiments used in this section are for buildings in which the ratio, m, of the vibration of the roof to that of the base is such that the axis of rock is not too far from the base. It is to be recalled that the assumptions of the theory demand that this axis should coincide with the axis of symmetry of the base.

Since only one measurement i.e. resonant frequency of rocking was made for each building at each site, it is not possible to determine Poisson's ratio and shear modulus independently. Therefore, shear modulus has been calculated for Poisson's ratio of 1/4,1/3,and 1/2 using the theoretical curves of figure 16. The shear modulus thus calculated has been compared with the corresponding value determined by the authors using the wave propagation method as quoted in figure 7 of their paper This comparison is shown in Table 4 in which m is the above ratio of roof to base vibrations and T is the time period of rocking.

TABLE 4

House No.	m	T sec.	G (present theory)- lb./sq.in. for Poisson's ratio of			G(Kanai et al.) lb/sq.in.
			1/4	1/3	1/2	
1	3.7	0.32	12,200	10,300	8,040	11,100
3	4.0	0.22	22,400	20,000	16,200	20,700

TABLE 4 (continued)

14	[illegible]	0.18	19,000	17,100	13,700	20,700
15	9.3	0.108	[illegible],500	32,700	16,200	34,500

Assuming the experimental values to be correct, it is clear that Poisson's ratios can be obtained by plotting the theoretical values of G.

A specimen calculation is given for the case of house 15.

Mass per unit length = 100/3tons per metre = 22,800lb/ft.

If m is the above ratio of roof to base vibration, h is the height and b the semi-width, it is easily shown that the square of the radius of gyration about the axis of rock is given by

$$k_o^2 = \frac{b^2}{3} + \frac{h^2}{4}\left[\frac{1}{3} + \left(\frac{m+1}{m-1}\right)^2\right]$$ and the non-dimensional

[illegible] of figure 16 given by its definition in equation (7) is found to be 5.58 after use has been made of the given density 120 lb./cu.ft. and the values b=3.4m = 11.13 ft.

and h=9.04 m. = 29.7 ft.

With the determination of $\mathfrak{F}$, the corresponding frequency factors for the Poisson's ratios 1/4,1/3 and 1/2 are read from figure 16 as 0.54, 0.58 and 0.68 respectively from which the shear moduli are easily obtained.

CHAPTER 11

APPLICATION OF THE THEORY TO THE PRACTICAL DETERMINATION OF THE DYNAMIC ELASTIC CONSTANTS OF SOIL IN-SITU

11.1. Comparison of the method used here with other methods

The problem of determining the dynamic elastic constants of soil in-situ has been briefly discussed in the general introduction (See article 1.2.3.)

In this chapter is described a method of determining these constants based on the complete solution of the rigid circular body, vertical translation which is summarized by figure 7. In this figure more lines of constant Poisson's ratio besides the four cases of 0, $\frac{1}{4}$, $\frac{1}{3}$ and $\frac{1}{2}$ which were accurately determined have been added by plotting the points of intersection of any mass ratio line and the four calculated Poisson's ratio lines so that any other Poisson's ratio curve can be interpolated fairly accurately.

The method of applying figure 7 then follows simply. A rigid circular slab would be placed on the soil at the surface. The slab would be loaded with a vibrator exerting on it at the centre a vertical sinusoidal force. For known mass ratios, say $\tilde{m}_1$ and $\tilde{m}_2$, and corresponding resonant frequencies Ω_1 and Ω_2, figure 7 would show that, provided the shear modulus is constant in the two tests, there is only one line

of constant Poisson's ratio that will satisfy the necessary condition that the resonant frequency factor is proportional to the resonant frequency.** A check can be undertaken with yet another mass ratio. The shear modulus can then be calculated from any of the frequency factors and the corresponding frequency.

Although there is another way of using figure 7 which involves the measurement of force and amplitude, this chapter later shows why this method cannot be recommended. Indeed, any method which relies on the measurement of force or amplitude at resonance must be inaccurate as there will be some error due to thermal damping and the non-linear characteristics of soil. The frequency at resonance is, however, hardly affected by thermal damping and can be measured to a high degree of accuracy by electronic means.

Also, resonance methods which keep the force constant and vary the amplitudes will be inaccurate (See, for example, commentson the results of Jones

---

** It has been found essential, because of the non-linear characteristics of soil, to define resonance in terms of the minimum force that will maintain the same amplitude of vibrations throughout the frequency range. For reasons of the non-linearity again, the amplitude should be kept as small as possible.

(1958) in the last chapter) mainly because high amplitudes will set in near resonance and the non-linear effects of soil will certainly make the results unreliable.

An alternative method is to carry out a wave propagation test in which measurements of the wave velocities are made. As discussed later in this chapter, it is generally difficult with this method of test to determine independently the Poisson's ratio and the shear modulus because only one wave of propagation is clearly distinguishable. Also, this method yields indeed a value of the dynamic elastic modulus as an average for a large area of ground and not directly under the rigid body.

11.2. Subsidiary experiments before the field tests

11.2.1 Calibration of vibration pick-ups

The vibration pick-up used to measure the amplitude of vibration of the rigid body was a Dawe's moving coil (electrodynamic) type which generates a voltage proportional to the absolute velocity. The following procedure was adopted to determine the constant of proportionality.

The graticule of a compound microscope with an objective magnification of ten was first calibrated by focussing it against a standard micrometer scale in

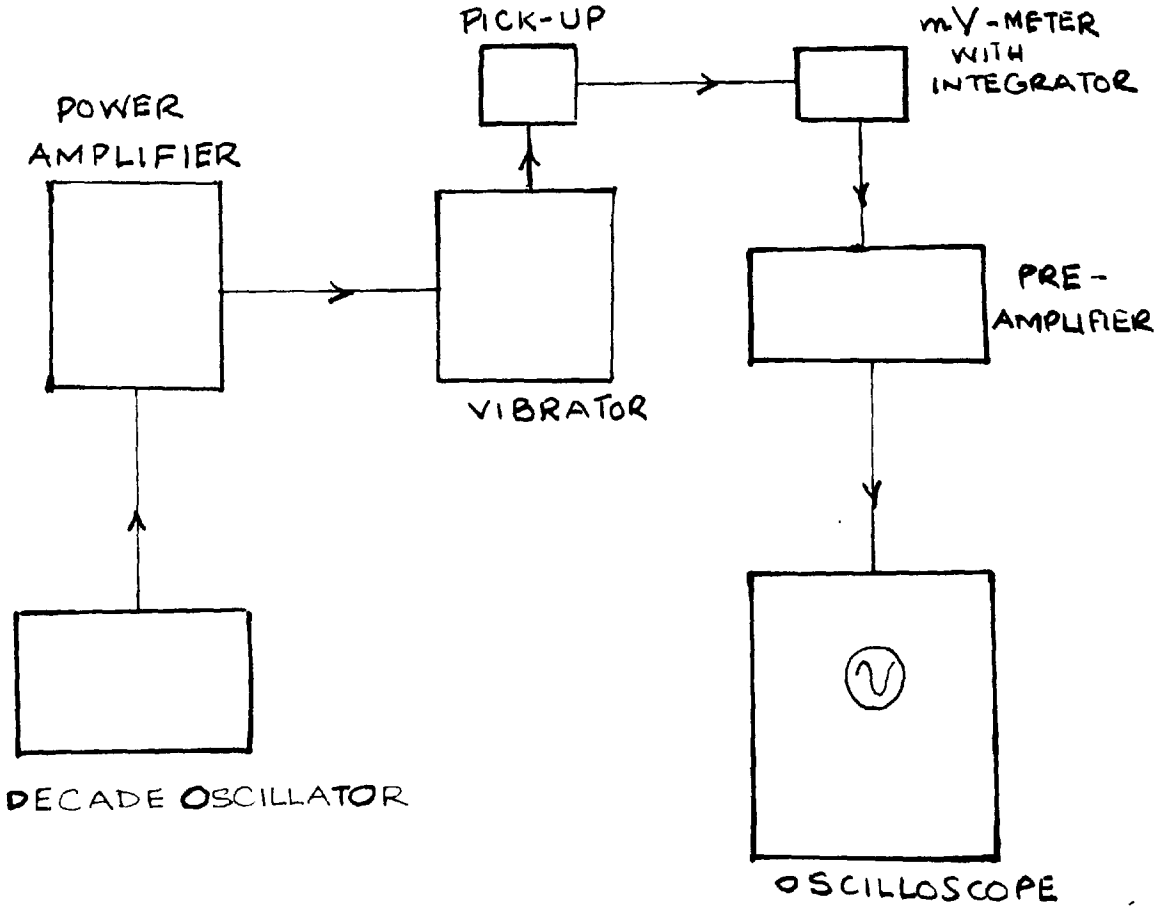


FIGURE 22: BLOCK DIAGRAM OF THE ELECTRONIC CIRCUIT USED IN BOTH CALIBRATION AND FIELD TESTS

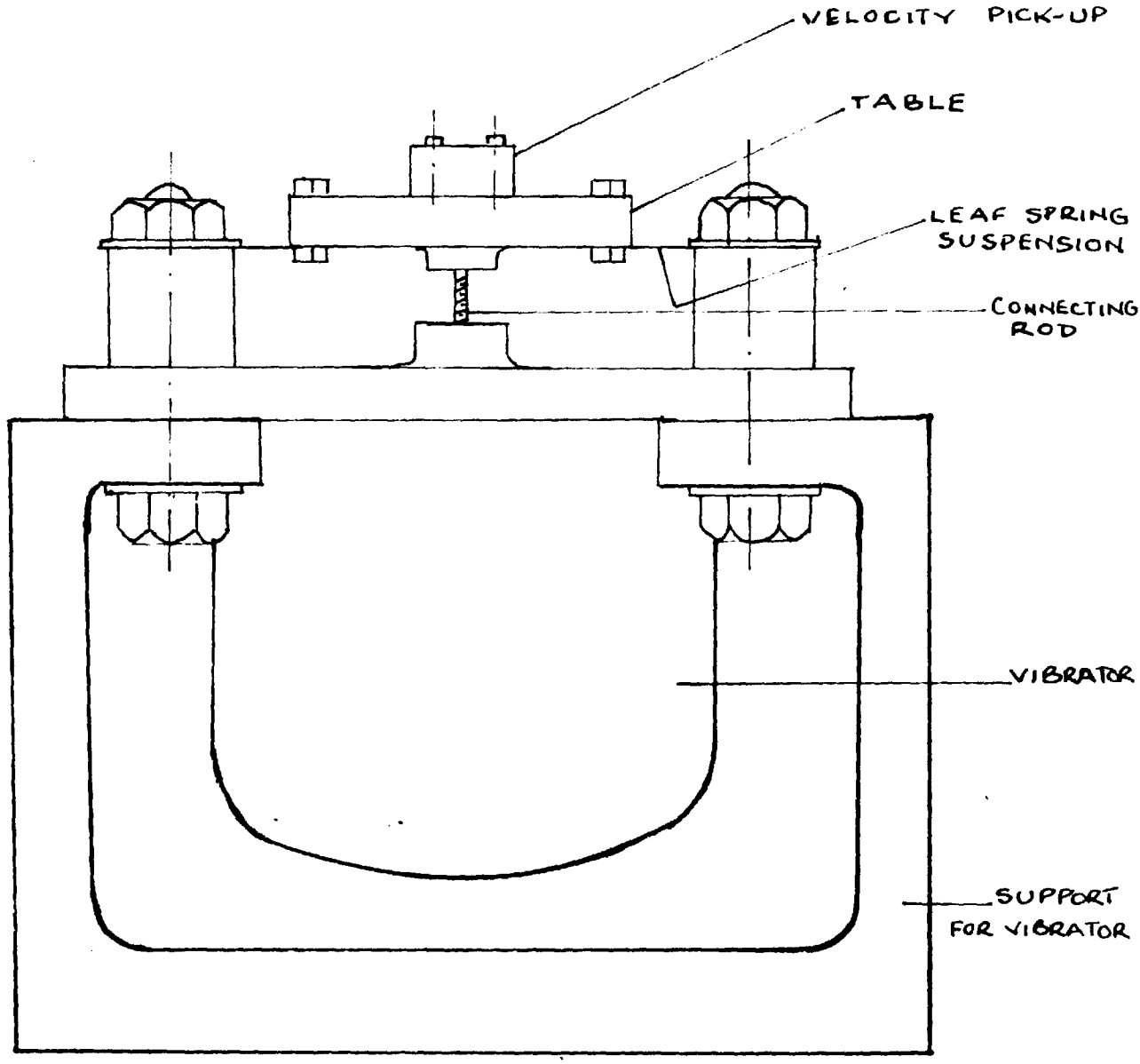


FIGURE 23 : ARRANGEMENT OF THE PICK-UP AND VIBRATOR DURING CALIBRATION OF PICK-UP.

which 1mm. is divided into a hundred parts. It was observed that ten divisions on the microscope coincided with 0.9 mm. on the scale thus giving the following factor for the microscope :

1 division = 0.00354 in.

A check was also made using a dial gauge. An auxiliary circular scale permitted the reading of the microscope to a hundredth of a division.

The pick-up was then fixed to a table supported by four leaf springs and connected to a vibrator by a short stud as shown in figure 23. This arrangement was part of the electronic circuit shown in figure 22. The millivoltmeter in figure 22 is a measuring box complete with differentiating and integrating circuits. It measures the output voltage from the pick-up by comparing the amplitude of the sinusoidal wave shown on the oscilloscope when a known mains voltage is fed into the box with the amplitude when the box is switched on to the circuit admitting the pick-up voltage. It is obvious that all pre-amplifier and oscilloscope settings that affect the wave amplitude should be the same in both cases. The frequency of excitation is read directly from the decade oscillator which reads accurately to 0.01 c.p.s..

A bright spot on the pick-up was focussed in order to measure the amplitude of vibration. Since, for harmonic vibrations,

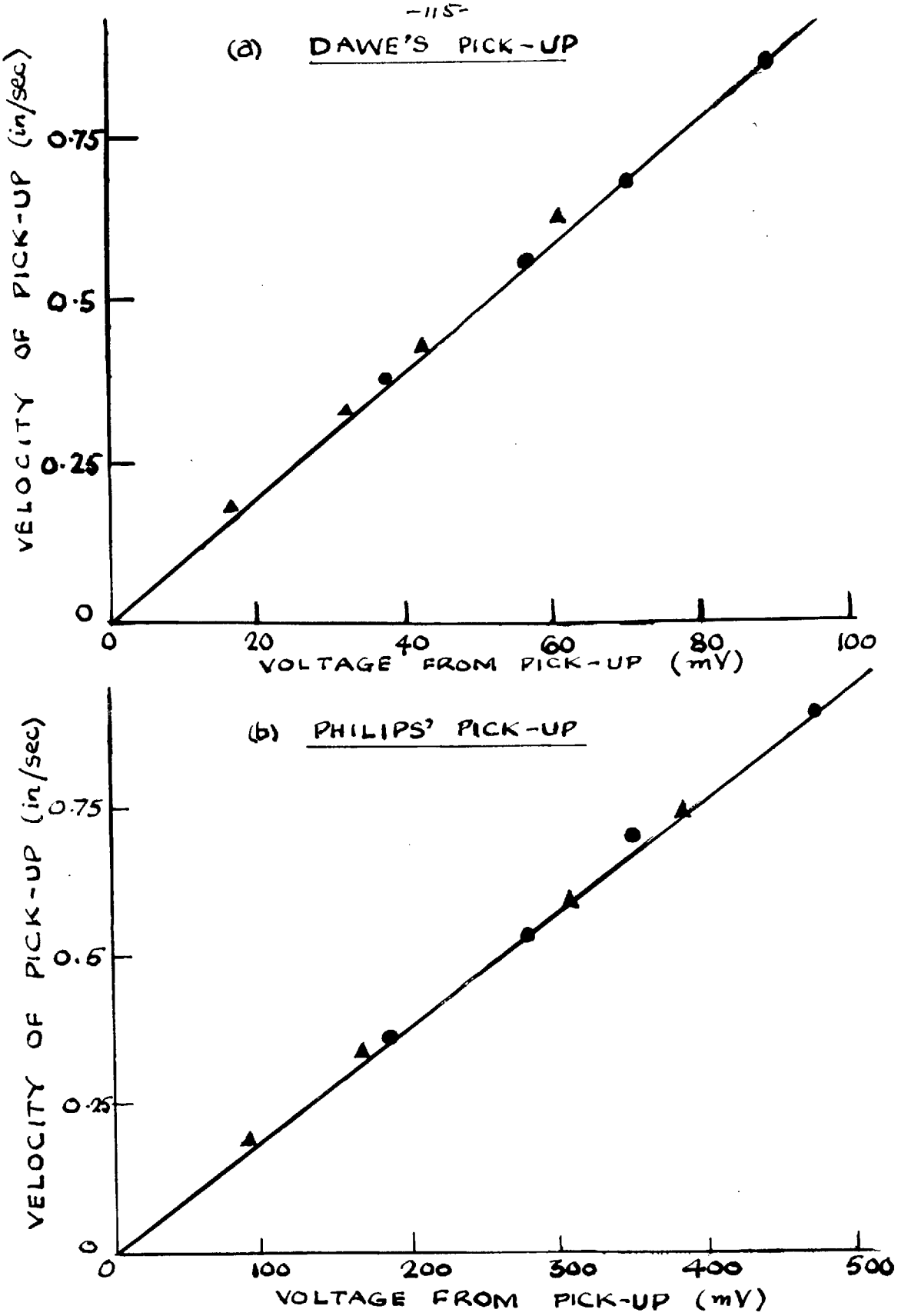


FIGURE 24: CALIBRATION CURVES FOR THE VIBRATION PICK-UPS

▲ 35 cps, ● 60 cps.

velocity = amplitude x angular frequency,

the velocity of the pick-up could be easily determined at any frequency while the corresponding voltage was read from the millivoltmeter as described above.

Figure 24(a) shows the results of the calibration from which the constant of the pick-up was found to be 104 mV (peak voltage) at 1 in. per sec.

Figure 24(b) shows similar results for a Philips' pick-up intended to be used for measuring ground vibrations at the surface away from the rigid body in the field tests.

11.2.2 Testing the equipments on the college site

Before taking the equipments to the field, it was thought advisable to try them out in the college premises. The quadrangle between the Civil, Mechanical and Electrical Engineering buildings was the chosen site. No difficulties were encountered and the equipments were considered fit for field tests.

11.3 Field tests at Silwood Park, Berkshire

The site chosen for the field tests is quoted by Jarman (1960) to be an unusually uniform medium of a low wave velocity soil (actually sandy clay) gradually merging to a 400 ft. depth of London clay. It corresponds to site 2 of his tests at the Imperial College Field Station, Silwood Park, Berkshire. The tests described here were performed in the last week of October

1964 during which the weather kindly remained fair. All equipments, with the exception of the vibrator, were inside a van about thirty feet from the vibrator. A pit, eight feet diameter and 1½ feet deep, was dug out to remove the loose top soil until uniform sandy clay was reached.

11.3.1. Resonance tests

11.3.1.1. Description of the set-up

The electronic circuit was connected up as shown in figure 22. An assembly diagram of the vibrator, pick-up and rigid circular body is shown in figure 25. The pick-up was placed in a recess machined out in the top circular disc as shon in the figure. The circular discs which are one foot diameter were ground flat on both faces. The device of two studs sticking out from the base plate and holes in the other discs enabled the mass of the rigid body to be increased with the least distu bance of the base plate and, therefore, of the soil. The least weight of the rigid body- consisting of the base plate, the top disc and pick-up, the vibrator and lead weights - was 231 lb.

An avometer was connected across the output of the power amplifier in order to measure the voltage applied to the vibrator.

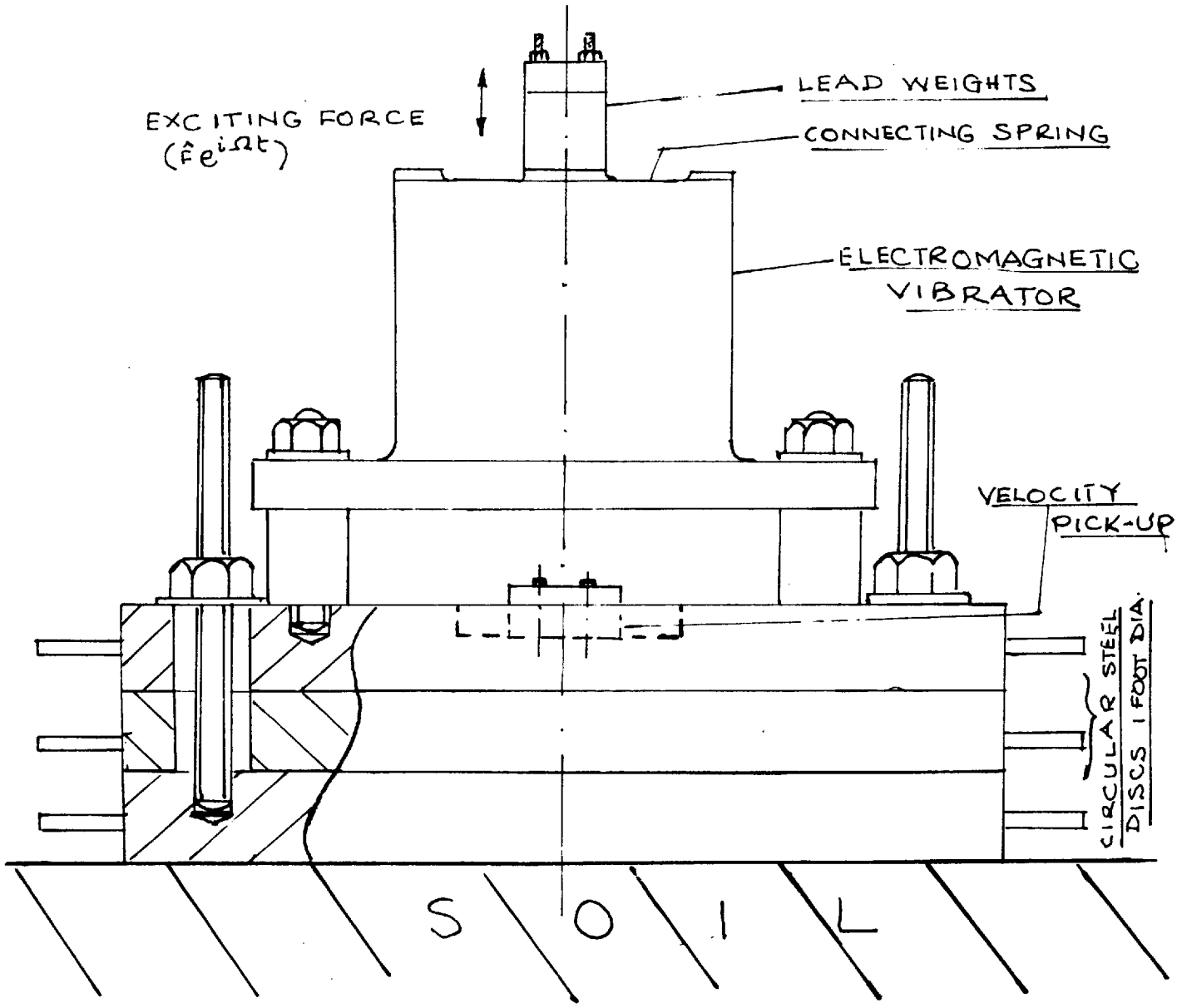


FIGURE 25 : ASSEMBLY DIAGRAM OF THE VIBRATING RIGID BODY IN-SITU.

11.3.1.2. Test procedure

The mains switches of the electronic equipments were put on for about half an hour to warm the sets. Stray radio waves and other external fields which were detected on the oscilloscope were suppressed as much as possible by using an earthing lead from the pick-up to the oscilloscope and by using the hum correctors on the preamplifier.

With the first mass - corresponding to the above least weight of 231 lb - on the soil, the E.H.T. of the power amplifier was switched on, the output knob was gradually turned from zero and the rigid body was set into vertical vibrations which were checked on the oscilloscope to be sinusoidal.

From the calibration factor of the pick-up, the amplitude of vibration was set to 0.303×10^{-3}in. at the arbitrary frequency of 42c.p.s.. The millivoltmeter measuring box was then switched on to the displacement (integrating) circuit and the height of the wave form was adjusted to occupy horizontal marks on the grid about 3in. apart. This height was to be maintained throughtout the test without touching any adjustment on the pre-amplifier or oscilloscope that would alter it, but only by controlling the output from the power amplifier was the height to be adjusted.

The test was then performed simply by changing the frequency (using the decade oscillator) and adjusting

the power amplifier output until the constant amplitude of vibration was attained when the voltage applied to the vibrator would be read on the avometer. The frequency range should include one frequency with the minimum applied voltage. At the end of each test, the amplitude of vibration was checked to be unaltered.

The results of all the tests, performed with six masses of the rigid body - 231, 295, 359, 423, 591 and 759 lb. - at various constant amplitudes of vibration, are shown graphically in figure 26 in which the applied voltages have been converted to forces using the calibration curves discussed in the next article and the above masses have been given as mass ratios using the density 130 lb./cu.ft. determined later. Also, the parts of the curves in the neighbourhood of resonance have been enlarged as shown in figure 27 in order to determine more accurately the resonant frequencies.

11.3.1.3. Conversion of the applied voltage to force

Since resonance has been defined in terms of minimum force that will maintain the same amplitude of vibration it is necessary to determine the force corresponding to each of the applied voltages. It is obvious that the exciting force on the rigid body is produced by the inertia force of the lead weights and the table to which they are fixed. Thus, by fixing the pick-up to the lead weights and measuring the amplitude x, say, of vibration at various frequencies, the force is easily given by $m\Omega^2 x$ where m, the total moving mass was 11 lb. for the tests. The corresponding applied

voltage was again read on the avometer.

The result of the calibration is shown in figure 28 from which we notice the effect of the variation of the combined impedance of the power amplifier and the vibrator with frequency. This is shown by the subsidiary curve in the same figure 28 in which, by direct projection of points as indicated for one point, the variation of frequency with applied voltage for a constant force of 25 lb. is given. An easier procedure might have been to read current instead of voltage since, theoretically, electromagnetic force is independent of frequenc at a given current. However, the above procedure is seen to throw light on the impedance characteristics of the vibrator with the amplifier.

11.4. Analysis of the results of resonance tests

11.4.1. Determination of the soil density

The density of the soil is required in the determinatio of the mass ratios and in the calculation of the shear modulus from the resonant frequency factor.

It was easily determined by cutting out two samples of soil 3/2 x 1 1/16 x ⅝ and 1⅛ x 15/16 x ¾ inches, directly under the rigid base plate and weighing them immediately on a chemical balance. The first weighed 74 gm. and the second, 26.8 gm. The calculated densities were admirably close - 130 and 129.5 lb./cu.ft. respectively.

11.4.2. Shear modulus and Poisson's ratio by the recommended method

It is to be recalled that the primary object of the

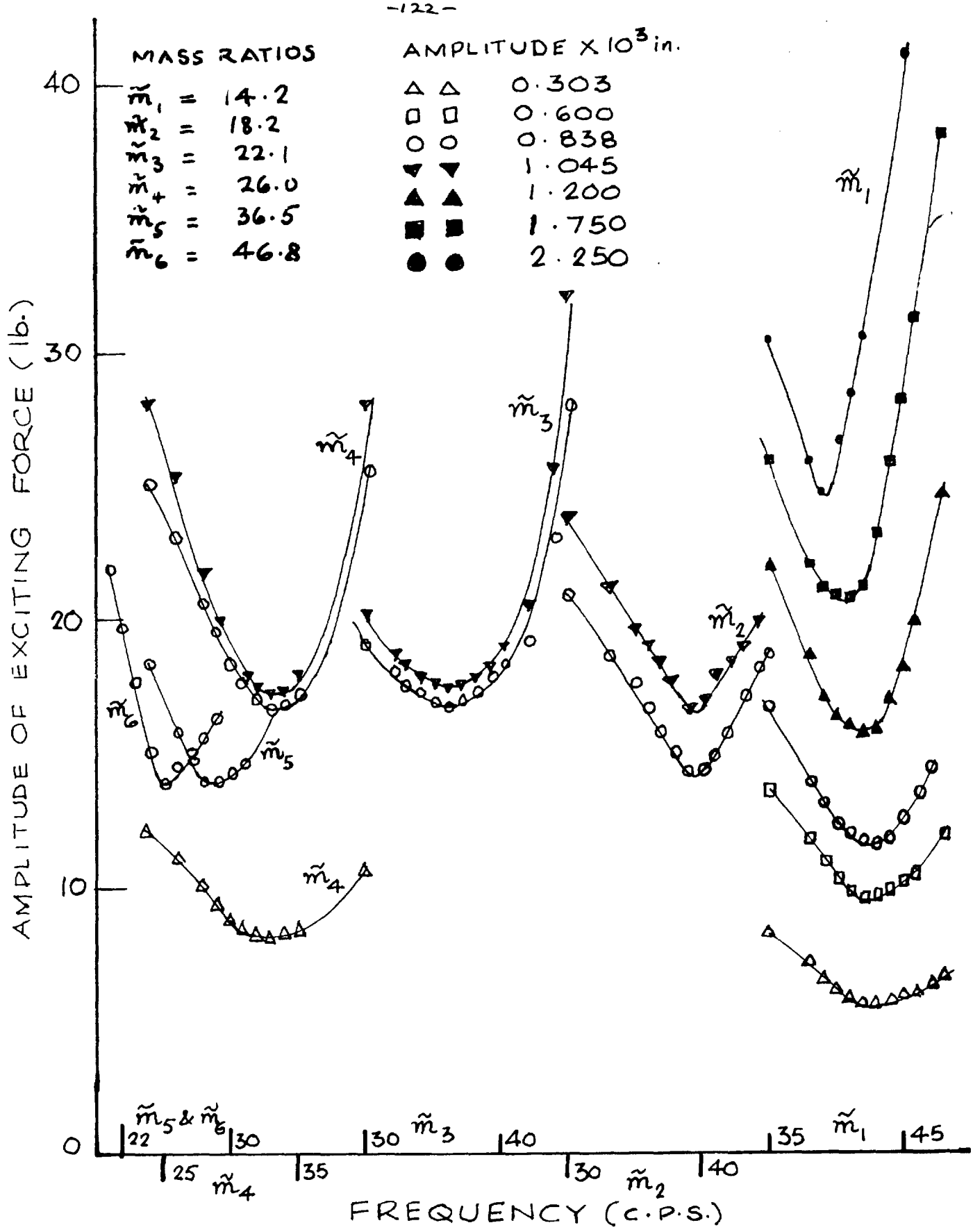


FIGURE 26: VARIATION OF EXCITING FORCE WITH FREQUENCY AT CONSTANT AMPLITUDE FOR $\tilde{m}_1$ to $\tilde{m}$

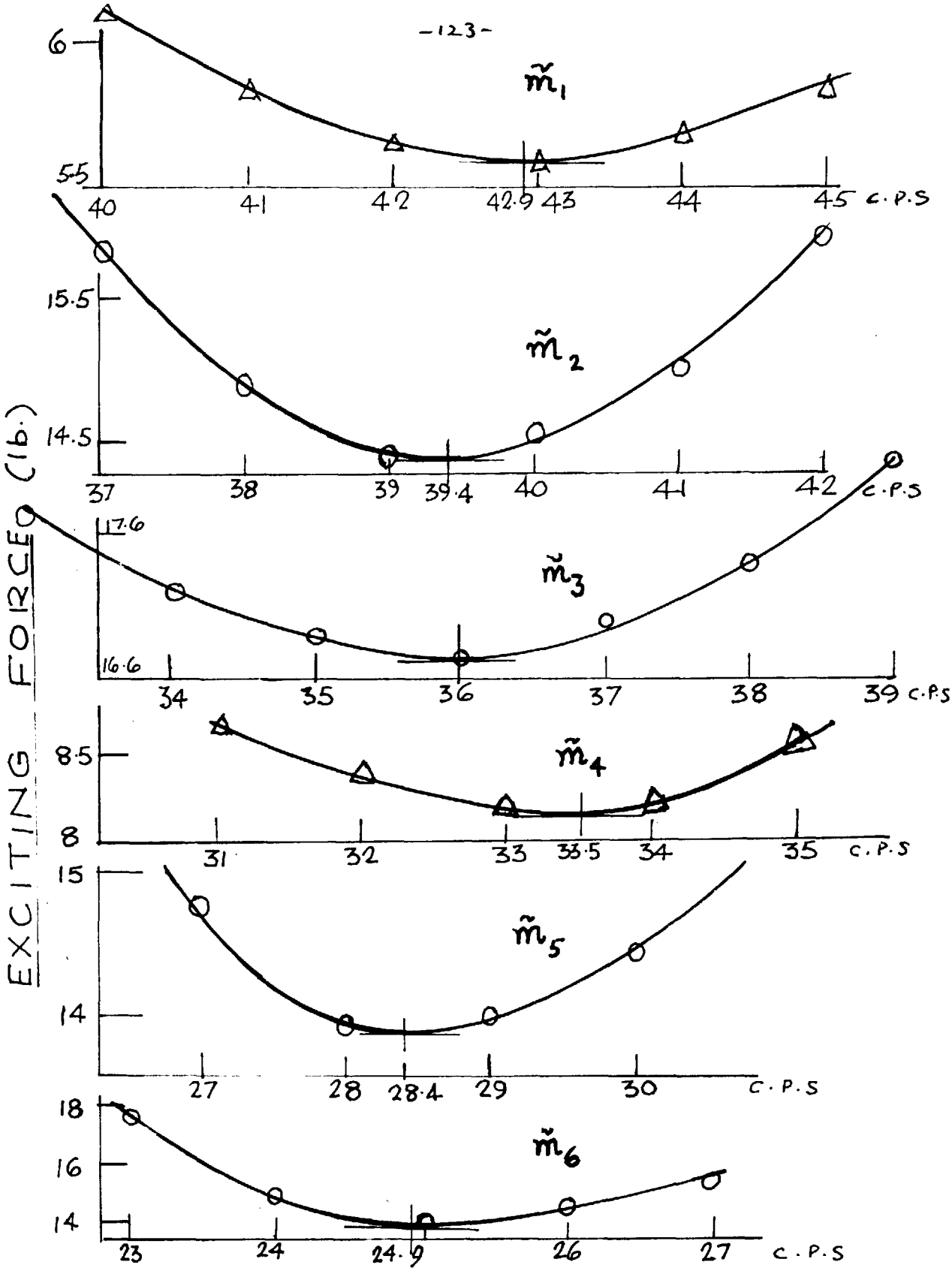


FIGURE 27: AN ENLARGEMENT OF FIGURE 26 IN THE NEIGHBOURHOOD OF THE RESONANT FREQUENCIES

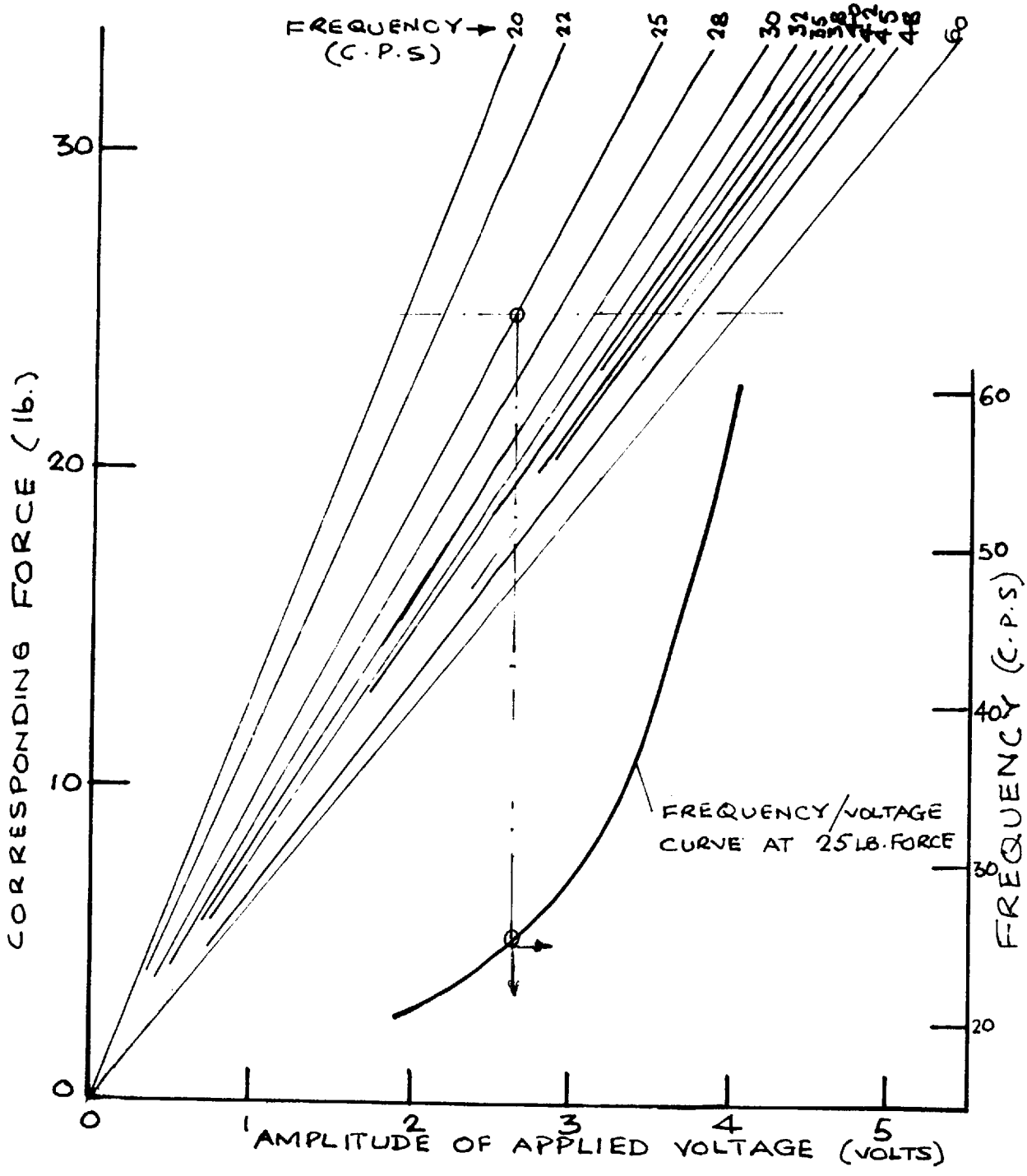


FIGURE 28: CALIBRATION CURVES FOR THE EXCITING FORCE PRODUCED BY THE ELECTROMAGNETIC VIBRATOR AND THE VARIATION OF FREQUENCY WITH APPLIED VOLTAGE AT 25 LB. FORCE

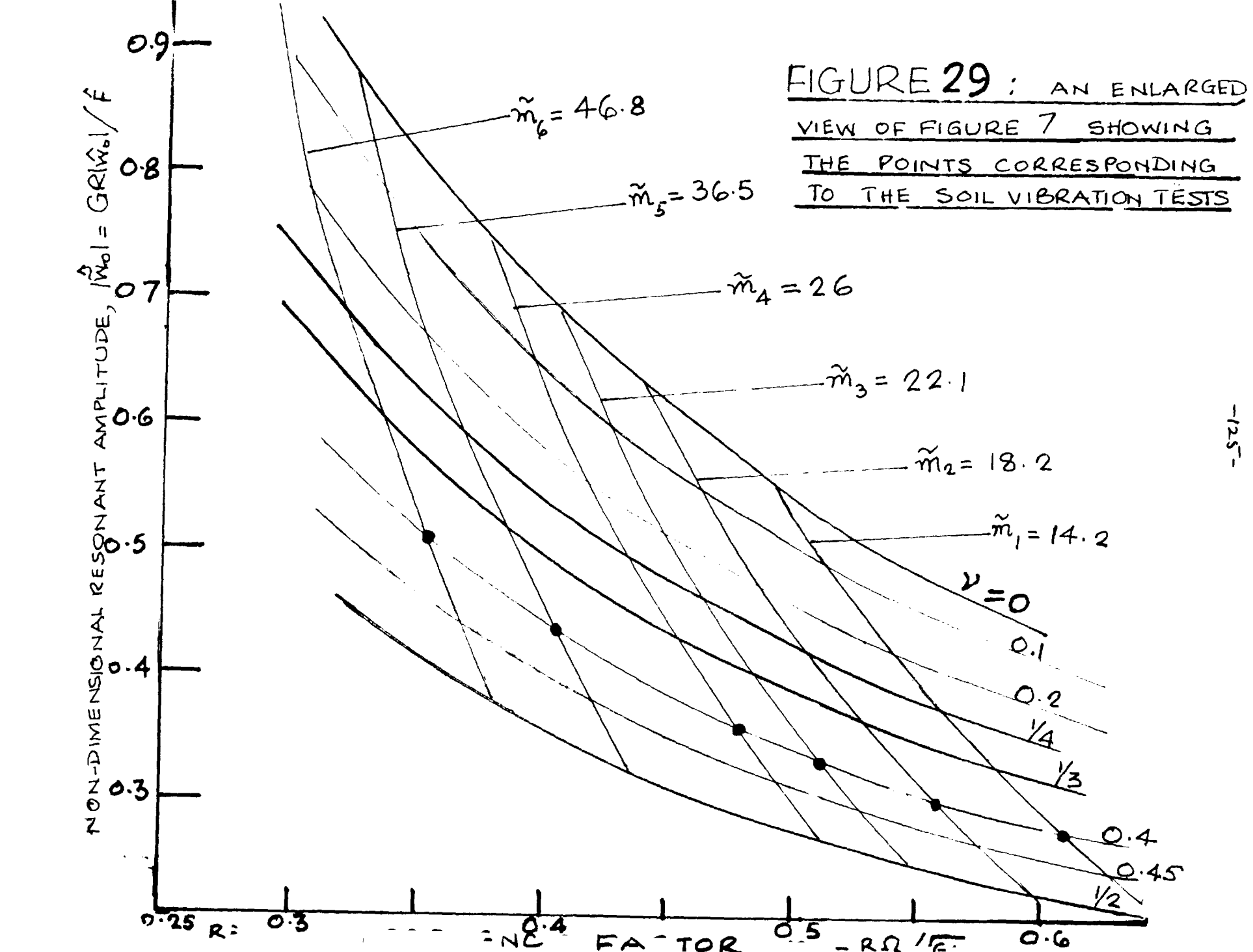


FIGURE 29 : AN ENLARGED VIEW OF FIGURE 7 SHOWING THE POINTS CORRESPONDING TO THE SOIL VIBRATION TESTS

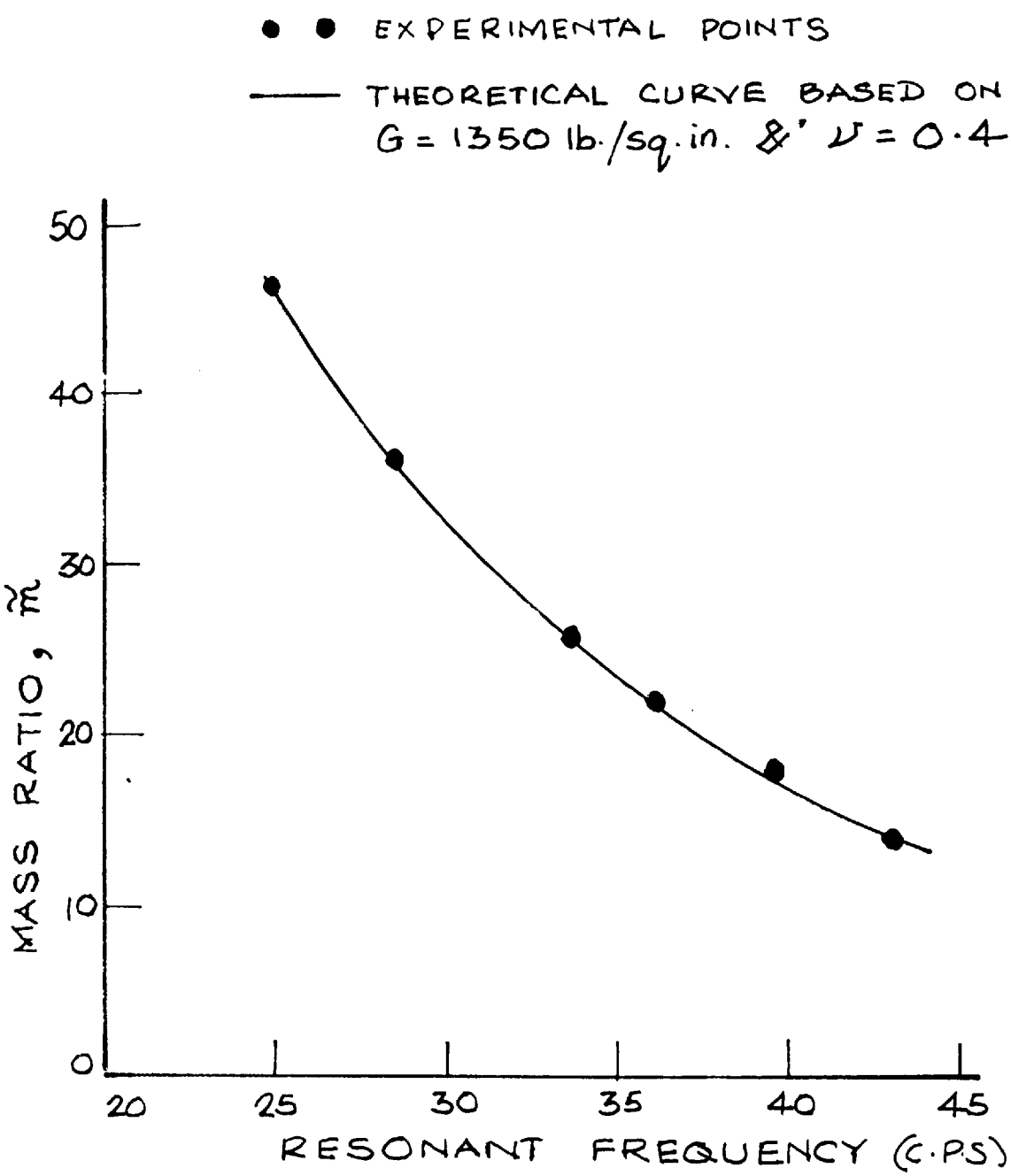


FIGURE 30: VARIATION OF MASS RATIO WITH RESONANT FREQUENCY

test is to solve the problem of the dynamic elastic constants as discussed in the introduction.

From the resonant frequencies shown in figure 27 and their correspomding mass ratios listed in figure 26, the procedure outlined in article 11.1. immediately gives, for any pair of mass ratios that the appropriate Poisson's ratio curve is 0.4 and the value of G, shear modulus, calculated from the resonant frequency factor and the corresponding resonant frequency for any of the six mass ratios is 1,350 lb./sq.in. This corresponds to a shear wave velocity (velocity of waves of distortion) of 220 ft./sec. and a velocity of waves of dilatation of 540 ft./sec.

The operating points are shown in figure 29 which is an enlarged view of figure 7 in the region of mass ratios tested. Figure 30 also shows the variation of mass ratio with resonant frequency.

11.4.3. Unreliability of elastic constants calculated from measured amplitude and force

It was mentioned in article 11.1. that there is more than one way of using figure 7 to determine the elastic constants but that the only method recommended is the one used above. The reasons given in that article are further substantiated here by considering figure 31(a) which shows the sub-linear characteristics of the soil under dynamic conditions. By comparison with the linear curve which a perfectly elastic medium would follow under the same conditions of loading, it is readily obvious that the error involved

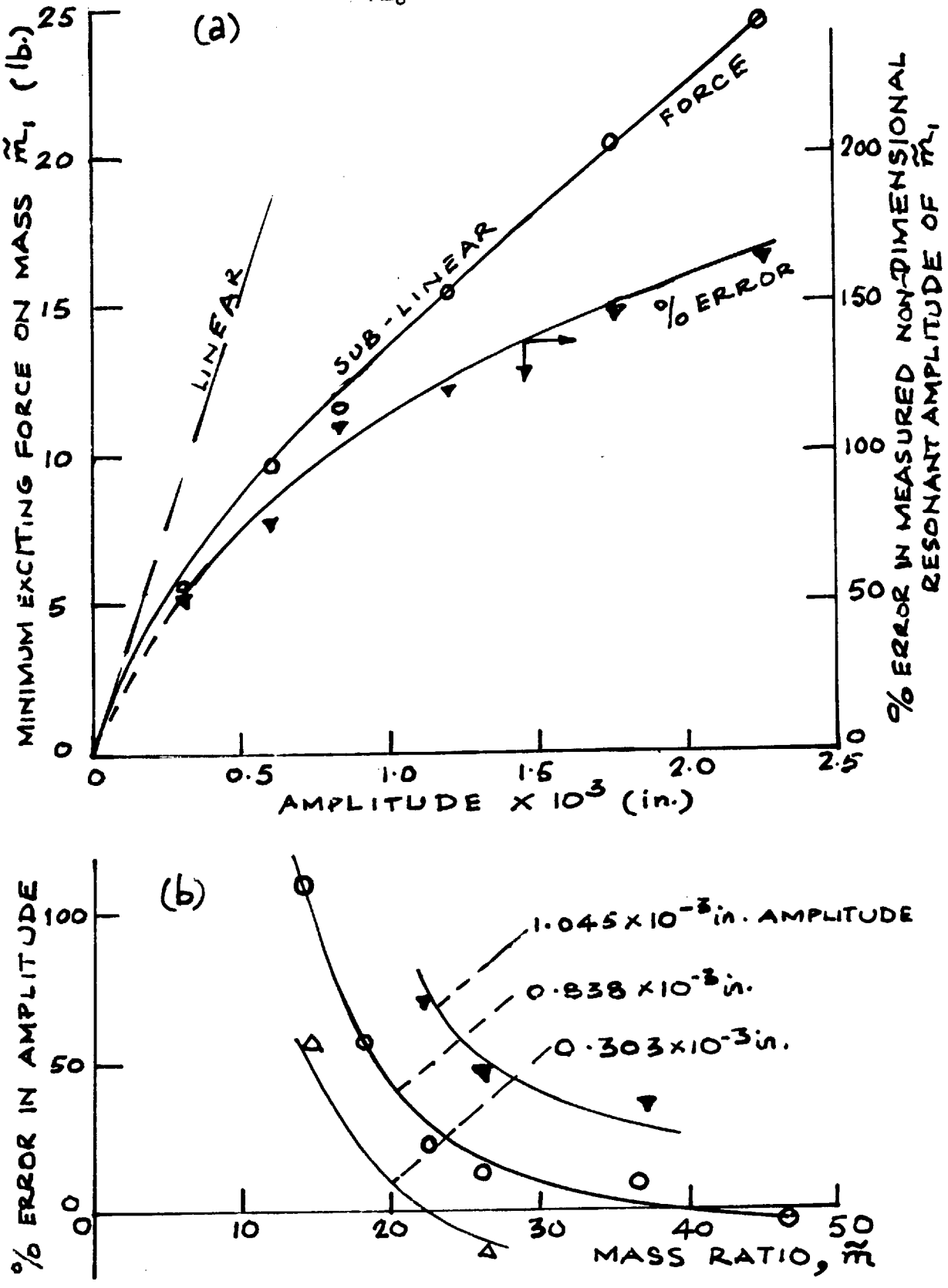


FIGURE 31 : EFFECT OF NON-LINEAR BEHAVIOUR OF THE SOIL ON MEASURED FORCE AND AMPLITUDE AT RESONANCE.

in the ratio of measured amplitude to force increases as we move away from the origin of the sub-linear curve. This has been shown in the same figure as the %ge error curve in the non-dimensional amplitude. Indeed, it has been checked that the tangent at the origin - which is the linear curve described above - gives practically no error in the non-dimensional amplitude at resonance.

The effect of this error on mass ratio as shown in figure 31(b) indicates that the error increases with decreasing mass. Thus, we can afford to work at higher amplitudes for larger masses with less error in the calculated non-dimensional amplitude at resonance. Also, when the error is negative i.e. from the points where the curves cross the horizontal axis, then linear elastic theory begins to take account of thermal damping in the medium.

All these show that methods of determining dynamic elastic constants of soil based on measured force and amplitude and assuming elastic theory are completely unreliable unless the sub-linear curve is accurately determined and the tangent at the origin properly obtained. This requires testing at very low amplitudes for a sufficient number of points and determining the best equation that fits the points. The differential coefficient at the origin would then be taken as the gradient of the linear curve of figure 31(a). The practical difficulties of testing at very low amplitudes and the effect of thermal damping which is not accounted for - and whose nature, in actual fact, is not really known for soil - make this method to be inferior to the one recommended.

11.5. Measurement of the velocity of waves of dilatation

As a check on the value of the shear modulus determined by the recommended method (article 11.4.2.), a test was carried out to measure the velocity of waves of dilatation.

A geophone was placed on the spot where the rigid body had been during the resonance tests and was connected to an M.D.1 refraction seismograph which is essentially a timing unit with variable gain and was placed in the pit near the geophone. A long lead from the seismograph goes to a sledge-hammer which was used to hit on an 8'' diameter, ¾'' thick steel plate placed in holes dug to the same depth as the geophone and at measured distances from the geophone.

The time taken by the first pulse to reach the geophone was recorded on the seismograph. This corresponds to the arriva of the waves of dilatation since this is the fastest. The slower waves - shear and Rayleigh waves - are generally indistinguishable and, therefore, reliance is placed only on the first pulse.

The results of the test are shown in figure 32 in which it is to be noticed that several readings, corresponding to various seismograph gains, were taken at each distance. The unpainted circles are for the readings taken at about 120° from the common direction of the other three.

The gradient of the graph gives the velocity of waves of dilatation as 540 ft./sec. corresponding to 1,350 lb./sq.in. on the assumption of 0.4 Poisson's ratio. This is in very good agreement with the value predicted from the resonance

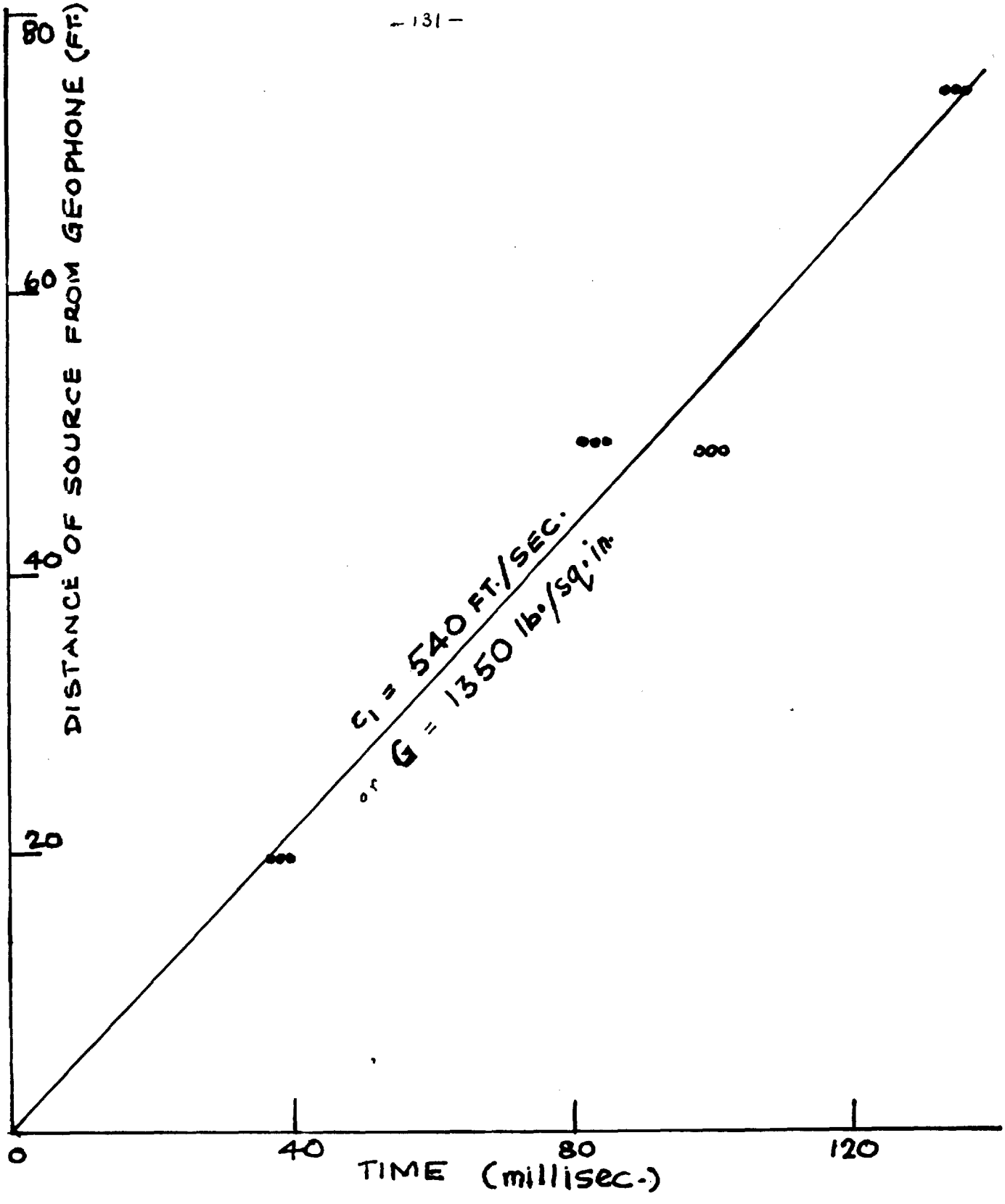


FIGURE 32 : MEASUREMENT OF THE VELOCITY OF WAVES OF DILATATION IN THE SOIL

tests results. It is, however, difficult to determine shear modulus and Poisson's ratio independently unless the arrivals of shear and Rayleigh waves can be distinguished.

The author hereby acknowledges the help and cooperation of Mr. Morgenstern of the Civil Engineering department and Dr.Krill of the Geology department with whom this test was performed.

11.6. Static tests

In the discussion on the problem of the dynamic elastic constants in the introduction (see article 1.2.), it was mentioned that the static modulus of elasticity is much lower than the dynamic modulus for soils. Tests on the soil used above have confirmed this statement and show that factors as large as ten may be involved if laboratory static modulus is used.

11.6.1. In-situ static determination of the shear modulus

The base plate was placed on the same spot as it was in the vibration tests. Two steel strips, 2ft. by 2" by ⅛" were symmetrically placed at 6" apart on the base plate and were maintained in a non-slip position by placing on them another disc. Two 0.0001" dial gauges were placed, one on each strip, diametrically opposite each other. The gauges were supported from a net-work constructed from handy iron angles whose ends were four feet from the discs - a distance which would ensure that the deflection of the soi there did not affect the readings of the gauges. Two beams were placed across the pit to form bridges on which the

loading weights were placed and which enabled loading to be effected without resting the feet near the loaded area.

The results of the tests are shown in figure 33 in which load has been plotted against deflection as read from the dial gauges. Figure 7 shows that at a Poisson's ratio of 0.4, the static non-dimensional amplitude is 0.15 - a result which can also be derived from Boussinesq's equation. Hence, from the linear portion of figure 33, we obtain the values of the shear modulus as 1,000 lb./sq.in. from gauge A and 790 lb./sq.in. from gauge B which are much lower (26% and 41.5%) than the dynamic modulus of 1,350 lb./sq.in. .

11.6.2. Triaxial laboratory test

Mr. Morgenstern kindly consented to conduct a laboratory test on cylindrical samples of the soil taken from the core of a lump which was dug from the spot on which the rigid body was resting.

The stress-strain characteristics of three samples as obtained from triaxial tests are shown in figure 34. The values of Young's modulus obtained from the linear portions of these graphs are quoted on the figure. Remembering that Young's modulus is 2.8 times shear modulus for a Poisson's ratio of 0.4, the important conclusion to be drawn from this test is that elastic constants derived from laboratory static tests and applied to field vibration problems can only lead to very wrong results because soil in the laboratory, under artificial loading, does not behave as the same soil in-situ.

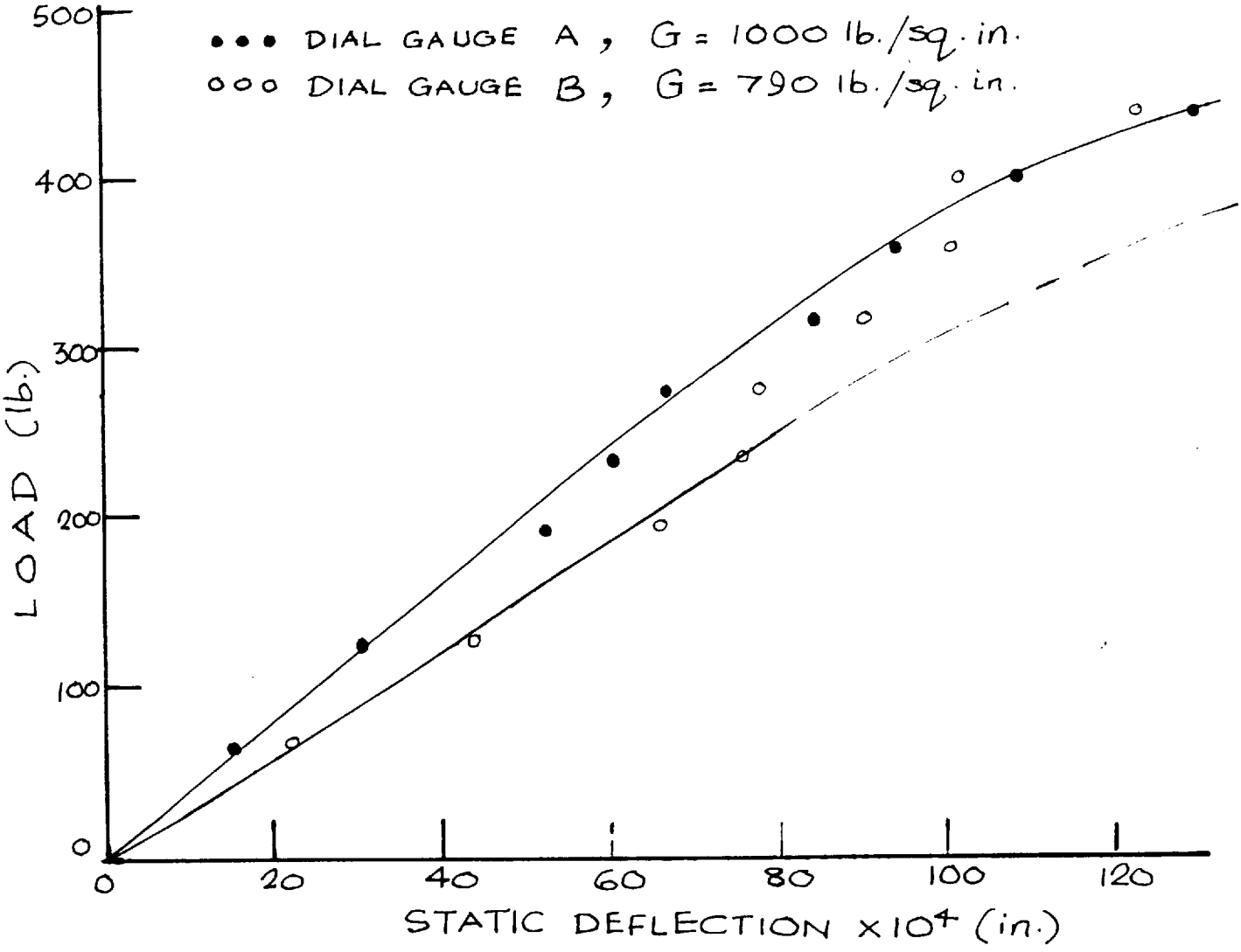


FIGURE 33 : IN-SITU DETERMINATION OF THE STATIC SHEAR MODULUS OF THE SOIL.

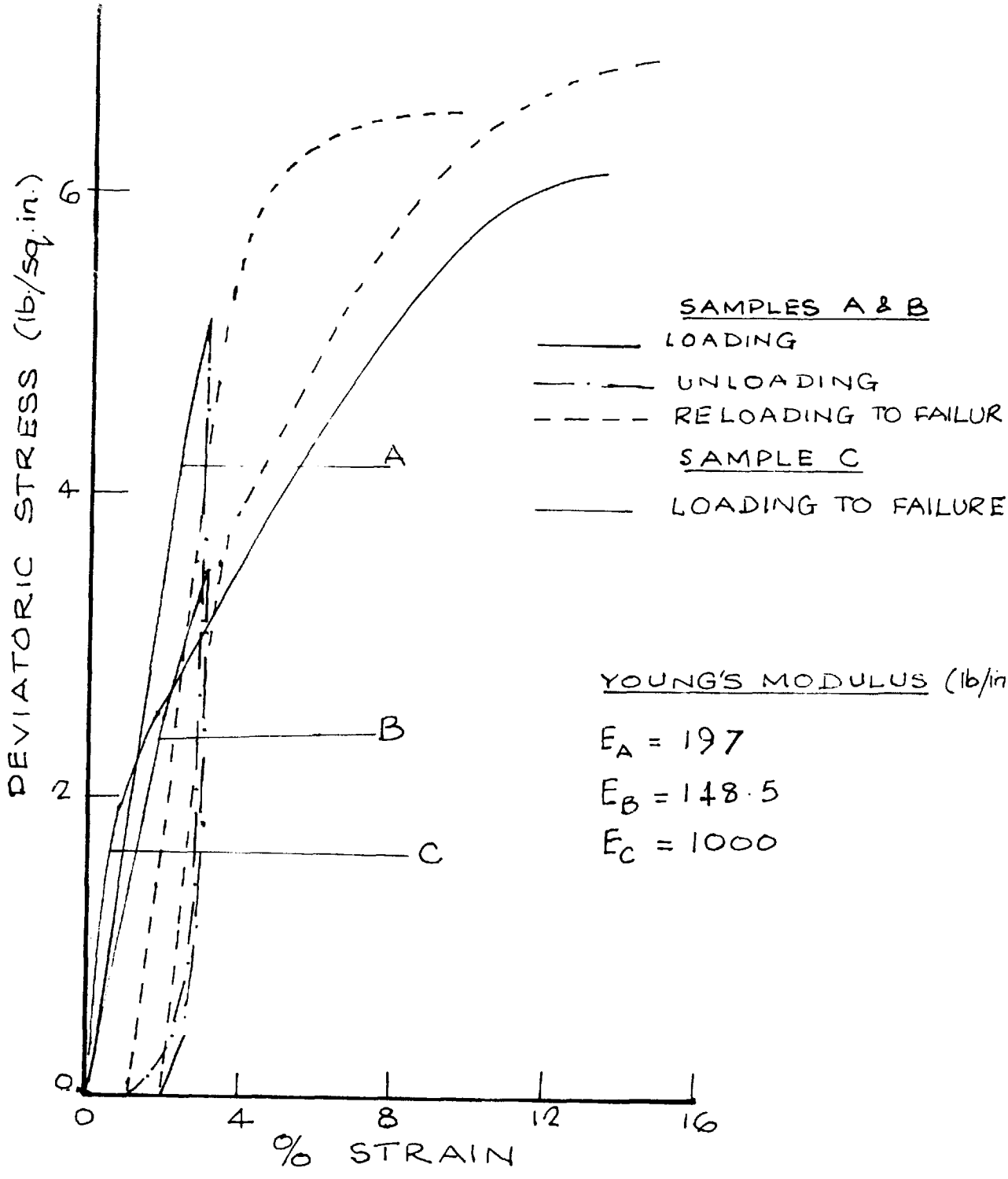


FIGURE 34: STRESS ~ STRAIN CURVES FOR THREE SAMPLES OF THE SOIL FROM TRIAXIAL TESTS.

APPENDIX 1

DERIVATION OF THE GOVERNING EQUATIONS OF MOTION

The equations of motion - the three components of equation (1) - are generally quoted in published papers and sketchily or inadequately derived in elasticity text-books, for example, Timoshenko (1951) and Love (1944). The following derivation is given for the purpose of completeness. The equations have been derived in cylindrical polar coordinates but it should be remarked that they can readily be transformed to corresponding equations in other coordinate systems by well-known techniques of orthogonal curvilinear coordinates.

Nomenclature

r, θ, z - cylindrical polar coordinates of P in figure A1

$r', \theta', z' = r+dr, \theta+d\theta, z+dz.$ - coordinates of P'

u, v, w - components of the displacement vector $\vec{s}$ of a particle at P in the directions r, θ, z.

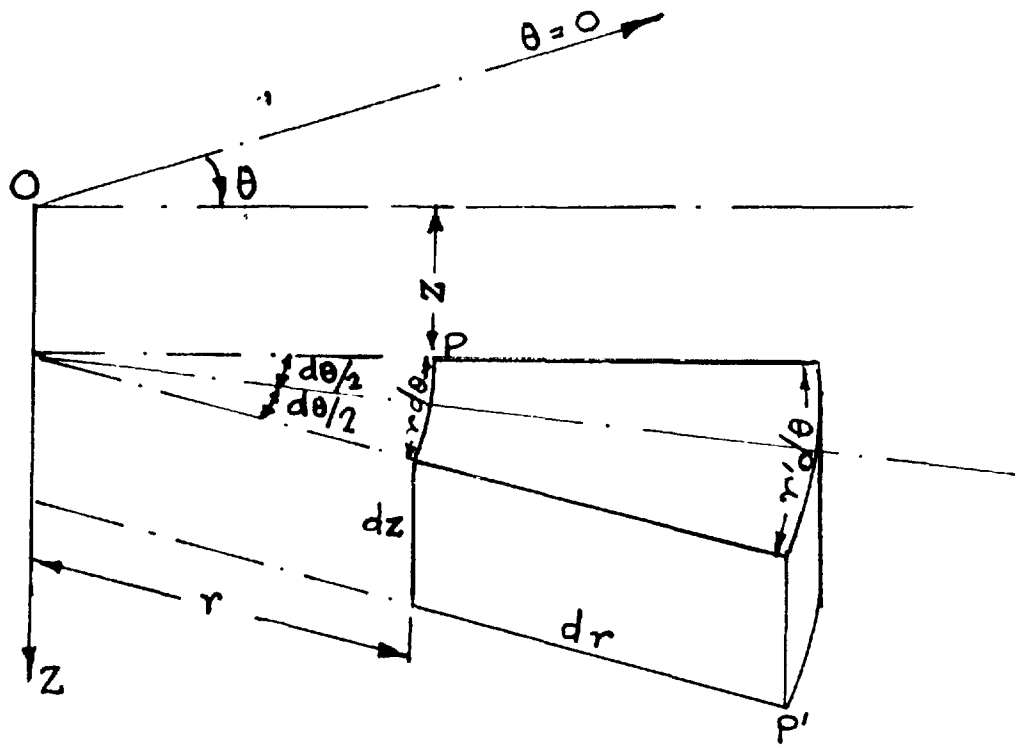
$\omega_{r,\theta,z}$ - components of the rotation vector $\vec{\omega}$ at P.

σ, ϵ - direct stress and direct strain respectively

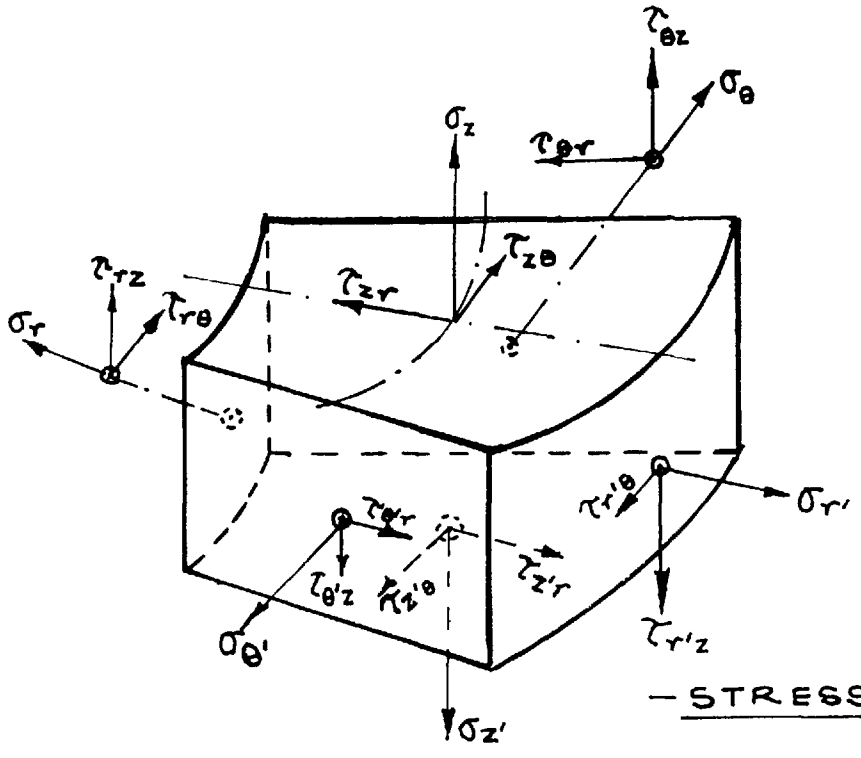
τ, γ - shear stress and shear strain respectively

ν, λ, ρ, G, E - Poisson's ratio, Lame's elastic constant, density, shear modulus and Young's modulus of the elastic medium respectively, where

$$\lambda = \frac{E}{(1+\nu)(1-2\nu)} \quad \text{and} \quad G = \frac{E}{2(1+\nu)}$$



— COORDINATE SYSTEM —



— STRESS SYSTEM —

FIGURE A1 — AN ELEMENT IN THE ELASTIC MEDIUM

Sign convention for stresses

Tensile stresses are positive. $\tau_{r\theta}$ is a shear stress on the face r is a constant and in the direction θ increasing. It is taken positive if the tensile stress on the same face is along the direction r increasing.

A1.1 Equations of motion in terms of stresses

The element in figure A1 is first considered as a rigid body acted upon by forces arising from the stresses shown in the figure. Resolving radially outwards along the mid-plane $\theta+d\theta$ = constant, resolving perpendicular to this plane and thirdly along the z-direction give the following equations of motion :-

$$\left.\begin{aligned}
&(\sigma_{r'}-\sigma_r)d\theta dz-(\sigma_\theta+\sigma_\theta)dr dz\frac{d\theta}{2}+(\tau_{z'r}-\tau_{zr})r d\theta dr+(\tau_{\theta'r}-\tau_{\theta r})dr dz=\rho dV\frac{\partial^2 u}{\partial t^2}\\
&(\sigma_{\theta'}-\sigma_\theta)dz dr+(\tau_{r'\theta}-\tau_{r\theta})d\theta dz+(\tau_{z'\theta}-\tau_{z\theta})r d\theta dr+(\tau_{\theta'r}+\tau_{\theta r})\frac{d\theta}{2}dr dz=\rho dV\frac{\partial^2 v}{\partial t^2}\\
&(\sigma_{z'}-\sigma_z)r d\theta dr+(\tau_{r'z}-\tau_{rz})d\theta dz+(\tau_{\theta'z}-\tau_{\theta z})dr dz=\rho dV\frac{\partial^2 w}{\partial t^2}
\end{aligned}\right\}\quad\ldots(A1)$$

Noting, for example, that as P' tends to P, $(\tau_{z'r}-\tau_{zr})=(\frac{\partial\tau}{\partial z}zr)dr$ and that the elemental volume $dV=r dr d\theta dz$, we find that equations (A1) reduce to

$$\left.\begin{aligned}
&\frac{\partial\sigma_r}{\partial r}+\frac{1}{r}\frac{\partial\tau_{r\theta}}{\partial\theta}+\frac{\partial\tau_{rz}}{\partial z}+\frac{\sigma_r-\sigma_\theta}{r}=\rho\frac{\partial^2 u}{\partial t^2}\\
&\frac{\partial\tau_{r\theta}}{\partial r}+\frac{1}{r}\frac{\partial\sigma_\theta}{\partial\theta}+\frac{\partial\tau_{\theta z}}{\partial z}+\frac{2\tau_{r\theta}}{r}=\rho\frac{\partial^2 v}{\partial t^2}\\
&\frac{\partial\tau_{rz}}{\partial r}+\frac{1}{r}\frac{\partial\tau_{\theta z}}{\partial\theta}+\frac{\partial\sigma_z}{\partial z}+\frac{\tau_{rz}}{r}=\rho\frac{\partial^2 w}{\partial t^2}
\end{aligned}\right\}\quad\ldots(A2)$$

It should be noted that the above equations are statically indeterminate as they do not take into consideration the deformation of the element.

A1.2 Compatibility of stress and strain

Hooke's law gives the following expressions for the direct strains in terms of the direct stresses :-

$$\begin{aligned} \sigma_r - \nu\sigma_\theta - \nu\sigma_z &= E\epsilon_r \\ -\nu\sigma_r + \sigma_\theta - \nu\sigma_z &= E\epsilon_\theta \\ -\nu\sigma_r - \nu\sigma_\theta + \sigma_z &= E\epsilon_z \end{aligned}$$

By solving these simultaneous equations, we obtain the direct stresses in terms of the direct strains; for example,

$$\sigma_r = \frac{E}{\Delta(\nu)}\begin{vmatrix} \epsilon_r & -\nu & -\nu \\ \epsilon_\theta & 1 & -\nu \\ \epsilon_z & -\nu & 1 \end{vmatrix} \quad \text{where } \Delta(\nu) = \begin{vmatrix} 1 & -\nu & -\nu \\ -\nu & 1 & -\nu \\ -\nu & -\nu & 1 \end{vmatrix}$$

$$= (1-2\nu)(1+\nu)^2$$

After some reductions, it is found that

$$\sigma_r = \frac{E[\nu\epsilon + (1-2\nu)\epsilon_r]}{(1-2\nu)(1+\nu)} \quad \text{where } \epsilon \text{ is the dilatation i.e.}$$

$\epsilon = \epsilon_r + \epsilon_\theta + \epsilon_z$. By introducing now the elastic constants G and λ, we finally express σ_r in the symmetric form

$$\left.\begin{aligned} \sigma_r &= \lambda\epsilon + 2G\epsilon_r \\ \sigma_\theta &= \lambda\epsilon + 2G\epsilon_\theta \\ \sigma_z &= \lambda\epsilon + 2G\epsilon_z \end{aligned}\right\} \quad \text{and in a similar manner} \quad \ldots\ldots\ldots\ldots\ldots\ldots (A3)$$

Shear stresses are directly related to corresponding shear strains by Hooke's law i.e.

$$\left.\begin{aligned} \tau_{r\theta} &= G\gamma_{r\theta} \\ \tau_{\theta z} &= G\gamma_{\theta z} \\ \tau_{zr} &= G\gamma_{zr} \end{aligned}\right\} \quad \ldots\ldots\ldots\ldots\ldots\ldots\ldots\ldots (A4)$$

A1.3 Expressions for strains in terms of displacements

From the geometry of the deformation of the element, it is shown by Timoshenko (Pages 65,66 & 305) and Love (P.56) that the components of strain are related to the components of displacement by the following expressions :-

$$\epsilon_r = \frac{\partial u}{\partial r}, \quad \epsilon_\theta = \frac{1}{r}\frac{\partial v}{\partial \theta} + \frac{u}{r}, \quad \epsilon_z = \frac{\partial w}{\partial z} \qquad \text{.....(A5)}$$

$$\gamma_{r\theta} = \frac{1}{r}\frac{\partial u}{\partial \theta} + \frac{\partial v}{\partial r} - \frac{v}{r}, \quad \gamma_{\theta z} = \frac{\partial v}{\partial z} + \frac{1}{r}\frac{\partial w}{\partial \theta}, \quad \gamma_{zr} = \frac{\partial u}{\partial z} + \frac{\partial w}{\partial r} \qquad \text{....(A6)}$$

Also, the components of rotation are shown to be given by

$$2\omega_r = \frac{1}{r}\frac{\partial w}{\partial \theta} - \frac{\partial v}{\partial z}, \quad 2\omega_\theta = \frac{\partial u}{\partial z} - \frac{\partial w}{\partial r}, \quad 2\omega_z = \frac{\partial v}{\partial r} + \frac{v}{r} - \frac{1}{r}\frac{\partial u}{\partial \theta} \qquad \text{...(A7)}$$

A1.4 Expressions for the derivatives of shear strains

It is obvious from the stress equations of motion (equations (A2)) that, after the elimination of the stress components by using equations (A3) and (A4), we require expressions for the derivatives of strains with respect to the spacial variables. These are found after some differential operations on equations (A5) to (A7) to be given by :-

$$\frac{\partial \gamma_{zr}}{\partial z} = \frac{2\partial \omega_\theta}{\partial z} + \frac{2\partial \epsilon_z}{\partial r}, \quad \frac{\partial \gamma_{r\theta}}{\partial \theta} = \frac{2\partial^2 v}{\partial r \partial \theta} - \frac{2\partial \omega_z}{\partial \theta}, \quad \frac{\partial \gamma_{r\theta}}{\partial r} = \frac{2\partial \omega_z}{\partial r} + \frac{2\partial \epsilon_r}{r\partial \theta} - \frac{2}{r}\gamma_{r\theta}$$

$$\frac{\partial \gamma_{\theta z}}{\partial z} = \frac{2\partial \epsilon_z}{r\partial \theta} - \frac{2\partial \omega_r}{\partial z}, \quad \frac{\partial \gamma_{rz}}{\partial r} = \frac{2\partial \epsilon_r}{\partial z} - \frac{2\partial (r\omega_\theta)}{r\partial r} + \frac{2\omega_\theta}{r}$$

$$\frac{\partial \gamma_{\theta z}}{\partial \theta} = \frac{2\partial \omega_r}{\partial \theta} + \frac{2r\partial \epsilon_\theta}{\partial z} - \frac{2\partial u}{\partial z}$$

A8

A1.5 Equations of motion in terms of the components of displacement, dilatation and rotation

Finally, we can now obtain the equations of motion in the forms in which they have been quoted in chapter 1 by successive substitutions of equations (A3) to (A8) in the stress equations (A2) and by introducing the velocities of waves of dilatation (c_1) and waves of distortion (c_2) which are related to the elastic constants by

$$c_1^2 = \frac{\lambda + 2G}{\rho} \qquad c_2^2 = \frac{G}{\rho}$$

After a few reductions the final equations of motion are found to be

$$\left.\begin{aligned} c_1^2 \frac{\partial \epsilon}{\partial r} - \frac{2c_2^2}{r}\frac{\partial \omega_z}{\partial \theta} + 2c_2^2 \frac{\partial \omega_\theta}{\partial z} &= \frac{\partial^2 u}{\partial t^2} \\ c_1^2 \frac{1}{r}\frac{\partial \epsilon}{\partial \theta} - 2c_2^2 \frac{\partial \omega_r}{\partial z} + 2c_2^2 \frac{\partial \omega_z}{\partial r} &= \frac{\partial^2 w}{\partial t^2} \\ c_1^2 \frac{\partial \epsilon}{\partial z} - \frac{2}{r}c_2^2 \frac{\partial}{\partial r}(r\omega_\theta) + \frac{2}{r}c_2^2 \frac{\partial \omega_r}{\partial \theta} &= \frac{\partial^2 w}{\partial t^2} \end{aligned}\right\} \quad \ldots\ldots\ldots (A9)$$

which are easily shown to reduce to equations (2) and (4) of chapter 1 for the vertical translation and torsional oscillation of the rigid circular body respectively.

A1.6 Composition of equations (A9) into the vector equation

By using the definitions of the curl and divergence of a vector and the gradient of a scalar (in this case, the volumetric dilatation) in cylindrical polar coordinates as given, for example, in Pipes (1958, Pages 397 & 398), it is readily shown that the vector equation of motion - equation (1), chapter 1 - is the composition of equations (A9). This completes the derivation of the governing equations of motion

APPENDIX 2

APPLICATION OF THE SOLUTION TO RELATED PROBLEMS OF SUPERSONIC AEROFOIL THEORY AND DIFFRACTION OF ELECTROMAGNETIC WAVE

The general nature of the solution presented here is indicated by quoting the above examples of other mixed boundary-value problems which have been reduced to dual integral equations that have not been satisfactorily solved.

It has been shown by Gunn (1947) that the linearised supersonic aerofoil theory for the case of a supersonic steady flow past a finite rectangular plate aerofoil at incidence can be reduced to the pair of equations :-

$$\int_0^\infty \sqrt{p^2+q^2}\, a(q)\cos(kqx)\,dq. \quad = e/pk \quad 0<x<b$$

$$\int_0^\infty a(q)\cos(kqx)\,dq. \quad = 0 \quad x>b$$

where b is the semi-span of the aerofoil which has its leading edge lying symmetrically along the x-axis, p,e and k are constants and a(q) is the unknown function required in the determination of the velocity potential.

After referring to the original work of Titchmarsh (1937), Gunn's comments on these equations are : " Its direct solution does not appear to present a simple analytical problem ". He then went on to methods which evaded the mixed boundary-value problem.

It is clear that, by a mere change of parameters, that the above equations can be re written in the convenient form :-

$$\int_0^{\infty} \frac{F(\eta)}{\left(\eta^2+a^2\right)^{-1/2}} \cos(\eta\tilde{x})d\eta. \quad = c \quad 0 < \tilde{x} < 1$$

$$\int_0^{\infty} F(\eta)\cos(\eta\tilde{x})d\eta. \quad = 0 \quad \tilde{x} > 1$$

By expanding $\left(\eta^2+a^2\right)^{-1/2} = \alpha$ as a power series in η/a where a is here a constant, a first approximation solution follows immediately by adopting the procedure of chapter 7. It is readily noticed that the leading term in this solution is the same as the second term (inertia component) for the case of the vertical translation of the rigid rectangular body and successive terms can be obtained from this solution also.

A suitable contour for the derivation of the complete solution is given in figure A2 and its image in the lower-half plane. The signs of the double-valued function α are shown and the only pole within the contour is by-passed by the branch-cuts and very small circle.

The above equations are also known to occur in the problems of the diffraction of an unsymmetrical electromagnetic wave incident upon a slit of arbitrary width. For the case of normal incidence, it is readily shown that the poles of the function move to the real axis as in the case of the torsional oscillations of the rigid circular body. Some of these problems have recently been discussed by Schmeltzer and Lewin (1964) who have attempted a solution of the problem by what they call the function theoretic solution.

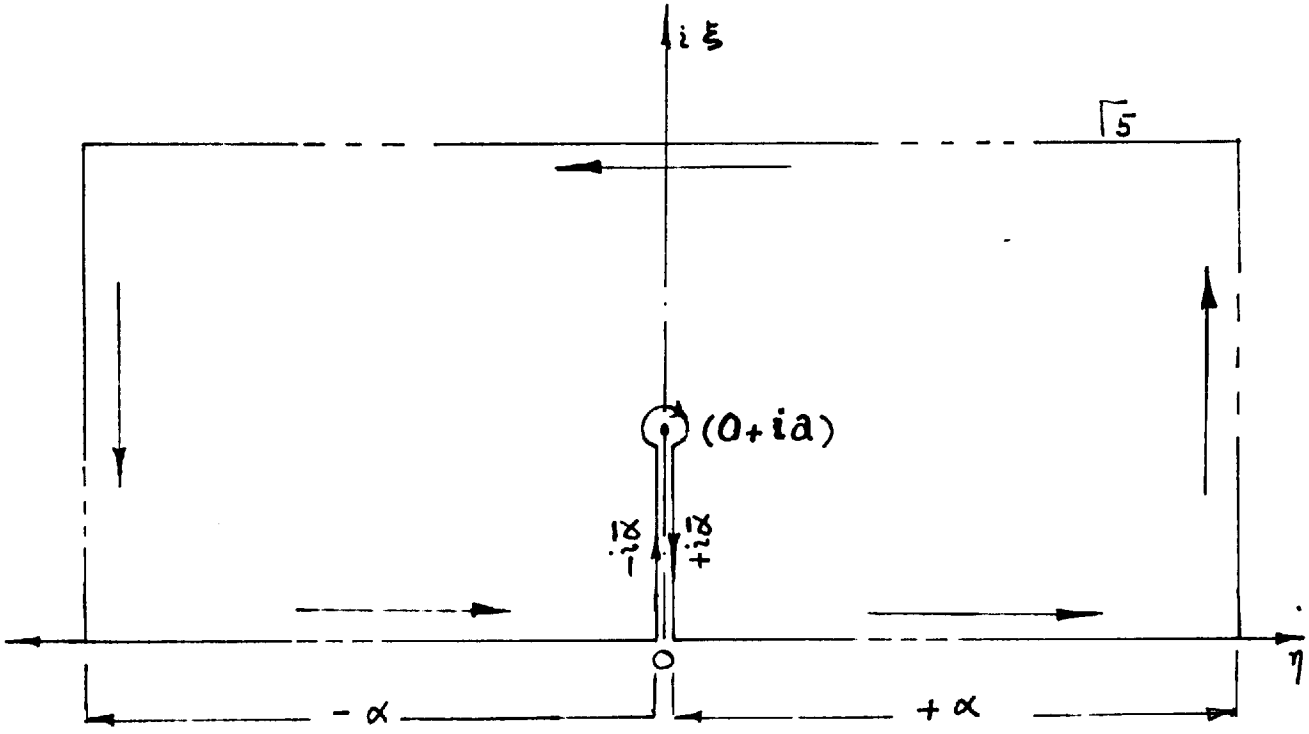


FIGURE A2 - THE CONTOUR Γ_5

REFERENCES

Alpan, I., 1961, Geotechnique, 95.

Arnold, R.N., Bycroft, G.N. and Warburton, G.B., 1955, J. Appl. Mech. 22, 391.

Bateman, H. and Erdelyi, A., 1954, Tables of Integral Transfo Vol. 2, McGraw Hill, N.Y.

Bernhard, R.K., 1953, A.S.T.M., S.T.P. No.156, 225.

Biot, M.A., 1943, Trans. Amer. Soc. Civ. Engrs., 108, 365.

Busbridge, I.W., 1938, Proc. Lond. Maths. Soc., 44, 115.

Bycroft, G.N., 1959, Proc. Inst. Mech. Engrs., 173, 469.

Crockett, J.H.A. and Hammond, R.E.R.,1949, Proc. Inst. Mech. Engrs., 163, 512.

Dawance, G. and Guillot, M., 1963, Ann. Inst. Tech. Bat. Travaux Publics, 16, 185, 511.

Eastwood, W., 1953, Structural Engr., 82.

Gordon, A.N., 1954, J. Lond. Math. Soc. 29, 360.

Gunn, J.C., 1947, Phil. Trans. A.,240, 327.

Hsieh, T.K., 1962, Proc. Inst. Civ. Engrs. 22,211.

Jacobson, L.S. and Ayre, R.S., 1958, Engineering Vibrations, McGraw Hill, N.Y.

Jarman, B., 1960, PhD Thesis, Univ. of London.

Jones, R., 1958, Geotechnique, 8, 1.

Kanai, K. and Yoshizawa, S., 1961, B.E.R.I., Tokyo, 39, 477.

Lamb, H., 1904, Phil. Trans. A., 203, 1.

Lorenz, H., 1950, Proc. 3rd. Int. Conf. Soil Mech., Zurich, 1, 460.

Love, A.E.H., 1944, A treatise on the mathematical theory of elasticity, 4th. Ed., Dover.

Miller, G.F. and Pursey, H., 1954, Proc. Roy. Soc. A., 223,521.
1955, Proc. Roy. Soc. A., 233, 55.

Novak, M., 1957, Acta technica, 2, 365.

Pipes, L.A., 1958, Applied Mathematics for Engineers and Physicists, 2nd. Ed., McGraw Hill, N.Y.

Quinlan, P.M., 1953, A.S.T.M., S.T.P. No. 156, 3.

Rao, H.A.B. and Nagaraj, C.N., 1960, Structural Engr., 310.

Rayleigh, J.W.S., 1885, Proc. Lond. Math. Soc. 17, 4;
Scientific Papers 2, 441.

Reissner, E., 1936, Ing.-Archiv., 7, 381.

Reissner, E. and Sagoci, H.F., 1944, J.Appl. Phy. 15, 652.

Sadowsky, M., 1928, Z. Angew. Math. Mech., 8, 107.

Schmeltzer, R.A. and Lewin, M.,1964, Qtly. Appl. Math.21,269.

Sneddon,I.N., 1947, J. Appl. Phy., 18, 130.

Sung, T.Y., 1953, A.S.T.M., S.T.P. No. 156, 35.

Terzaghi, K., 1942, Theoretical Soil Mechanics.

Timoshenko, S. and Goodier, J.N., 1951, Theory of Elasticity, McGraw Hill, N.Y.

Tranter, C.J., 1951, Oxf. Quart. J. Math., 2, 160.

Tschebotarioff, G.P.,1951, Soil Mechanics Foundation and Earth Structures, McGraw Hill, N.Y.

U.S. Army Engr. Waterways Expt. Station, Corps of Engrs..
Tech. Report 1, July 1963.

Warburton, G.B., 1957, J. Appl. Mech., 24, 55.

Watson,G.N., 1922, A treatise on the theory of Bessel functions Cambridge University Press.

INDEX OF PRINCIPAL NOTATION (see also Appendix 1)

$a_{1,2,3..}$ - coefficients in the expansion of $\emptyset/\alpha_1$

b - semi-width of rectangular body

$c_{1,2}$ - dilatational and shear wave velocities

m - mass or mass per unit length of rigid body

$\tilde{m}$ - mass ratio, $m/\rho R^3$ or $m/\rho b^2$ where R = radius of circular body

p - transform parameter

u,v,w - components of displacement

G - shear modulus of the elastic medium

$\tilde{J}$ - Non-dimensional polar inertias (equations 38b and 40b)

$\alpha_{1,2}$ - double-valued functions (equations 9a and 9b)

β_1 - ratio of the wave velocities c_2/c_1, $\beta = c_1/c_2 = 1/\beta_1$

η_2 - frequency factor, $R\Omega/c_2$ or $b\Omega/c_2$

Ω - angular frequency of excitation

F - exciting force

$\emptyset$ - Rayleigh function (equation 18)

$\sim$ - sign for non-dimensional quantities

$\wedge$ - sign for maximum value